RI/RD87-207-2

Interim Study Report for the Space Transportation Main Engine Phase A' Study

Rockwell International

Rocketdyne Division
6633 Canoga Avenue
Canoga Park, California 91304

FOREWORD

This report presents the results of the Space Transportation Main Engine Study performed under the Phase A' extension to National Aeronautics and Space Administration Contract NAS8-36869. The work was performed during the period of June 1, 1987, through December 31, 1987. This program was conducted under the direction of National Aeronautics and Space Administration--Marshall Space Flight Center.

This volume is a supplement to Volume II of the final report describing the results of Phase A of the Space Transportation Main Engine, Report Number RI/RD87-207-2.

ABSTRACT

The Space Transportation Main Engine Phase A' Study was conducted over a 7-mo period as an extension to the Phase A Study. The Phase A' program was designed to expand the study effort completed in Phase A, focusing on the baseline engine configuration selected. Analysis and trade studies were conducted to further optimize some of the major engine subsystems. These changes resulted in improvements to the baseline engine. Several options were evaluated for consideration by vehicle contractors.

CONTENTS

CONTENTS

CONTENTS

TABLES

TABLES

TABLES

FIGURES

FIGURES

FIGURES

FIGURES

ACRONYMS

ALS	Advanced Launch System
ASI	Augmented spark ignitor
CEI	Contract end item
CMS	Condition monitor system
DDD	Design definition document
EDM	electrical discharge machining
ELI	extra low interstitial
FASCOS	Flight acceleration safety cutoff system
FPL	Full power level
FSD	Full-Scale development
GG	Gas generator
GGFV	Gas generator fuel valve
GGOV	Gas generator oxidizer valve
GSE	General support equipment
HEE	Hydrogen embrittlement environment
HEV	Heat exchanger valve
HPFTP	High-pressure fuel turbopump
HPOTP	High-pressure oxygen turbopump
KSC	Kennedy Space Center
LCC	Life cycle cost
LEO	Low earth orbit
LOX	Liquid oxygen
LPFTP	Low-pressure fuel turbopump
LPOTP	Low-pressure oxygen turbopump
MCC	Main combustion chamber
MFV*	Main fuel valve
MOV	Main oxidizer valve
NASA	National Aeronautics and Space Administration
NPL	Nominal power level
NPSH	Net positive suction head
NPSP	Net positive suction pressure
OPF	Orbiter processing facility

SSME	Space Shuttle Main Engine
STBE	Space Transportation Booster Engine
STME	Space Transportation Main Engine
STS	Space Transportation System
TFU	Theoretical first unit
TVA	Thrust vector actuator
WBS	Work breakdown structure

1.0 INTRODUCTION

1.1 BACKGROUND

The Space Transportation Main Engine (STME) Configuration Study Plan for the Phase A' effort is designed to expand the study effort completed in Phase A. The Phase A' effort consisted of analyses and trade studies to further optimize the baseline gas generator (GG) engine selected. This engine is configured to operate with LO_2 and liquid hydrogen propellant in the main combustion chamber (MCC) and in the GG. Additionally, liquid hydrogen is used for MCC and nozzle cooling. The Phase A' program schedule and its relationship to Phase A is shown in Figure 1-1.

1.2 OBJECTIVES

The objective of the Phase A' Study effort was to further define the baseline engine selected during the Phase A Study and to evaluate issues and options that would enhance its low cost and high reliability attributes. The ultimate objective of this study is to expand on the development and study begun in Phase A.

1.3 SCOPE

The work for the Phase A' Study was divided into eight categories. These categories and their relationship to the Phase A Study are identified in Figure 1-1 and are as follows: Systems Analyses (Section 2.0), Turbomachinery Studies (Section 3.0), Combustion Devices Studies (Section 4.0), Control System Studies (Section 5.0), Start Transient Scope Analysis (Section 6.0), Launch Operations (Section 7.0), Producibility Studies (Section 8.0), and Cost Update (Section 9.0). These seven divisions of work entail the complete development effort of the STME.

A large portion of the STME Phase A' effort was devoted to the continued refinement of the GG cycle engine already developed during Phase A. Various

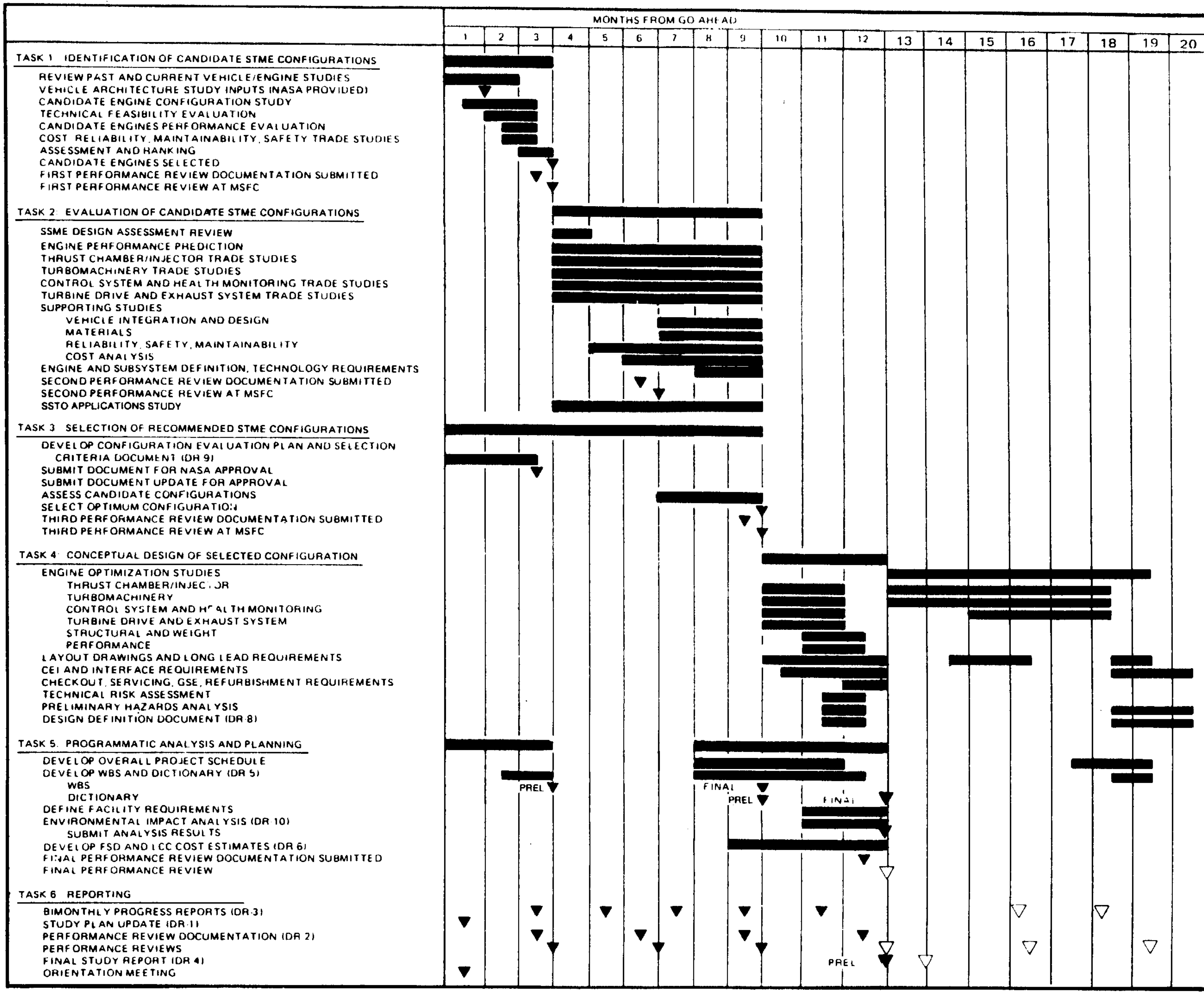

Figure 1-1. STME Program Schedule

implementations were incorporated into the design that would allow the engine to better reflect not only the engine mission and low-cost philosophy of Advanced Launch System (ALS), but also to better reflect actual flight data gathered from previous Rocketdyne engines such as the Space Shuttle Main Engine (SSME). The STME was further refined with the commonality study. Component design studies were conducted that addressed the idea of common use components on both the STME and its ALS counterpart, the Space Transportation Booster Engine (STBE). Additionally, the start transient model was updated to incorporate low cost, nonmodulating valves and a solid propellant GG start initiator.

The development of the STME was expanded during Phase A' with the definition, evaluation, and selection of a control system. The drivers in this study were the satisfaction of mission requirements and low cost.

The Phase A' effort also involved a number of studies that addressed low-cost issues. Launch operations were investigated with the intent of minimizing launch preparations and between flight maintenance, thus reducing costs and expediting the launch process. Further, a producibility study was pursued with the intent of easing the manufacture of the various STME components. This study reflects the recurring theme of STME development; i.e., reducing costs.

Finally, in keeping with the low-cost emphasis of ALS, a cost update was included. The cost update contains the complete projected costs of the STME, including the design, development, test, evaluation, production, and operations costs. Also included are studies that address the problem of reducing engine production costs.

2.0 SYSTEMS ANALYSES

2.1 INTRODUCTION

The Phase A' Systems Analyses effort sought to refine the baseline model and to begin to investigate cost versus performance tradeoffs. The baseline model was refined to better reflect actual operating conditions by incorporating parameters based on SSME flight data. Additionally, pump design characteristics were detailed and suction specific speed limits consistent with actual cavitation limits were established. Further, the Phase A' effort began to examine the varied trades associated with the low cost ALS design philosophy. Finally, various parametric studies were conducted to optimize chamber pressure and engine weight and size.

2.2 SUMMARY AND RESULTS

Several minor changes to the STME baseline engine balance were incorporated since the conclusion of the Phase A effort. Based on SSME flight data, the fuel and LO_2 inlet pressures were reduced. The minimum fuel inlet pressure was dropped from 30 to 24.5 psia and the LO_2 from 100 to 47 psia. In addition, the engine balance code was modified to include detailed modeling of the LO_2 boost pump. Also, a suction specific speed limit was set for the fuel pump consistent with the cavitation limits imposed by the lack of a boost pump. A summary of the pertinent baseline engine parameters as of the end of this report period is provided in Figure 2-1.

2.2.1 Performance Impacts

The STME differs from previous engines in that performance is not the primary design driver; low cost is the emphasis. Incorporated into the STME design are several features that enhance the low-cost aspects of the engine at the cost of performance. The following describes the impact of some of these features.

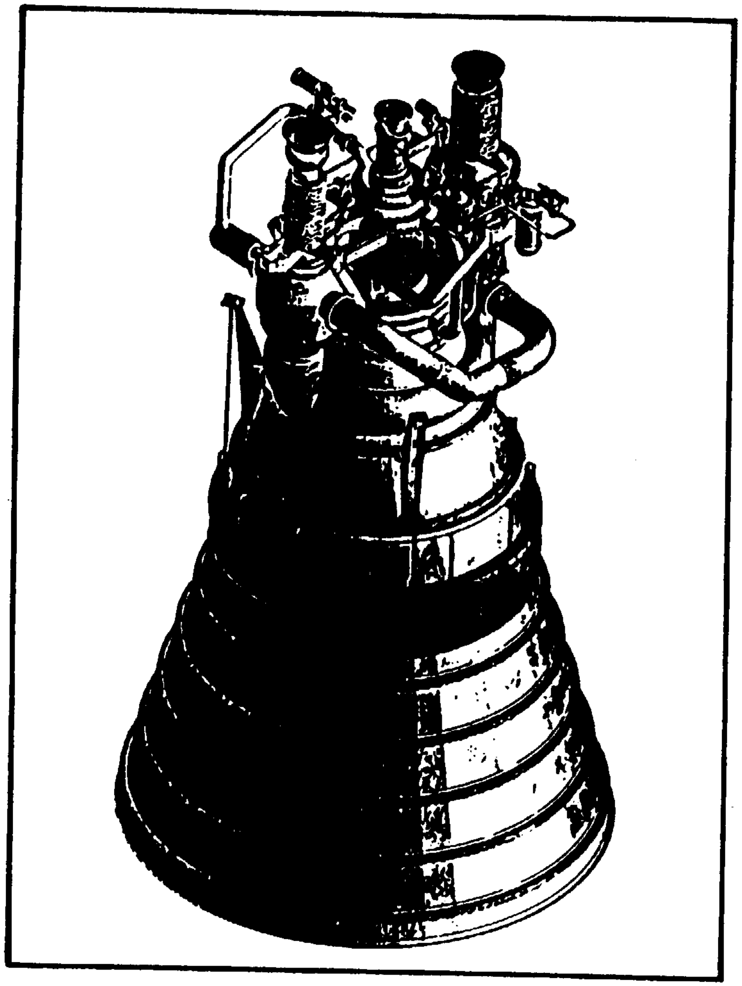

● Thrust (lb), Vac	
● Maximum	580,000
● Nominal	435,000
● Chamber pressure (psia)	
● Maximum	2,800
● Nominal	2,100
● Specific impulse(s), NPL	
● Vacuum	447
● Sea level	368
● Throttle range (% NPL)	80-133
● Weight (lb)	7,700
● Mixture ratio	6.0
● Area ratio	55/138
● Design life (missions)	100
● Gimbaling	
● Angle (deg)	±6
● Rate (rad/s^2)	10

Figure 2-1. Space Transportation Main Engine

87D-9-332B

The low cost conservative design philosophy of the STME is reflected in the nozzle selection. A retractable dual-bell contour nozzle was employed for reliability. If designed for maximum performance, an extendable/retractable Rao optimum contour nozzle would have been incorporated. Though this would have provided an increase in vacuum specific impulse of approximately 2.5 sec, it would require extension of the lower segment over the exhaust plume during ascent. This approach would entail additional technical risk.

In order to maximize reliability, durability, and low cost, a conservative fuel turbine inlet temperature of 1600°R was chosen. An increase in this temperature to 2000°R would provide an extra 2.3 sec of vacuum specific impulse but would compromise the conservative design.

In order to accommodate probable vehicle acceleration limits, the baseline engine has the capability to throttle down to 60% of the maximum thrust. If this throttling capability was reduced to only 75% of maximum thrust, an additional 0.1 sec of vacuum specific impulse could be realized. Conservative injector, valve, and system pressure drops were also incorporated to enhance stability and control and to provide thermal margins. If minimum pressure losses were used instead, the vacuum performance could have been improved by another 1.0 sec.

Finally, a low-cost injector design was employed, yielding a combustion efficiency of 99.0%. By increasing the number of injector elements, and consequently the cost, an additional 2.3 sec of vacuum impulse could be achieved.

The net impact of this conservative philosophy upon engine performance is approximately 8.0 sec. These design features are highlighted in Table 2-1.

The STME flow schematic and system layout are also provided in Figures 2-2 and 2-3 respectively.

Table 2-1. STME Features Low Cost Conservative Design

Baseline Engine	Engine Designed to Maximize Performance	Vacuum (ΔI_S, sec)
Retractable dual-bell contour nozzle to improve reliability	Extendable/retractable RAO optimum contour nozzle	+2.5
Turbine temperature = 1600° R for reliability, durability and low cost	Turbine inlet temperature = 2000° R	+2.3
Minimum thrust = 60% maximum thrust to accommodate probable acceleration limits	Minimum thrust = 75% thrust	+0.1
Conservative ΔP's to enhance stability, control and thermal margins	Minimum pressure losses	+1.0
η_C = 99% with low cost injector	Increase number of elements η_C = 99.5%	+2.3
	Total	~ 8
	Baseline Engine	447
	High performance engine	~455 sec

87D-9-2476

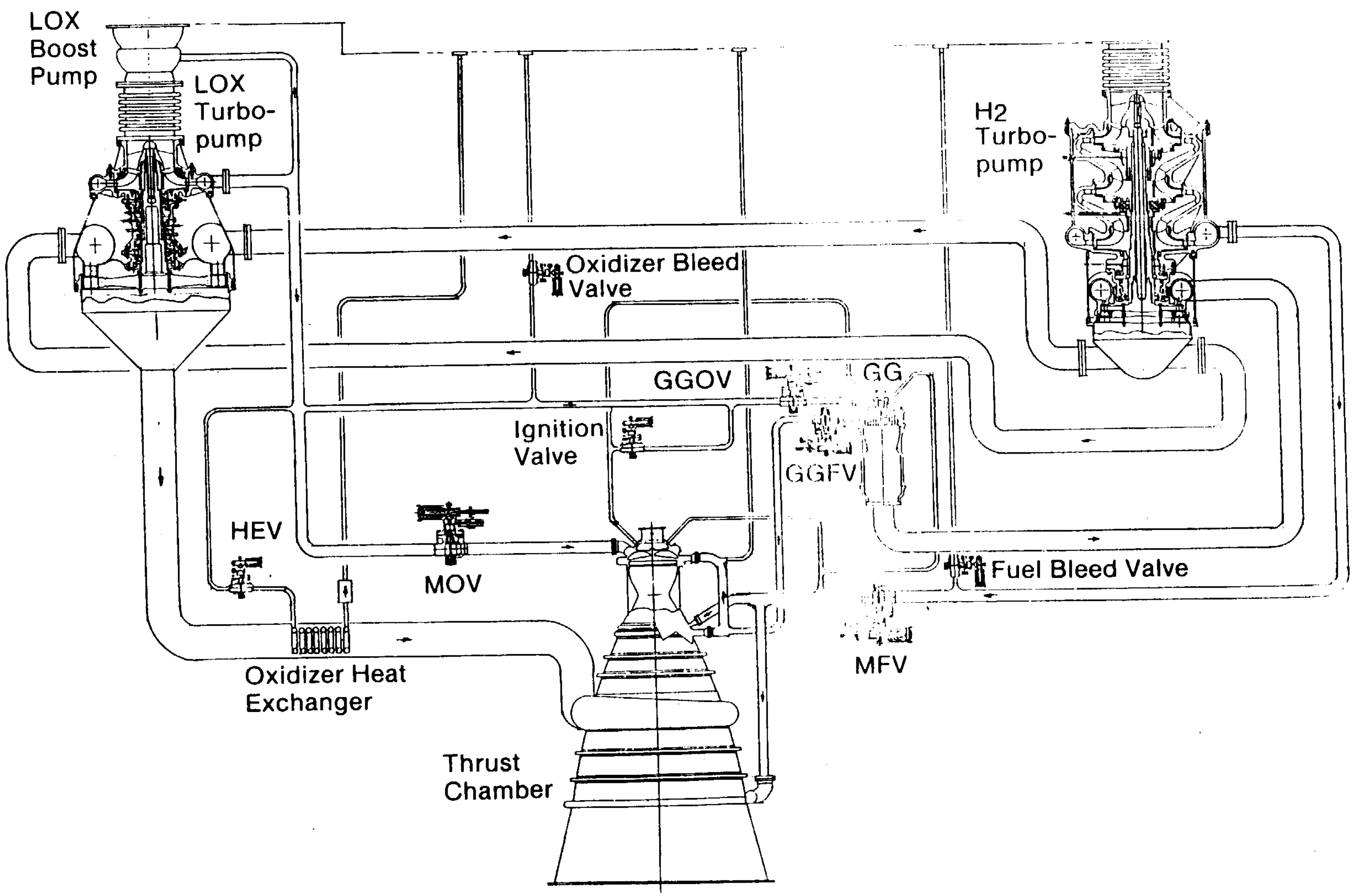

Figure 2-2. Baseline STME Flow Schematic

87D-9-2470A

ORIGINAL PAGE IS
OF POOR QUALITY

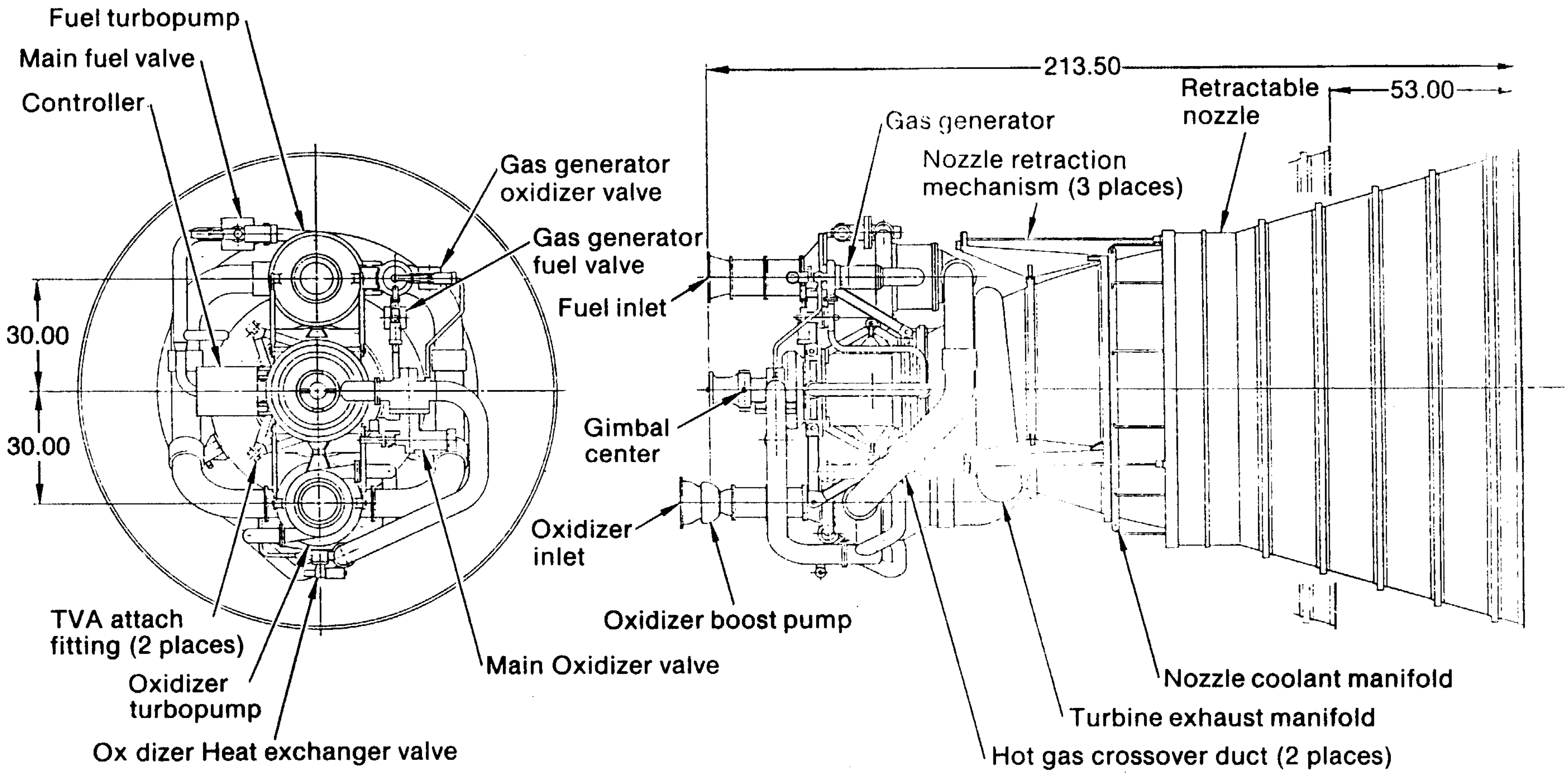

Figure 2-3. Baseline STME Layout

87D-9-2469A

2.2.2 Parametric Studies

The effects of chamber pressure upon engine envelope, weight, and performance were investigated at the 580 klbf thrust level. The pressures ranged from 2,500 to 3,000 psia. By increasing the chamber pressure to 500 psia, the nozzle exit diameter decreased only 0.5% while the engine length decreased 2.2%. These results are presented in Figure 2-4. The reason for the relatively minimal effect upon envelope is that, for this parametric scan, the nozzle exit pressure was held constant. Therefore, as the chamber pressure increases, a larger expansion ratio is required, resulting in a larger nozzle.

A plot of sea level and vacuum performance as a function of chamber pressure is presented in Figure 2-5 for both the nominal and full power levels. As can be seen, the maximum full power level vacuum specific impulse occurs at the baseline chamber pressure of 2,800 psia. The vacuum performance increases at the throttled nominal power level of 435 klbf, since the lower chamber pressures require less flow to power the turbines and therefore have fewer secondary losses. It should be noted that the performances plotted are for a fixed Rao optimum nozzle. Therefore, the vacuum values would have to be decreased by approximately 2.5 sec for a dual-bell configuration. The sea level specific impulses are for the large full area ratio nozzles and therefore are very low.

Finally, the effect of chamber pressure on engine weight is provided in Figure 2-6. The weight is decreasing with chamber pressure because the combustor size is decreasing. This effect is greater than the increase in turbomachinery weight in the pressure range investigated and therefore results in a net decrease.

The effect of vacuum thrust was also investigated parametrically. As would be expected, the engine envelope increases with thrust. This effect is presented in Figure 2-7 for a thrust range from 300 to 900 klbf. The engine weight also increases with thrust but in a linear fashion, as can be seen in

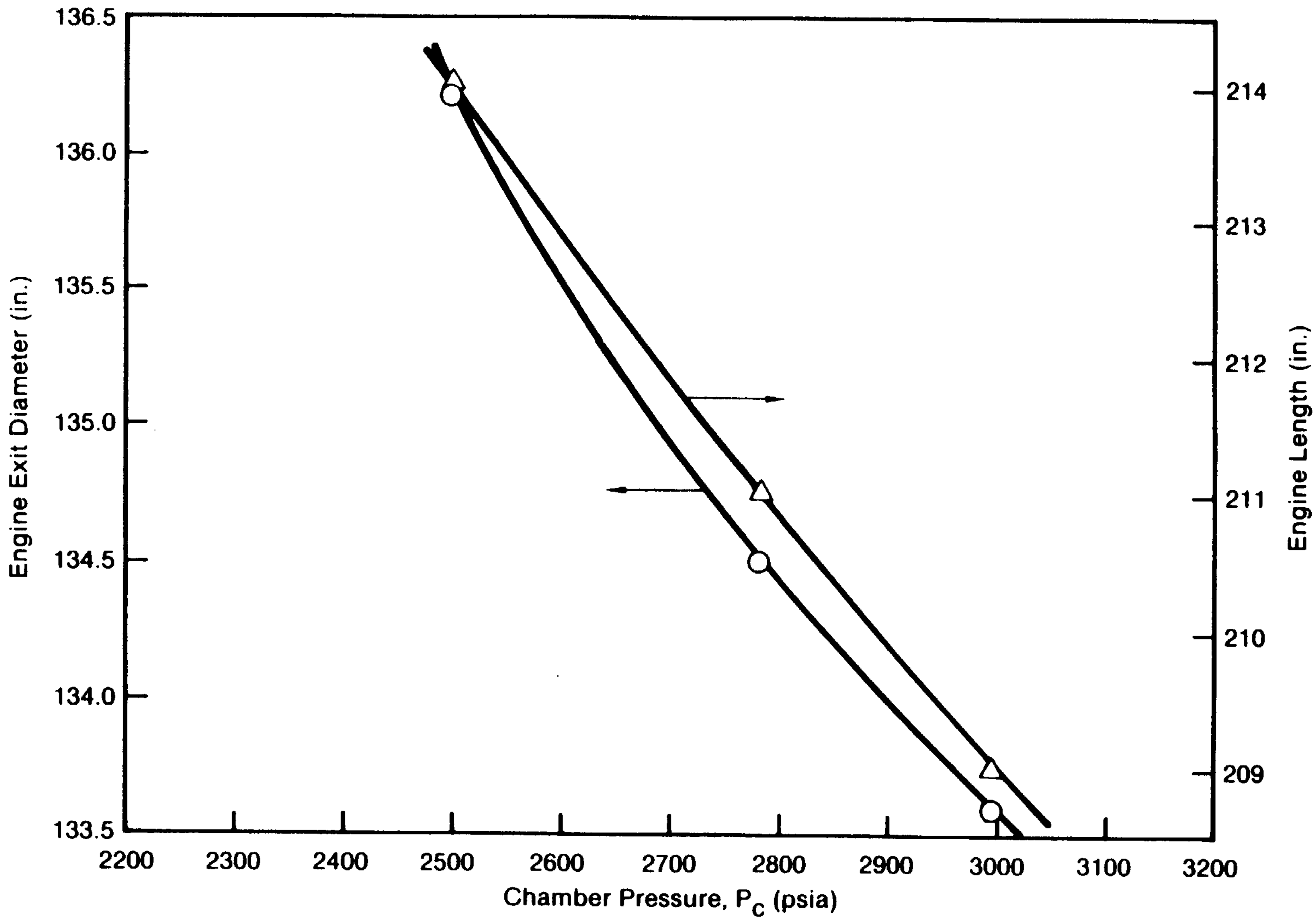

Figure 2-4. STME Geometry Parameters

87D-9-2486

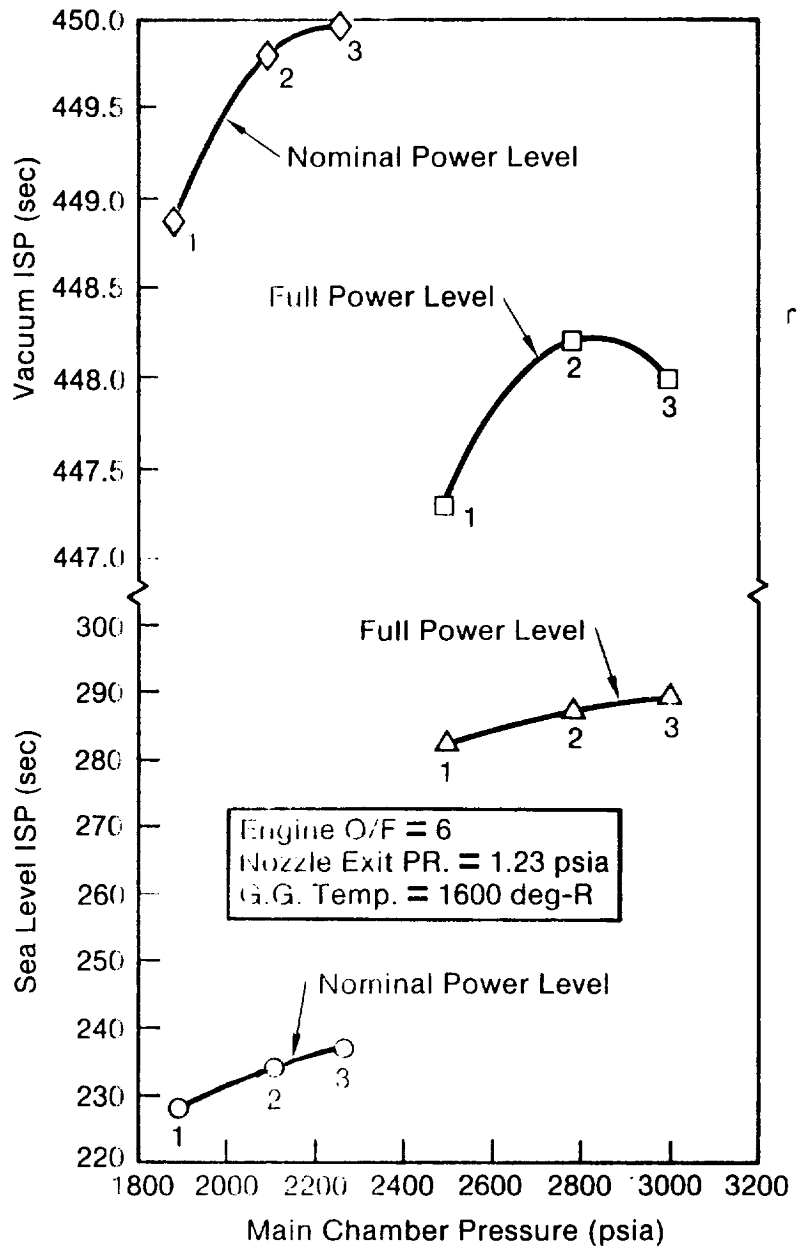

re

87D-9-2492

Figure 2-5. STME Performance versus Chamber Pressure

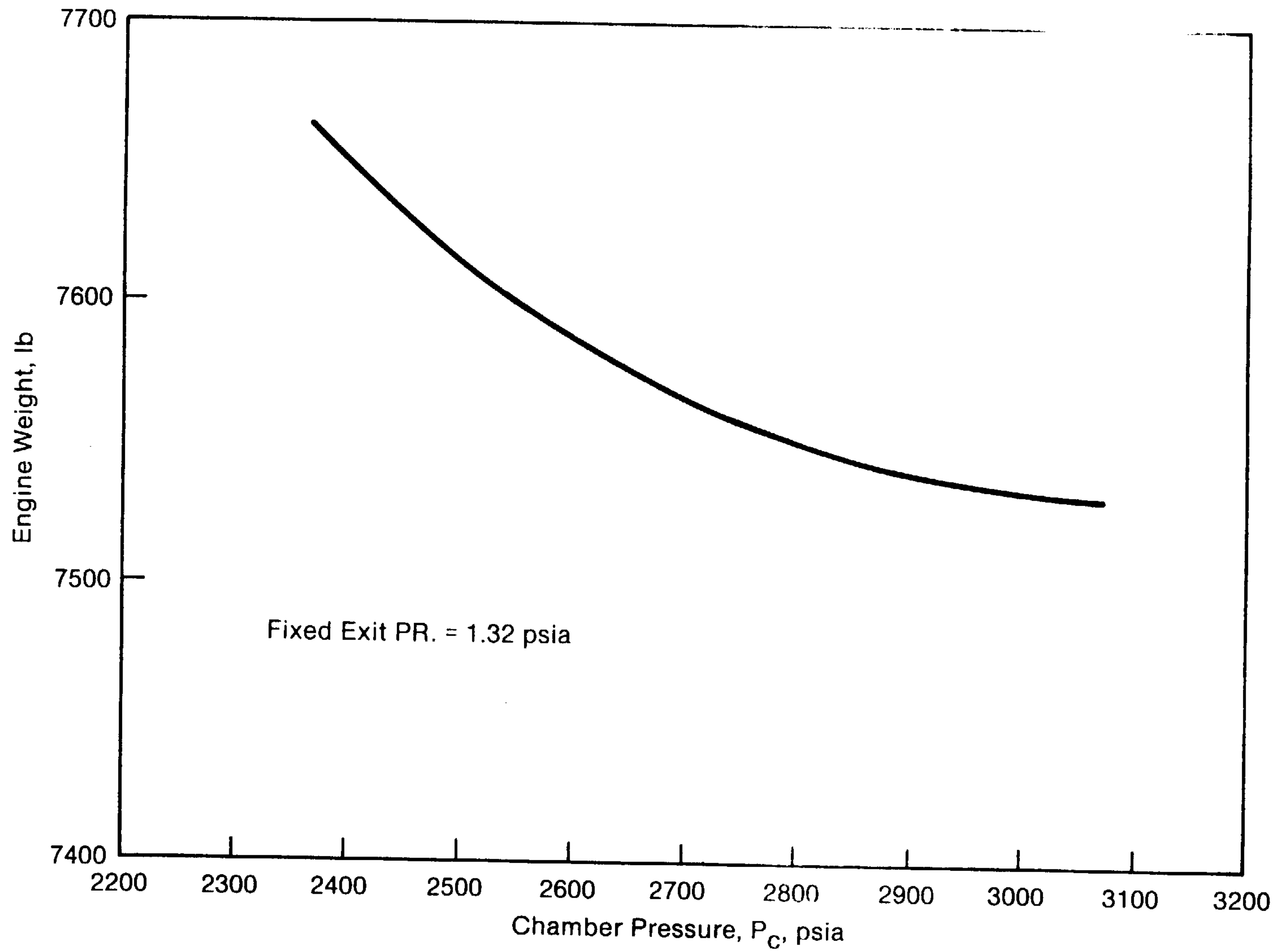

Figure 2-6. STME Engine Weight

87D-9-2493

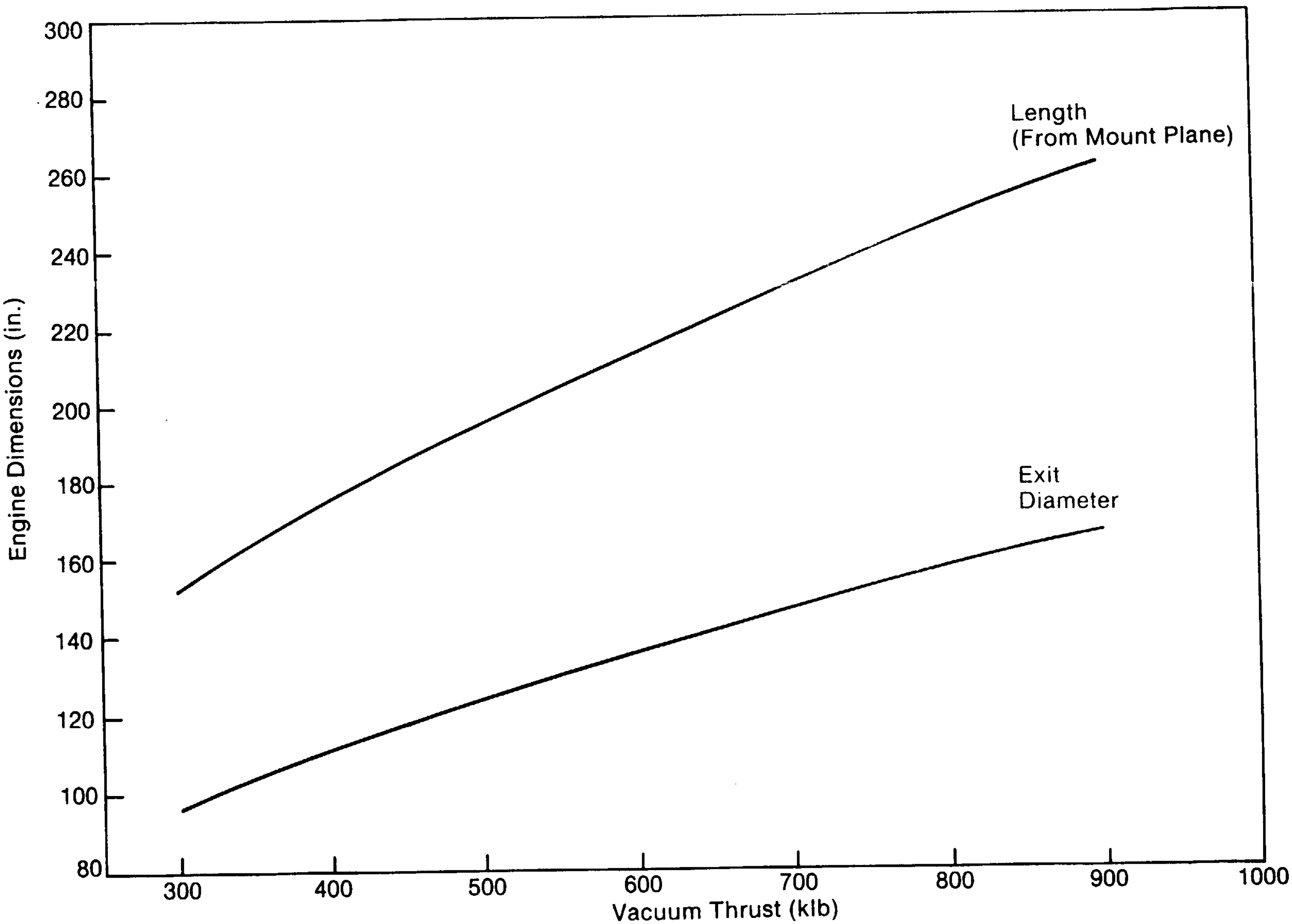

Figure 2-7. Engine Envelope versus Vacuum Thrust

87D-9-3215

Figure 2-8. Performance and optimum chamber pressure are only weak functions of the thrust level. These data are plotted in Figure 2-9.

2.2.3 Space Transportation Main Engine/Space Transportation Booster Engine Commonality

A major topic of study in the STME Phase A' effort was commonality. The commonality study is another facet of the ALS low-cost design philosophy. Commonality refers to the sharing, or "common" use, of components between the STME and its counterpart the STBE.

One approach investigated in the booster/main engine commonality effort was a common MCC. Three methods were analyzed: (1) optimum main engine combustor in a booster engine; (2) optimum booster engine combustor in a main engine; and (3) a common combustor, which is a compromise between both optimum main engine and optimum booster engine.

In the first approach, if the optimum main engine combustor at a chamber pressure of 2,800 psia and a vacuum thrust of 580 klbf was used in a booster engine at a vacuum thrust of 830 klbf, a booster engine chamber pressure of 4,200 psia would be required. This excessive pressure is required due to the smaller throat area of the optimum main engine.

In the converse approach, the optimum booster engine combustor at a chamber pressure of 3000 psia and vacuum thrust of 830 klbf was used in a main engine. At a vacuum thrust of 580 klbf, a main engine chamber pressure of only 2,040 psia is required. In this case, the low chamber pressure is due to the larger throat area of the optimum booster engine.

Finally, in a compromise between these two extremes, a chamber pressure of 3,600 psia was selected for the booster engine. If the MCC from this booster engine was used in a main engine at the 580 klbf vacuum thrust level, a chamber pressure of 2,450 psia is required in the main engine. A summary of

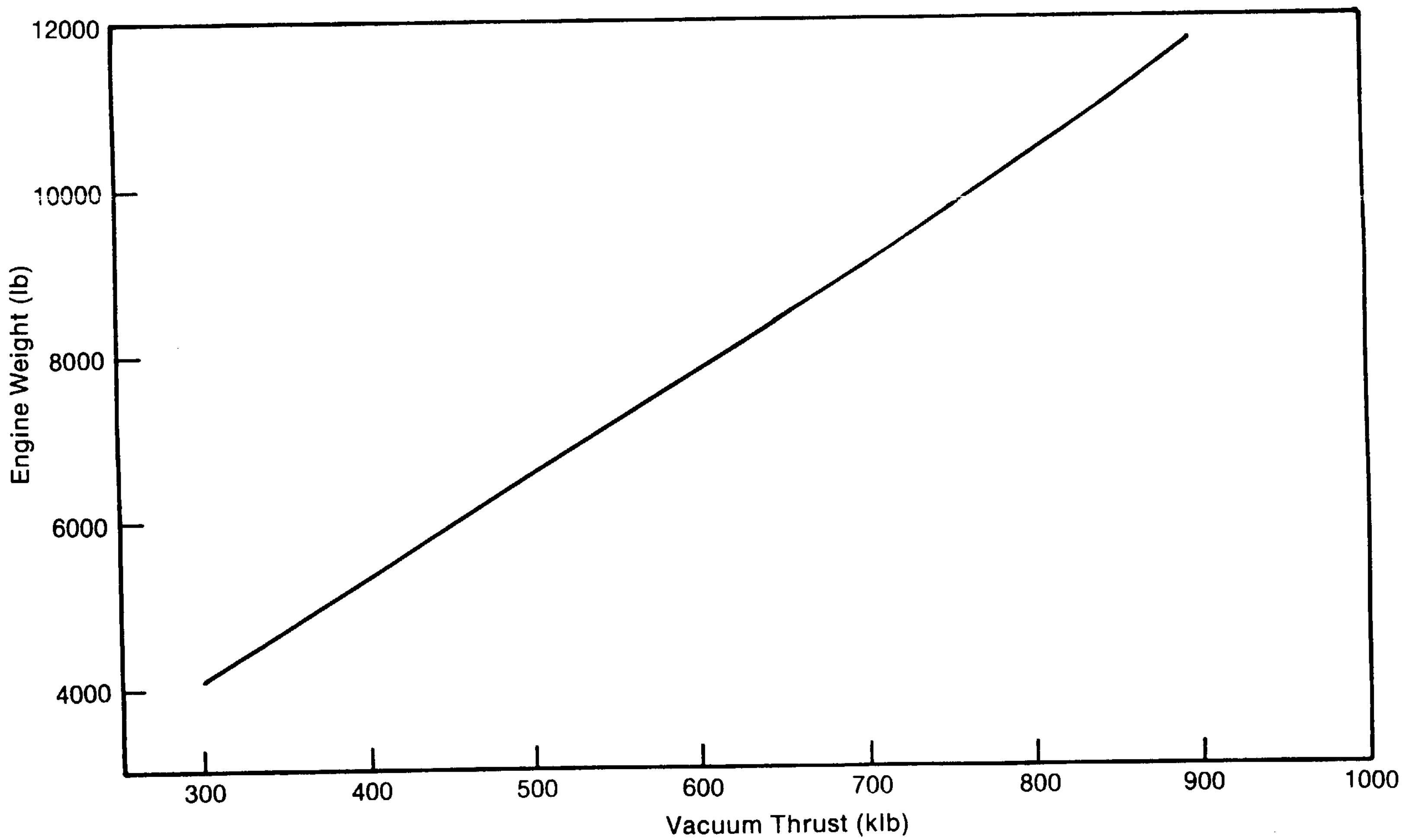

Figure 2-8. Engine Weight versus Vacuum Thrust

87D-9-3214

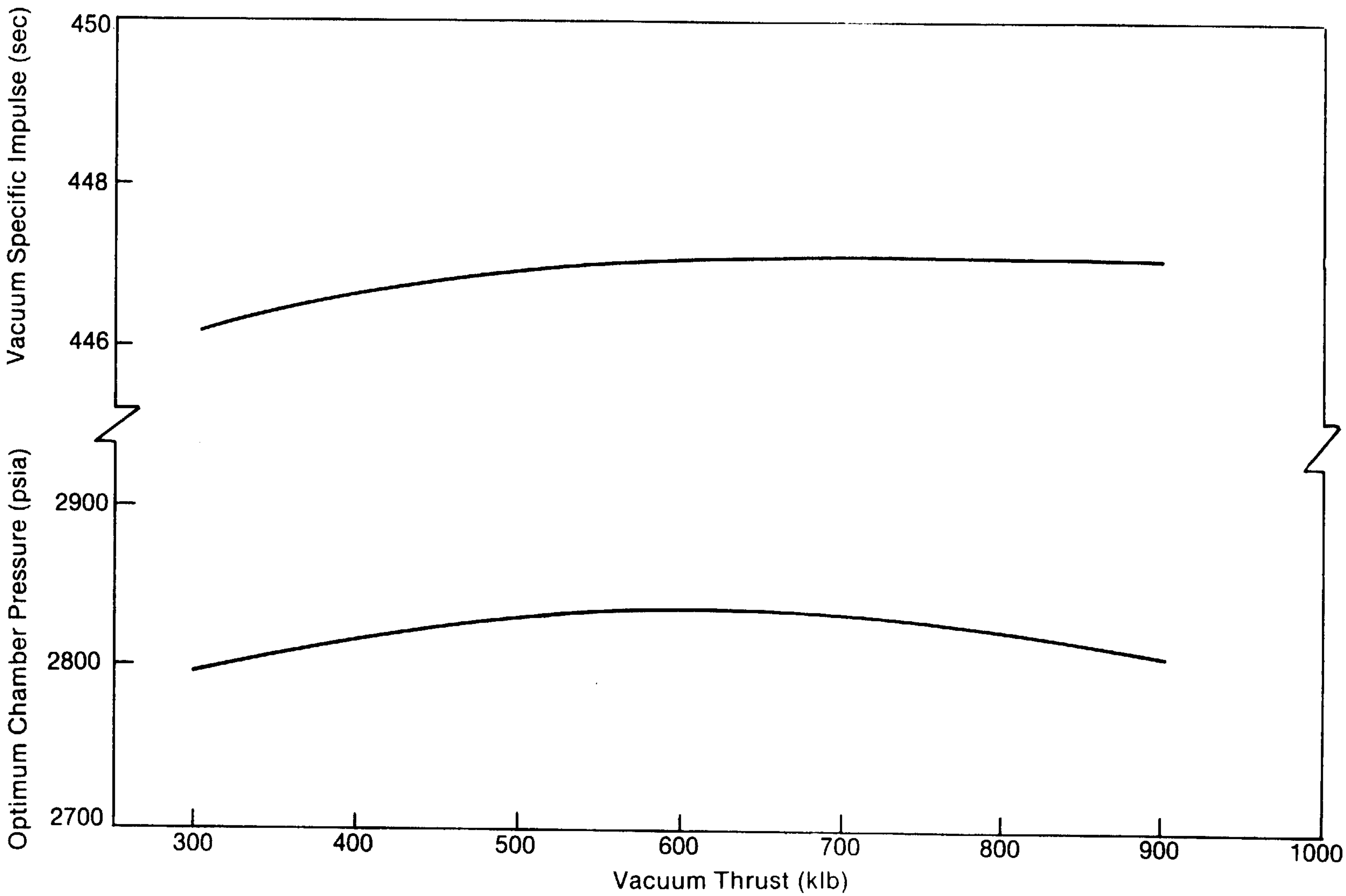

Figure 2-9. Engine Performance versus Vacuum Thrust

87D-9-3216

this commonality configuration evaluation, including the impact upon performance and engine weights, is presented in Table 2-2.

Based on this same philosophy of combustion chamber commonality, a more general analysis was conducted in which the thrust levels of the engines were allowed to vary. In this manner, a wide range of combinations of chamber pressures are achievable. This effort is summarized in Figure 2-10. The baseline commonality case described above with a main engine chamber pressure of 2,450 psia and a booster engine chamber pressure of 3,600 psia is highlighted in Figure 2-10.

Another option investigated under the commonality effort was to take an optimized booster engine tripropellant engine and, with minimal changes, run it in an off-design mode as a main engine. In order to accomplish this, the methane pump must be replaced with a new liquid hydrogen pump since the operating conditions are so dissimilar. Additional changes in turbomachinery include the replacement of the LO_2 pump inducer and impeller and the changeout of the nozzles in the hydrogen and oxygen turbines. Pressure drops in the injectors must also be adjusted for stability requirements and therefore will require the replacement of face nuts. Finally, a nozzle extension would be added to achieve the expansion required for main engine operation.

The resulting chamber pressure at the 580 klbf thrust level is 2,420 psia. The penalty in performance for this level of commonality is 6 sec of vacuum specific impulse relative to the baseline main engine. In addition, a weight increase of 1,470 lb is also necessary. A summary of this effort is presented in Table 2-3.

5349e/crp

Table 2-2. Commonality Configuration Evaluation Summary

	STME			STBE		
Thrust (vac, klb)	580	580	580	830	830	830
P_c (psia)	2800	2040	2450	3000	4200	3600
Δ I_{sp} (vac, sec)	0	-3.0	-2.0	0	—	+2.0
Δ Weight (lb)	0	+230	+60	0	+	+
Combustion devices	Optimum	STBE	Common	Optimum	STME	Common

87D 9-3165

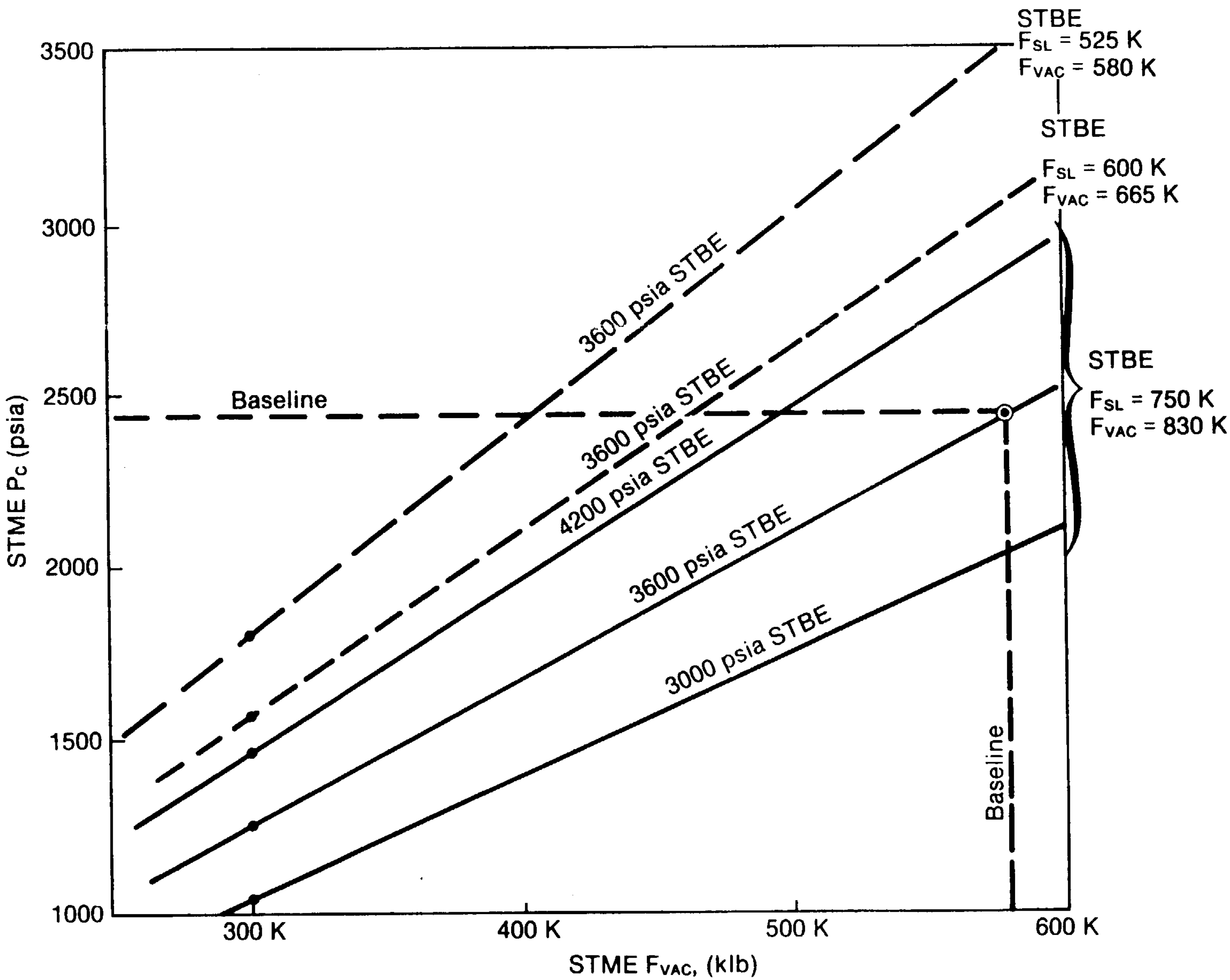

Figure 2-10. STBE/STME Commonality

87D-9-3192A

Table 2-3. STME/STBE Commonality Option

- **STME derived from 3600 psia Pc STBE (tripropellant) with minimal changes**
    - Replace CH_4 turbopump with LH_2 turbopump
    - Replace nozzles in STBE H_2 and O_2 turbopump turbines
    - Replace LOX pump inducer/impeller
    - Change injectors facenuts
    - Add nozzle extension
- **Resulting STME characteristics**
    - 2420 psia P_c at 580 K thrust
    - I_{sp} loss - 6 sec (1.3%)
    - Weight gain - 1470 lb (13%)

87D-9-3044A
220

3.0 TURBOMACHINERY STUDIES

3.1 INTRODUCTION

The turbomachinery objectives for this report period were to characterize the turbomachinery requirements of the STME, develop preliminary conceptual layouts of the analyzed turbopumps, identify potential technology drivers to the designs, and conduct trade studies in areas of low cost and producibility and of component commonality between STBE and STME turbopumps for reduced costs. At the conclusion of this report period, the baseline designs of the turbomachinery had been defined based on the ground rules previously stated for a reusable engine system. The turbopump component size had been characterized and a set of general conceptual layouts for each turbopump had been completed. With the general rotor definition available, preliminary rotordynamic analysis was completed and turbopump characteristics have been defined to support engine start model studies. A general evaluation of the turbomachinery material requirements and reviews of the low cost/producibility issues in the baseline designs have been addressed. The baseline designs used in these studies were invaluable in that they provided a basic frame of reference for comparative purposes. These turbopumps were conceptually designed in the baseline study. Positioning of the turbopumps in the engine schematic is shown in Figure 3-1. This includes the main hydrogen and oxygen turbopumps and the oxygen boost turbopump. The hydrogen main turbopump shown operates without a boost pump. The results of this effort will be presented in this section.

3.2 SUMMARY

3.2.1 Approach

Turbopump structural/mechanical constraints were determined earlier in the study. Hydrodynamic and aerodynamic design parameter criteria were established to ensure that the objectives of achieving highly reliable turbomachinery component designs were met. The ground rules were first implemented in

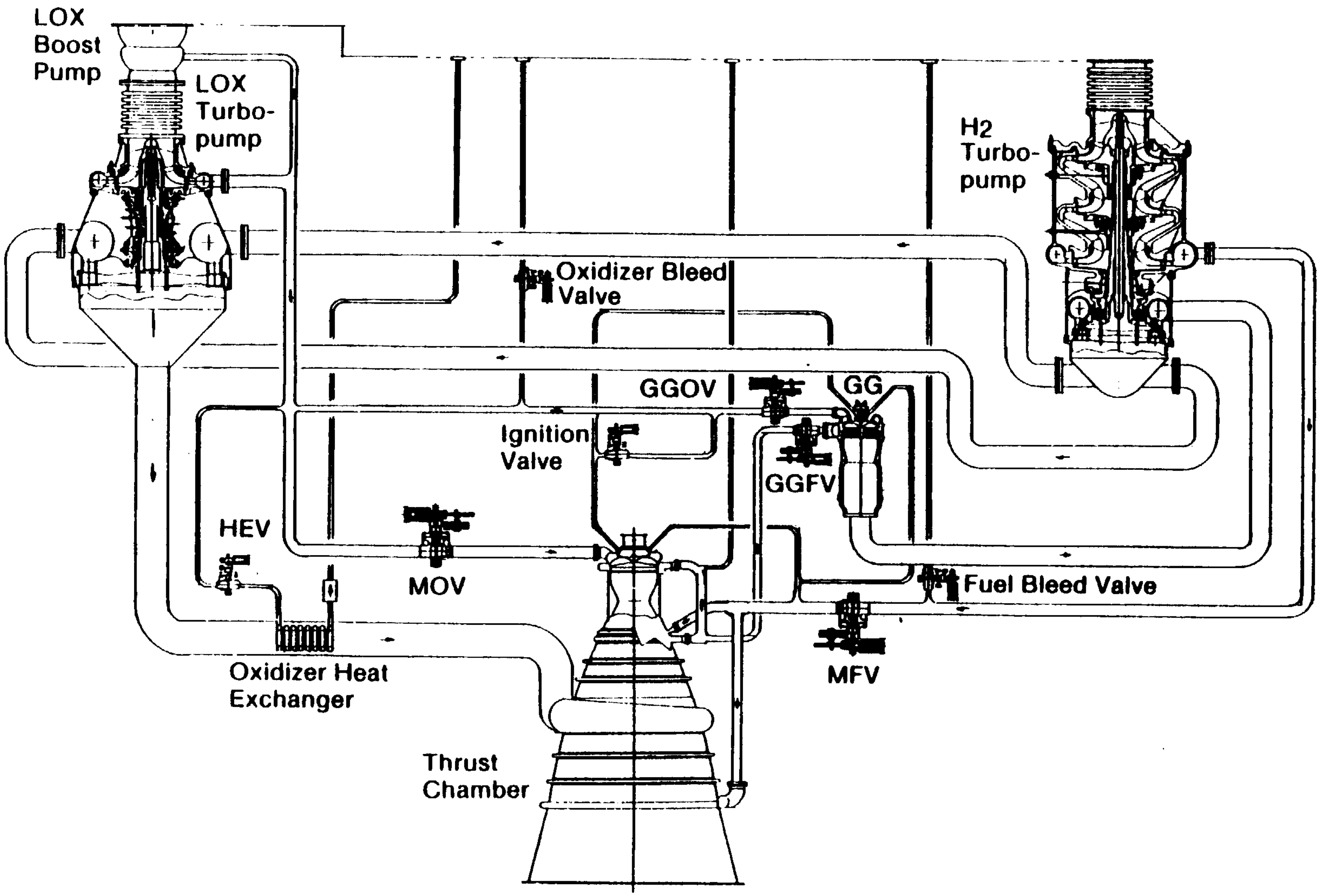

87D-9-2470A

Figure 3-1. Baseline STME Flow Schematic the preliminary engine balance development effort and continued to be incorporated into the detailed designs as they progressed through hydrodynamic and aerodynamic analysis and turbopump sizing. These criteria set adequate net pump suction head (NPSH) margins for the main LO_2 and hydrogen pumps and the LO_2 boost pump. They also defined maximum suction specific speed limits for main pump impellers, head and flow coefficient ranges, and maximum impeller eye-to-tip ratios to ensure efficient operation, good suction performance, and high reliability over the pump operating range.

General turbopump structural/mechanical constraints are set to provide high reliability turbomachinery designs with adequate structural margins for long life and durability. The criteria utilizes values that are considered current technology levels and are based on Rocketdyne's considerable rocket engine experience and other industry data.

Turbine inlet temperature and tip speed limits were defined so as to maintain conservative margins of operation within the turbine similar to those provided in the pumping elements. Recognizing that turbine blade speed and maximum inlet gas temperature are major drivers in mechanical/structural integrity as well as materials costs in the turbine, limit values of these parameters were set at 1,550 ft/s mean blade speed and 1,600°R maximum gas generator supplied inlet gas temperature. These upper limit values are well within the current technology. In addition to this, other sizing and cost considerations were utilized in the design to reduce the operating values to well below their allowable limits.

3.2.2 Pump Sizing Approach

Rocketdyne's preliminary analysis programs (INDANA and CPLOSS) were used to refine the original sizing performed during the Phase A contract, set inlet and discharge blade angles, and generate H-Q and efficiency curves for each of the pumps. These programs use one-dimensional loss analyses to calculate the magnitudes of the various loss contributions (e.g., friction, incidence, diffusion, etc.) and sum these to calculate a pump head and efficiency. Both axial and volute discharge boost pumps were considered to assess the effect of the different configurations and to accommodate the various candidate engine ducting configurations.

The parameters required to size the pumps were taken from the updated engine balances and are listed in Table 3-1. The single-point 580,000 thrust engine balance was used since the pumps' maximum operating suction specific speeds were at this thrust level and it was necessary to ensure adequate NPSH margin for this condition. The ground rules used for the preliminary design were the same as for the Phase A contract and are listed in Tables 3-2 and 3-3.

Discharge pressure requirements for the boost pumps were set to ensure adequate NPSH margins for the main pumps. Realistic ducting losses based on SSME experience were used to ensure accurate modeling of the overall pump system. Hydraulic turbines using flow recirculated from the main pump discharge were assumed for the boost pump turbine and the main pump inlet flows were adjusted accordingly. The main pump and boost pump operating points for the configurations with boost pumps were set using an iterative process that analyzed the overall pump system and optimized main pump speed.

3.2.3 Turbine Sizing Approach

Turbines were sized for the STME turbopump. A propellant flow schematic for the engine is shown in Figure 3-1. The following turbines are summarized in this report:

- STME LO_2 main turbopump turbine
- STME LH_2 main turbopump turbine
- STME LO_2 boost turbopump turbine.

The main turbines are driven by LO_2-LH_2 combustion products while the LO_2 boost turbine is driven by LO_2 tapped off from the main pump discharge. The turbines for the main pumps were sized with the Rocketdyne GASPATH program. A program for hydraulic turbines that was developed for the low-pressure oxygen pump turbines on the SSME was used for the STME LO_2 boost

Table 3-1. Engine Balance Requirements

	BASELINE ENGINE (P_C = 2689 PSI)		COMMON MCC (P_C = 2464 PSI)	
	LOX	HYDROGEN	LOX	HYDROGEN
FLOWRATE, GPM	6996	18881	7156	18850
INLET PRESSURE, PSIA	47	24.5	47	24.5
DISCHARGE PRESSURE, PSIA	4189	4544	3672	4201

Table 3-2. Pump Hydrodynamic Design Parameters

NPSH MARGIN FOR BOOST PUMP OR MAIN PUMP ALONE	20%
NPSH MARGIN FOR MAIN PUMP FOLLOWING BOOST PUMP	100%
MAXIMUM SUCTION SPECIFIC SPEED FOR IMPELLER FOLLOWING INDUCER	5000
INDUCER FLOW COEFFICIENT	0.05 TO 0.3
IMPELLER FLOW COEFFICIENT	0.14 TO 0.36
INDUCER HEAD COEFFICIENT	0.15 TO 0.25
IMPELLER HEAD COEFFICIENT	0.4 TO 0.5 LOX 0.45 TO 0.55 FUEL, LH_2
MAXIMUM IMPELLER EYE-TO-TIP DIAMETER RATIO	0.75

Table 3-3. Pump Structural/Mechanical Constraints

MAXIMUM IMPELLER TIP SPEED, FT/SEC-LOX	900
LCH_4	1490
LH_2	2000
MAXIMUM INDUCER TIP SPEED, FT/SEC-LOX	500
LCH_4	830
LH_2	1110
MINIMUM ROLLING ELEMENT BEARING SIZE, MM	20
MAXIMUM BEARING DN, MM RPM, DIA 30 MM	$2x10^6$
DIA 30 MM	$1.5x10^6$
MAXIMUM NUMBER OF IMPELLERS ON A SHAFT	3

turbine. To support development of a low-cost design, turbine sizing was performed for common turbines for the STME and STBE turbopumps.

3.2.4 Turbopump Conceptual Layout Design

Hydrodynamic and aerodynamic sizing of the baseline turbomachinery and several alternative designs were completed during this report period. This sizing and analysis exercise provided performance verification data for the engine system balance as well as basic sizing data for the preliminary conceptual layout. The preliminary conceptual layout of the baseline turbomachinery has been completed. These baseline layouts provided a reference base from which alternative design studies for improved reliability and reduced cost could be addressed and from which commonality issues could be determined.

3.2.5 Turbopump Commonality Studies

During the Phase A' contract, preliminary optimized pump sizing was performed. The issue of pump commonality between the STME LO_2 pump and the pumps on the STBE tri-propellant engine was addressed, and the use of the SSME high-pressure fuel turbopump (HPFTP) for the STME LH_2 pump was investigated.

3.2.6 Turbopump Rotordynamic Analysis and Approach

Rotordynamic considerations often play a key role in the design of rocket-engine turbomachinery. Rocketdyne integrates rotordynamics analysis throughout the design and development process, from conceptual layouts through detail design, fabrication, and test. STME turbopump designs have been evaluated to determine potential rotordynamic problem areas and identify technology and development risk issues for consideration in subsequent phases of STME development.

Undamped critical speeds for the STME main LO_2 pump, main hydrogen pump, and LO_2 boost pumps have been analytically determined and compared to the applicable design guidelines. The LO_2 boost pump operates below its first critical speed and is rotordynamically acceptable. The main LO_2 and main hydrogen pumps operate between their first and second critical speeds and can be made to meet the design criteria with additional refinement. Several candidate designs were evaluated during this phase of the program. The resulting final configurations have been designated as the baseline turbopump designs for future phases of the program.

Undamped critical speeds for STME turbopumps were determined using an in-house finite-element program. Bearings and seals have been represented with linear springs to ground at the applicable locations. Bearing and seal stiffness estimates were provided by the Mechanical Elements group based on inputs provided them from the design function. Hydrostatic bearing stiffness is derived from turbopump discharge pressure; thus, bearing stiffness is defined and implemented in a speed-dependent manner. Values from 0% to 50% of the pump pressure rise are utilized as the range of hydrostatic bearing pressure differentials for this study.

Damping effects and cross-coupled stiffness effects have not been accounted for in this analysis. These effects, along with unbalanced response predictions and nonlinear boundary condition simulations, will be conducted in subsequent phases of the STME program as the turbopump designs mature. The approach taken in this analysis allows enough depth to identify rotordynamic issues that would impact turbopump design.

Rotordynamic margin requirements have been determined in the "Rocketdyne Task Support Policy." In summary, this policy requires steady-state operation within 20% of a critical speed should be avoided to prevent high-amplitude resonant vibration. At this early phase of the design process, rotordynamic stability issues are addressed by raising all natural frequencies above 50% of operating speed. This design practice precludes half-speed instability and greatly reduces development risk. A complete stability and response analysis will be completed for each turbopump as the designs mature. If these analyses indicate that sufficient damping is present (i.e., if the log-decrement stability parameter is greater than 0.2), then relaxation of the 20% margin rule is allowed by the referenced policy.

The rotordynamic outlook for the baseline STME turbopumps is very good for this early phase of the program. LO_2 boost pump design is rotordynamically acceptable as currently configured. The main LO_2 pump and main hydrogen pump will conform to rotordynamic margin requirements with the additional design refinements described herein.

Any changes to STME turbopump designs must continue to be reviewed for potential rotordynamic issues to ensure that adequate margins are designed into the baseline configurations. As the STME program matures, more in-depth analyses will be required, including damped critical speed and stability analyses, unbalanced response predictions, and nonlinear boundary condition simulations. Turbopump housing dynamics will also require review before full-scale development can be completed. Housing backup stiffness will be incorporated into the analysis in the next review period. As housing designs develop, the backup stiffness requirements and dynamic impact will be closely analyzed.

Accurate predictions of hydrostatic bearing and wear-ring seal coefficients are vital to meaningful rotordynamic analyses of STME turbopumps. In-depth review of these parameters is planned early in future phases of the STME program. Similarly, rotordynamic evaluation of subsequent design iterations will include damping and cross-coupled stiffness analysis for a more complete definition of their effects on critical speeds and stability.

3.3 OXYGEN TURBOPUMP

3.3.1 Main Oxygen Pump

The conceptual layout of the main LO_2 turbopump is given in Figure 3-2. Performance predictions, geometry, and hydrodynamic design parameters for the LO_2 main pump are presented in Figures 3-3 and 3-4 and Tables 3-4 through 3-6. The pump is a single-entry, single-stage centrifugal pump with an inducer upstream of the impeller to maximize suction performance. A vaned diffuser and double-discharge volute minimize the hydrodynamically generated radial loads on the rotor.

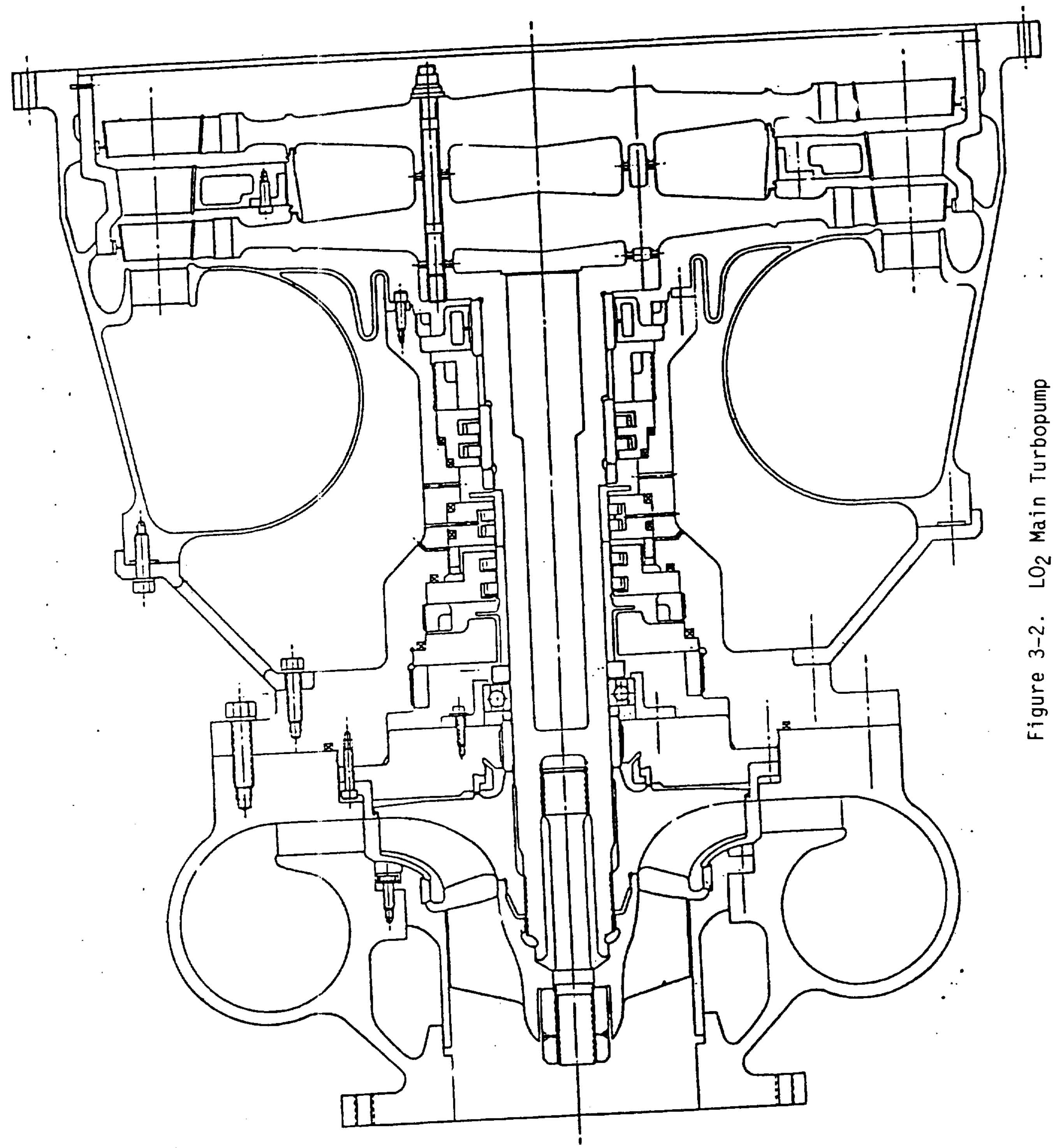

Figure 3-2. LO_2 Main Turbopump

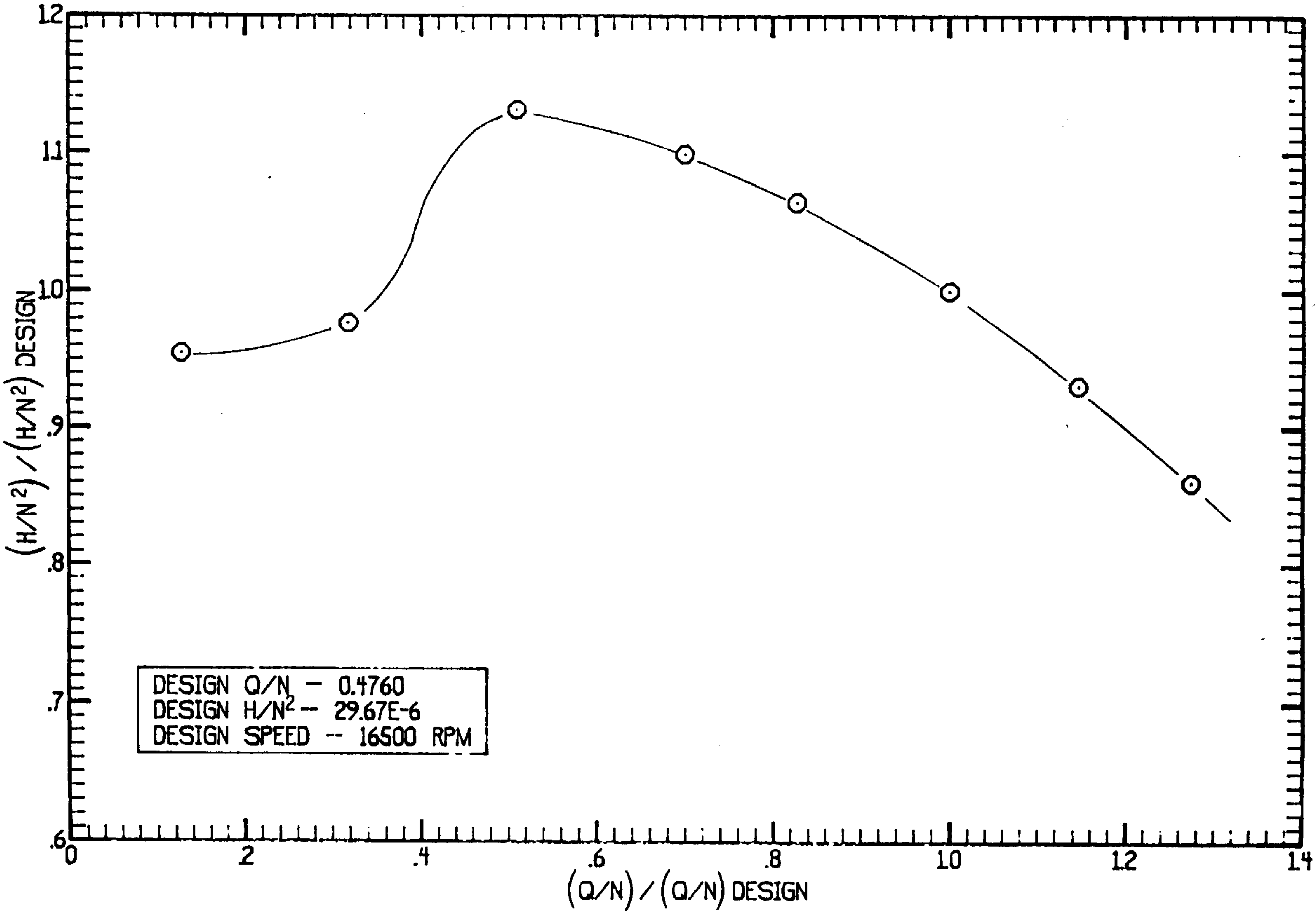

Figure 3-3. STME Main Oxygen Pump--Pump Performance

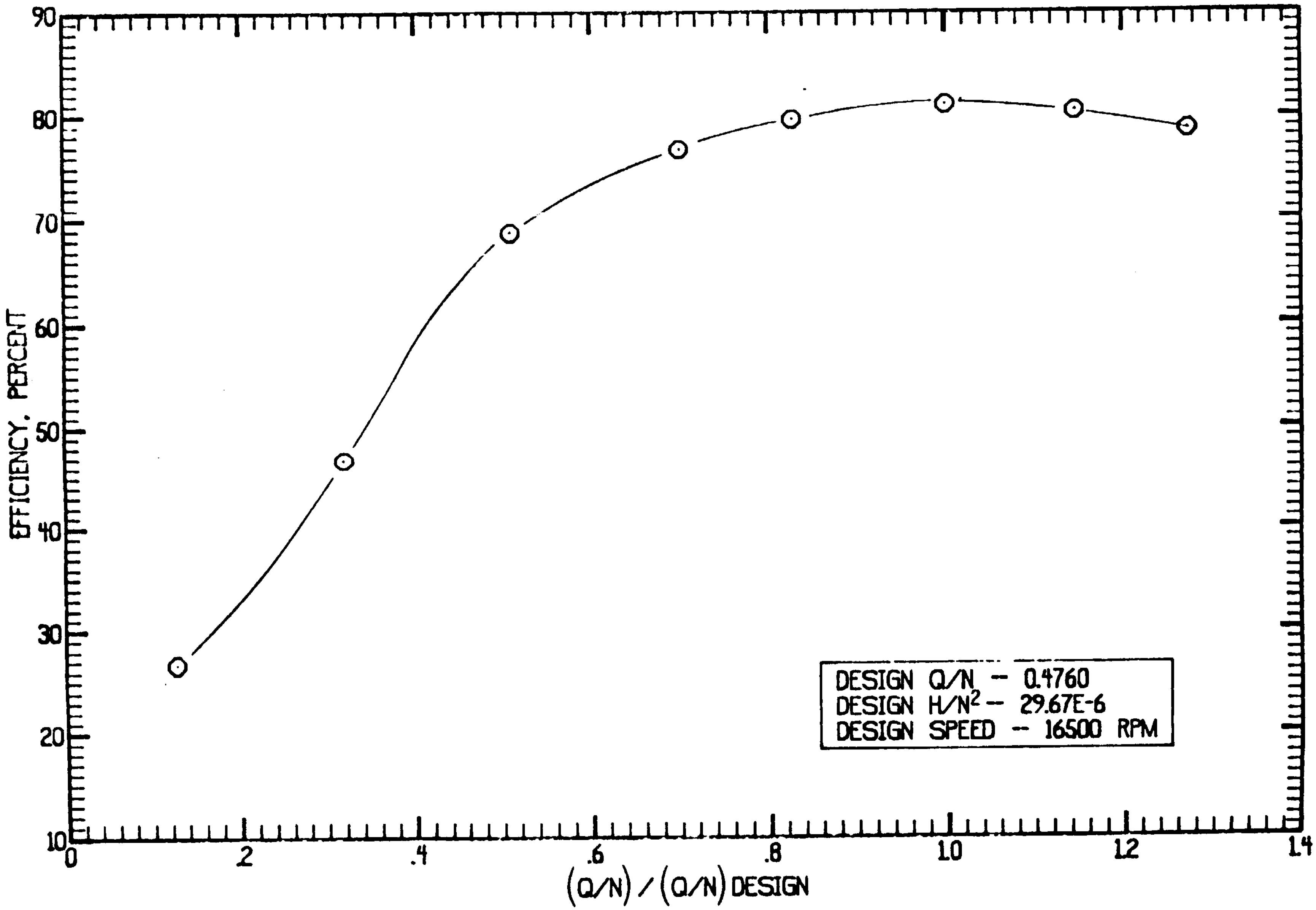

Figure 3-4. STME Main Oxygen Pump--Pump Performance

Table 3-4. LO_2 Main Design Conditions

PUMP TYPE	SINGLE STAGE CENTRIFUGAL
INLET FLOWRATE, GPM	7854.3
HEAD, FT	8077
SPEED, RPM	16500
EFFICIENCY	81
REQUIRED SHAFT POWER, HP	22595
TURBOPUMP WEIGHT, LB	721
MINIMUM INLET NPSH, FT	542
DISCHARGE PRESSURE, PSIA	4188.6
STAGE SPECIFIC SPEED	1716
MAX. OPERATING SUCTION SPECIFIC SPEED	13025
BOOST PUMP TURBINE RECIRC. FLOW	1053
BEARING DN, 10^6 MM RPM	1.14
SEAL RUBBING SPEED, FPS	245

Table 3-5. LO_2 Main Pump Geometry

INDUCER:		VOLUTE:	
TIP DIAMETER, INCH	6.945	TYPE	DOUBLE SCROLL
INLET HUB DIAMETER, INCH	2.78	AREA, INCH	7.82 (EACH SIDE)
DISCHARGE HUB DIAMETER, INCH	4.0	DIAMETER, INCH	19.2
INLET HUB TO TIP RATIO	0.4		
AXIAL LENGTH, INCH	1.87		
IMPELLER:		DISCHARGE DUCT:	
TIP DIAMETER, INCH	10.56	DIAMETER, INCH	4.0
TIP WIDTH, INCH	0.927		
EYE DIAMETER, INCH	7.1		
HUB DIAMETER, INCH	4.0		
DIFFUSER:			
INLET DIAMETER, INCH	11.4		
DISCHARGE DIAMETER, INCH	16.3		

Table 3-6. LO_2 Main Pump Hydrodynamic Design Parameters

	INDUCER	DIFFUSER	IMPELLER
INLET FLOW COEFFICIENT	.14		.182
DISCHARGE FLOW COEFFICIENT	.199		.123
HEAD COEFFICIENT	0.197		.45
TIP SPEED, FT/SEC	500		760
NO OF BLADES	4		7
TIP SOLIDITY	1.5		1.3
INLET BLADE ANGLE, DEG	14		25
INCIDENCE, DEG	2.2		2.2
DISCHARGE BLADE ANGLE, DEG	24		30
DEVIATION, DEG	2.2		13.3
RMS D-FACTOR	.40		
		DIFFUSER	
NO. OF BLADES		12	
THROAT ASPECT RATIO		.863	
LENGTH/THROAT WIDTH RATIO		3.45	
INLET BLADE ANGLE, DEG		13.1	
INCIDENCE, DEG		0.1	
DISCHARGE FLOW ANGLE, DEG		37.5	
VELOCITY RATIO		.71	
		VOLUTE	
DISCHARGE VELOCITY, FT/SEC		161	

3.3.2 Main Oxygen Turbine

Figure 3-5 shows the configuration with dimensions of the LO_2 main turbopump. The turbine is a two-row pressure compounded design. Table 3-7 presents the basic turbine design parameters, and Table 3-8 describes the turbine geometry. Turbine power is split equally between the two stages. For this initial turbine sizing, turbopump envelope was not a significant constraint, allowing a large enough diameter to achieve a reasonable efficiency of 83.7%. The velocity ratio, stage reactions, stage-loading coefficients, and Zwiefel coefficients are all within comfortable ranges. The blade dimensions and aspect ratios are reasonable and within Rocketdyne's design experience. Table 3-9 summarized the parameters along the hot-gas flow path through the turbine. Figures 3-6, 3-7, and 3-8 present the predicted performance of this turbine. Figure 3-6 shows the predicted efficiency as a function of velocity ratio for a range of shaft speeds with the design point selected in a relatively flat region near the peak of the efficiency curve. Figures 3-7 and 3-8 summarize the variation in turbine flow parameter as a function of pressure ratio and as a function of velocity ratio for a series of shaft rotating speeds.

3.3.3 Main Oxygen Turbopump Design

The main LO_2 turbopump baseline design is given in Figure 3-9. The figure shows the major fluid flow paths and the preliminary selection of materials used. The pumping elements consist of an axial inlet with an axial inducer followed by a single impeller stage. The impeller back face is used as a balance piston, and a front wear ring may be used as a damping seal as necessary. An integral diffuser/volute collects and diffuses the impeller discharge flow in an efficient manner while the diffuser vanes also support the separating pressure loads of the volute.

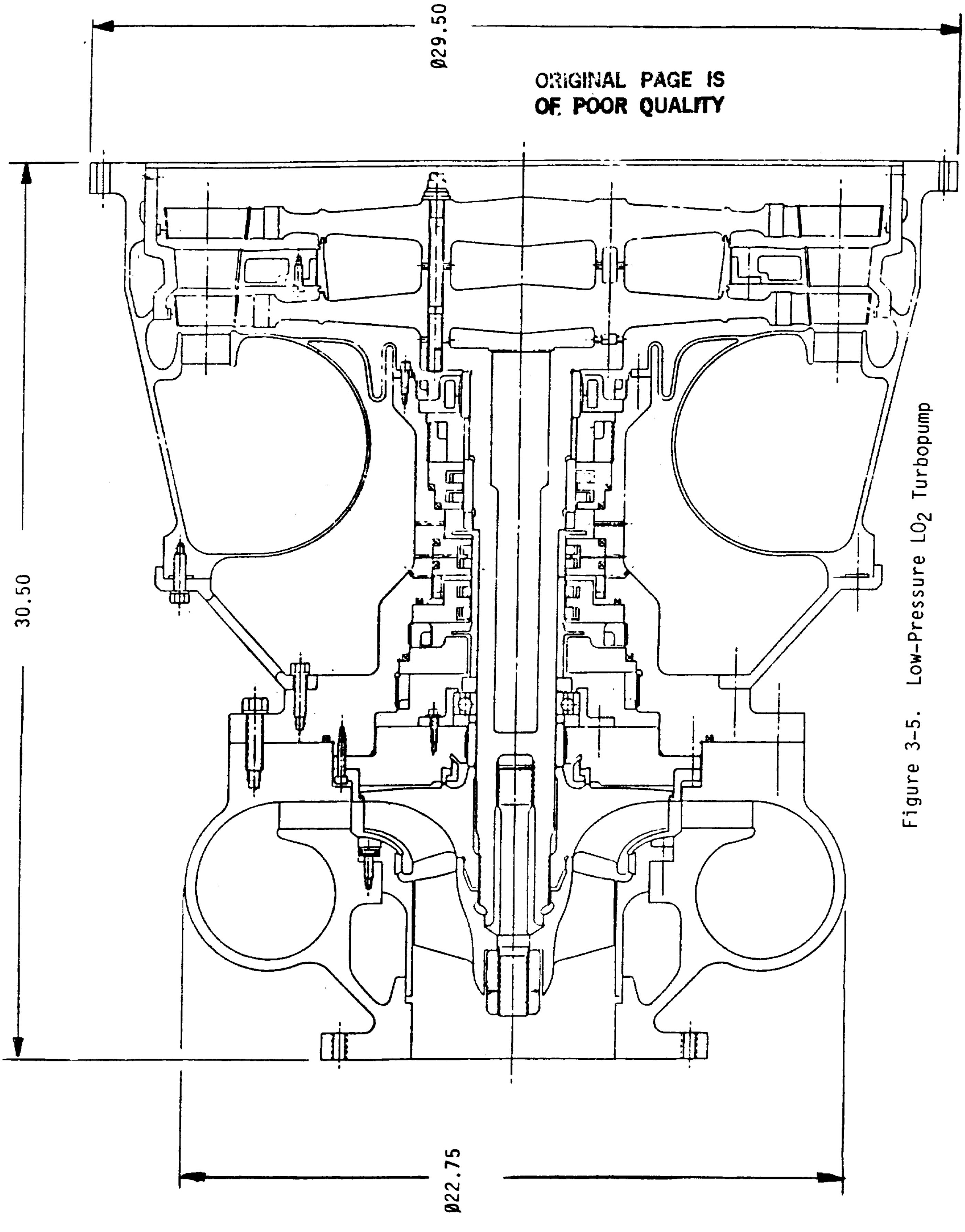

Figure 3-5. Low-Pressure LO_2 Turbopump

Table 3-7. STME LO_2 Main Turbopump Turbine Design Parameters (2 Stages)

• TURBINE TYPE	2 ROW PRESSURE COMPOUNDED	
• STAGES	2	
• PRESSURE RATIO	2.06	
• FLOW	43.875	LBM/S
• SHAFT POWER	22300	HP
• SPEED	16500	RPM
• EFFICIENCY	83.7	
• MEAN DIAMETER	21.65	INCH
• MEAN BLADE SPEED	1550	FT/S
• OVERALL TURBINE VELOCITY RATIO	0.34	
• STAGE VELOCITY RATIO	0.485	T-T STAGE 1
	0.484	T-T STAGE 2
• STAGE MEAN REACTION (NASA)	0.178	STAGE 1
•	0.160	STAGE 2
• STAGE LOADING COEFFICIENT	1.88	STAGE 1
	1.86	STAGE 2
• STAGE POWER SPLIT	50%	STAGE 1
	50%	STAGE 2

Table 3-8. STME LO_2 Main Turbopump Turbine Preliminary Design Geometry (2 Stages)

STAGE	1	1	2	2
BLADE ROW	NOZZLE	ROTOR	NOZZLE	ROTOR
NUMBER BLADES	76	83	91	97
% ADMISSION	100	100	100	100
MEAN DIAMETER (INCH)	21.653	21.653	21.653	21.653
BLADE DATA				
HEIGHT (IN)	1.665	2.093	2.178	2.804
WIDTH (IN)	1.0	1.0	1.3	1.0
PITCH (IN)	0.895	0.820	0.748	0.701
AXIAL SOLIDITY	1.117	1.220	1.739	1.426
ZWEIFEL COEFFICIENT	0.575	0.965	0.405	0.827
INLET FLANGE AREA (IN^2)	114.16			
DISCHARGE FLANGE AREA (IN^2)	216.80	FOR M = 0.15		

Table 3-9. STME LO_2 Main Turbopump Turbine GASPATH Summary (2 Stages)

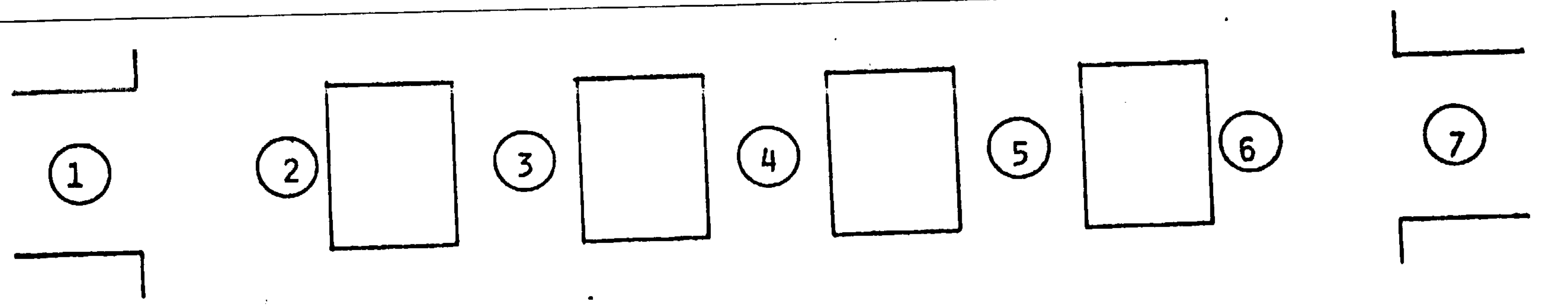

LOCATION			1	2	3	4	5	6	7
T_{TOT}	ABS	°R	1135	1135	1135	1049	1049	964	964
T_{TOT}	REL	°R			1078		992		
P_{TOT}	ABS	PSIA	276	272	267	196	191	137	134
P_{TOT}	REL	PSIA			222		156		
P_{STAT}		PSIA	272	272	207	191	146	134	132
DENSITY LBM/FT^3			0.0781	0.0778	0.0635	0.0596	0.0484	0.0454	0.0446

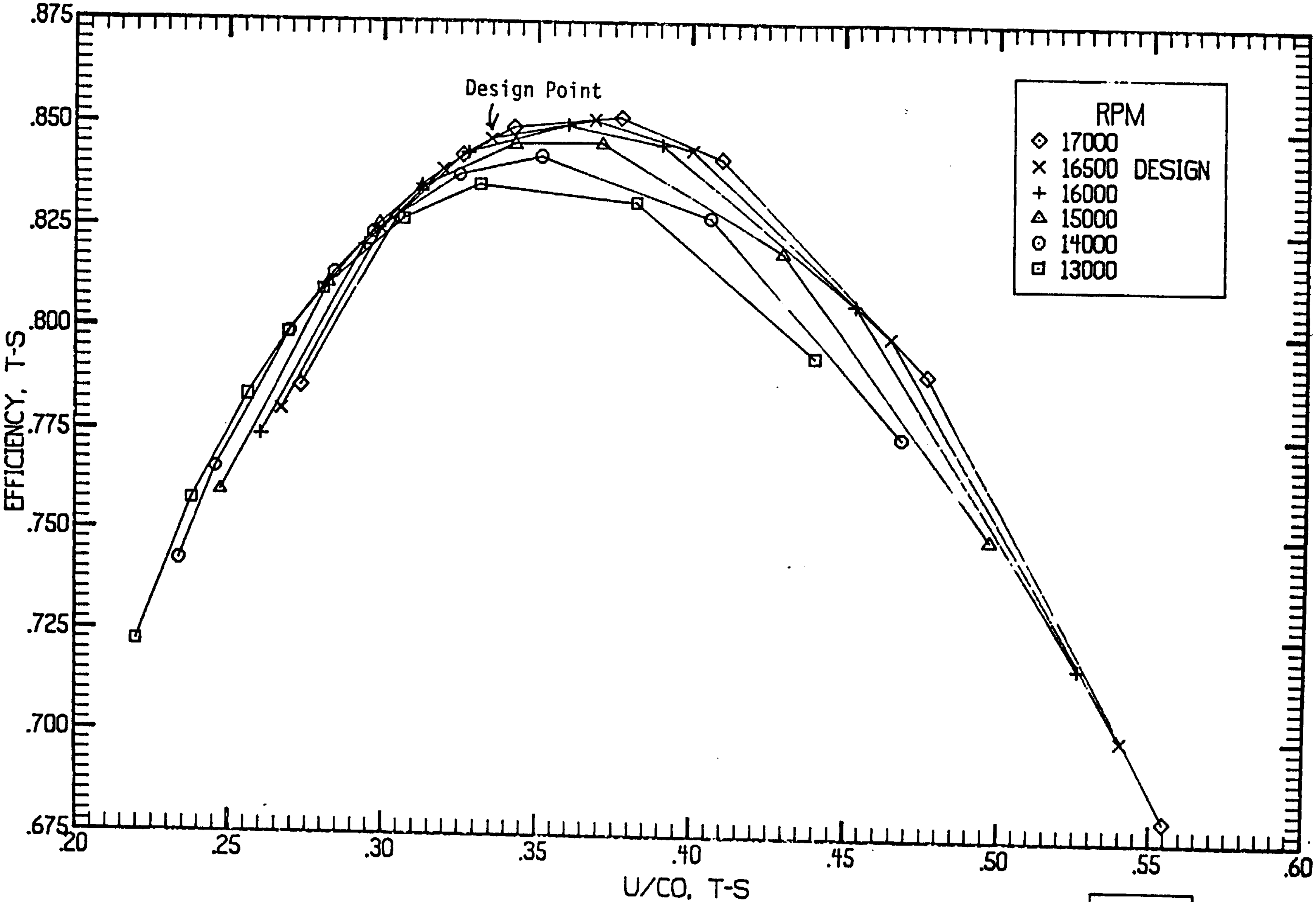

Figure 3-6. STME LO_2 Turbopump Turbine Performance

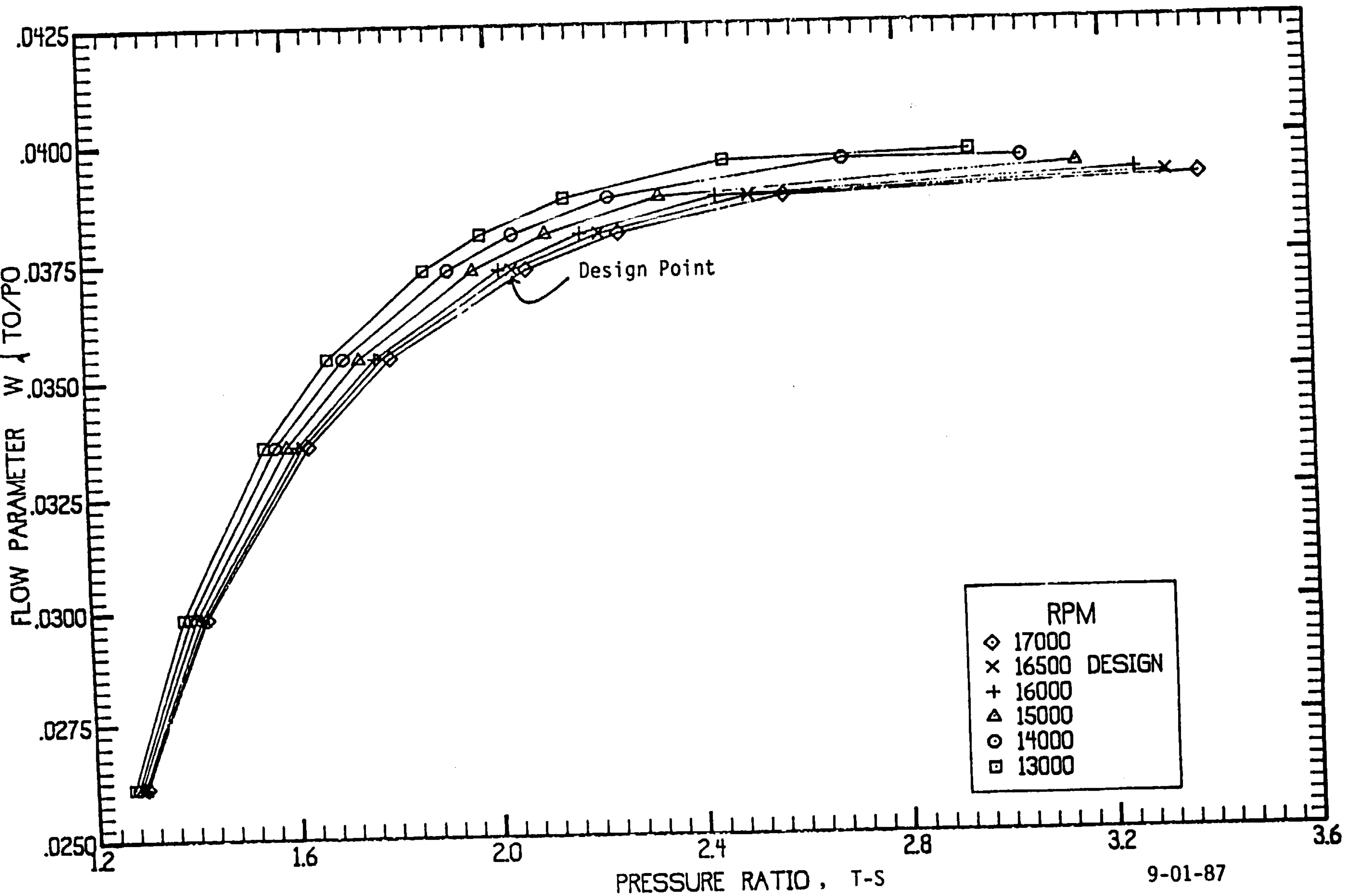

Figure 3-7. STME LO_2 Main Turbine Flow Performance

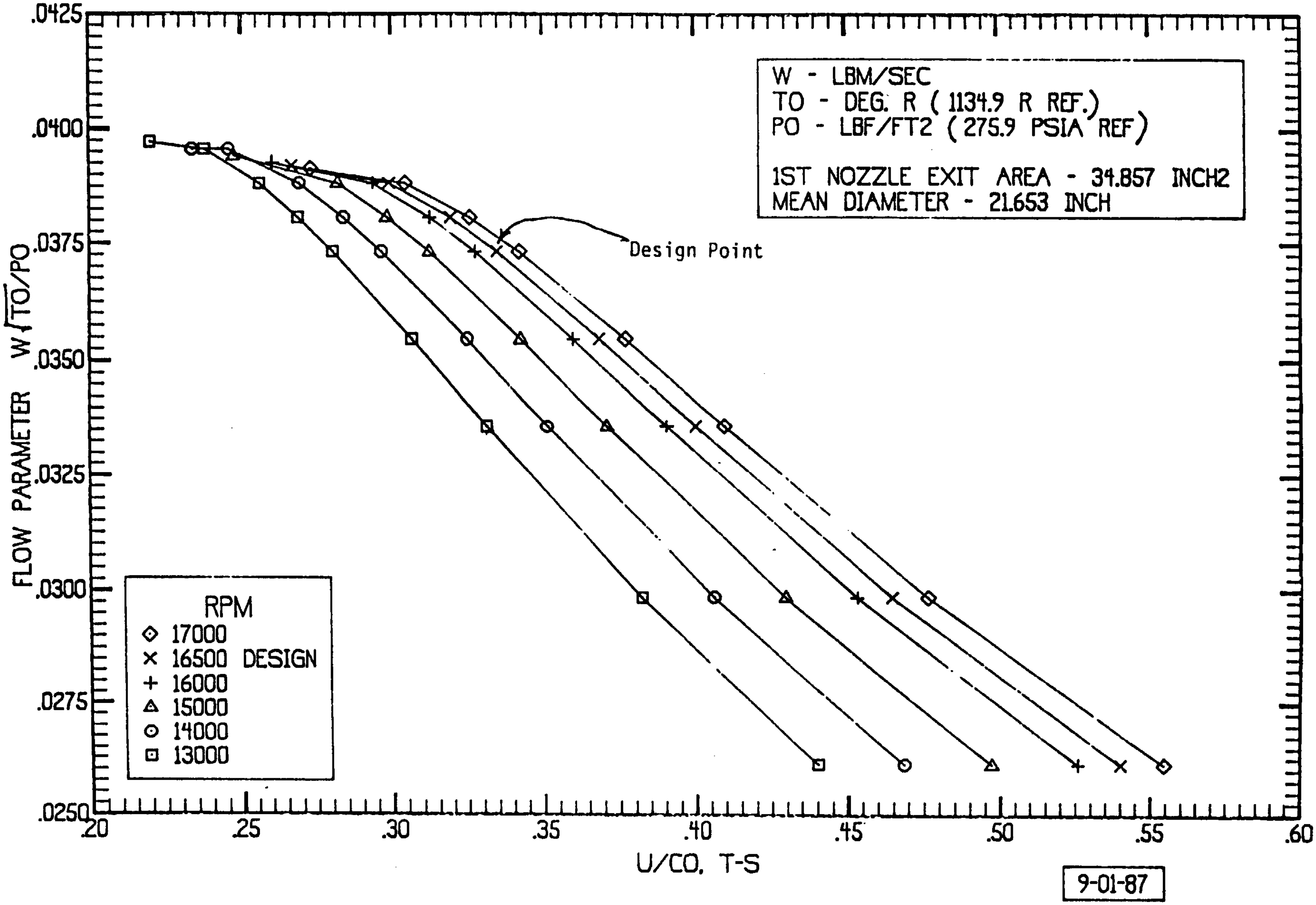

Figure 3-8. STME LO_2 Main Turbine Performance

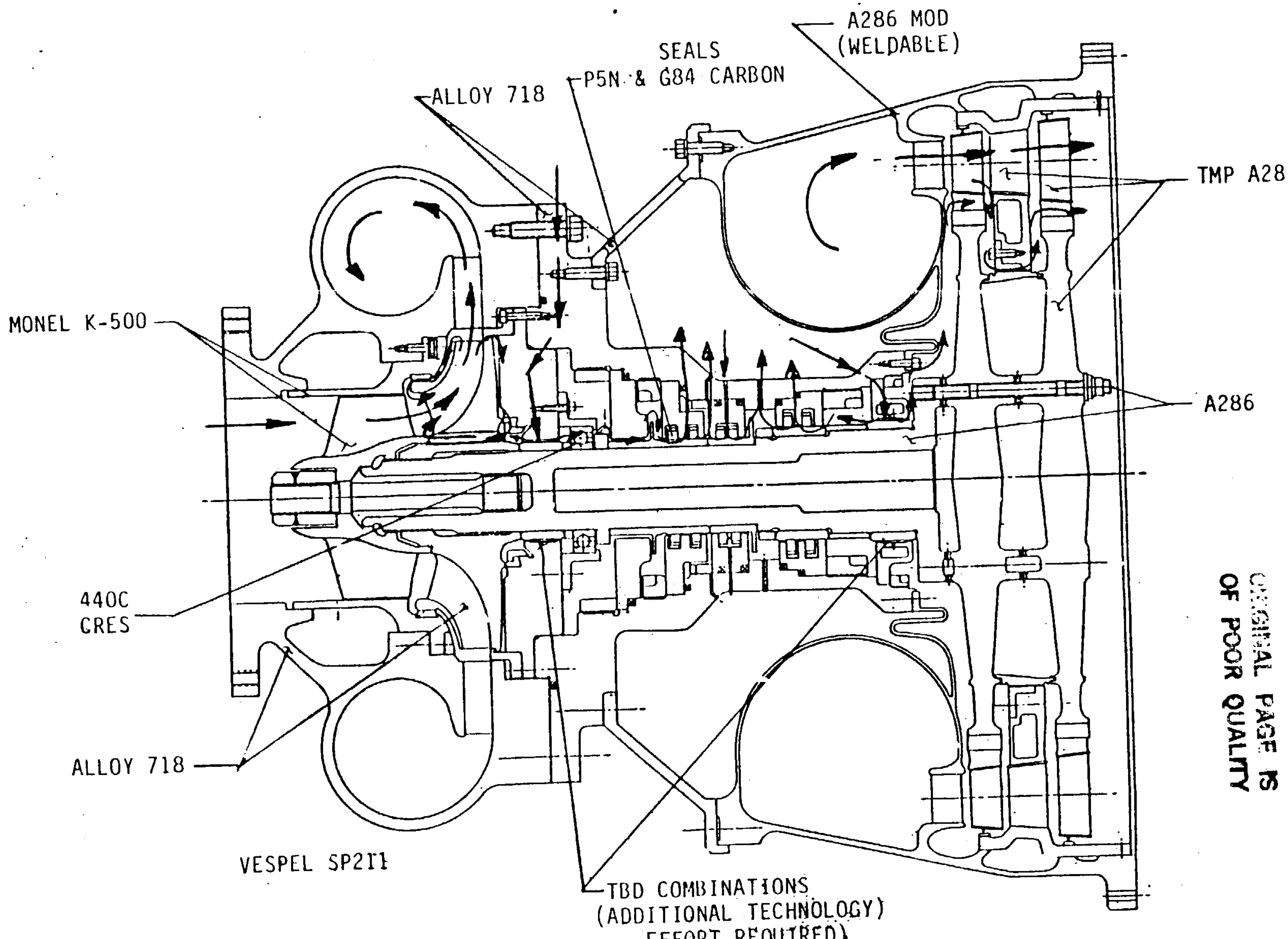

Figure 3-9. STME LO_2 Main Turbopump Baseline Design

The volute is rolled over to minimize the envelope for engine packaging purposes and is a double-discharge volute to minimize radial loads. An integral part of the housing forming the balance piston is a LO_2-fed hydrostatic bearing that supports the pump-end radial loads and controls the shaft rotordynamics. Adjacent to the hydrostatic bearing is a transient axial thrust ball bearing to control axial thrust during startup and shutdown. This bearing is in operation only during the transient periods of operation. Additional studies are planned to determine if the transient bearing could be located on the turbine bearing end to remove it from the LO_2 environment. This study will be completed during the next report period. The turbopump is equipped with a series of lift-off and floating ring seals, purges, and drains to isolate the LO_2 during pre-chill and startup and to maintain a positive barrier from the turbine end during operation. The turbine-end hydrostatic bearing will be supplied hydrogen from the main hydrogen pump discharge as shown in the figure. The turbine is a two-row pressure compounded design with a mean diameter of 21.65 in.

The turbopump housing consists of low-cost cast components with an effort to minimize welding where possible. Although the turbomachinery is in the very earliest stages of conceptual design, the producibility issues and material selection issues need to be addressed to ensure minimum cost, highly reliable components. The reusable maintenance history accumulated at Rocketdyne over the years greatly influenced the current STME designs. Analysis of SSME and other programs inspection and maintenance history provides major guidelines to the design features that require addressing in the new design. The results of the evaluation are presented in Table 3-10 for the oxygen turbopump. The table indicates the major maintenance inspection requirements and causes for those inspections. The table also presents the STME features used in order to eliminate the cause or the need for inspection. The major problem areas shown are for bearings, impellers, and inlet life and turbine hot-end component life (both rotating and static). The design features considered for the STME designs use the lessons of the past in this manner to provide a low-maintenance design.

Table 3-10. Reusable Maintenance History Influences STME Designs LO_2 Turbopump

Inspection Required in Maintenance History	Cause	STME Design Features
Bearings: Balls - wear, spalling Cage-wear, delamination Races - cracks	High radial loads High fluid dynamics Stress corrosion	Double discharge volute Hydrostatic bearings No loaded inner races Transient axial thrust bearing Balance piston
Impellers, inlets	Cavitation damage	Increased NPSP margin Inducers on main T/Ps Axial entry inlets Reduced tip speeds
Turbine housing cracks Turbine sheet metal cracks Nozzle cracks, erosion Blade erosion	Thermal induced LCF High temp spikes Blades cooled	GG-cycle controlled start Eliminate temp spikes Lower temp to 1600°R Material changes Segmented nozzles
Blade shroud chipping	Forced blade response High cycle dynamics	Shroud damping Material changes
Disk/blade gold plating loss	Assy/operation	Improved materials Eliminate plating

87D-9-2581

In a similar fashion, a preliminary producibility evaluation of the designs was made as the conceptual design progressed. In this study, the turbopump conceptual drawings were reviewed as to how they would be fabricated and what producibility issues were inherent in the design. This was done to ensure that the design will result in the simplest fabrication approaches available. This accomplishes a reduced component fabrication lead time as well as reduced net fabrication cost. The results of this analysis are given in Table 3-11 for the main oxygen turbopump. In this table, the component producibility issue is compared against the SSME equivalent component to assess how a better, more simple fabrication technique can be applied.

3.3.4 Main Oxygen Turbopump Rotordynamics

The baseline main LO_2 pump baseline design is shown in Figure 3-10. This pump operates between its first and second critical speed with acceptable critical speed margin as shown, but the frequency of the first mode must be increased slightly to satisfy the stability guideline described above. This will be accomplished by reducing overhang length and weight in subsequent design iterations. These are minor packaging changes and will not require substantial redesign. The second mode is controlled by mass distribution of the pumping elements and pump-end bearing stiffness and is acceptable as is. The speed-dependent bearing stiffness properties of hydrostatic bearings provide great critical speed separation and are a powerful tool for controlling the rotordynamics of this machine.

This design meets the Rocketdyne design criteria but does not satisfy the program goal of operating below its first critical speed. Subcritical operation will not be achieved for this machine without extreme mass reductions at the turbine end that may not be achievable within the baseline engine system design. The baseline turbopump design is the optimum design for this engine system as currently defined and super-critical operation should not be viewed as a liability as long as the basic guideline of margin and stability factors are maintained.

ORIGINAL PAGE IS
OF POOR QUALITY

Table 3-11. Producibility--STME Main LOX Turbopump

COMPONENT	MATERIAL	SSME EQUIVALENT	REMARKS
PUMP INLET DIFFUSER AND VOLUTE	• ONE PIECE CASTING INCO 718	• WELDMENT CASTING TO FORGING (INCO 718)	• ELIMINATE WELDING • ELIMINATE MACHINED DIFFUSER VANES • SINGLE AXIAL INLET REPLACES TWO RADIAL INLETS
TURBINE HOUSING	• WELDMENT MODIFIED A286	• WELDMENT INCO 718 AND 903 HEE PROTECTION • SHEET METAL LINER	• ELIMINATE HEE PROTECTION REQUIREMENTS • REDUCE COMPLEXITY • ELIMINATE NON-INSPECTABLE WELDS • ELIMINATES NEED FOR 2 COMPLEX SHEET METAL LINERS
MAIN PUMP HOUSING	• CASTING INCO 718	• WELDMENT INCO 718 HEE PROTECTION	• ELIMINATE WELDING • ELIMINATE NON-INSPECTABLE WELDS • REDUCE COMPLEXITY
TURBINE DISC	• FORGING TMP A286	• FORGING WASPALLOY HEE PROTECTION	• ELIMINATE PLATING FOR HEE PROTECTION
TURBINE BLADES	• FORGING TMP A285	• CASTING DS MAR-M-246	• ELIMINATE HEE ASSISTED CRACKING
TURBINE NOZZLE AND STATOR	• FORGING TMP A285	• CASTING MAR-M-246	• ELIMINATE HEE ASSISTED CRACKING
IMPELLER	• CASTING INCO 718	• FORGING INCO 718	• ELIMINATE COMPLEX MACHINING
INDUCER	• FORGING MONEL K-500	• FORGING INCO 718	• IMPROVED IGNITION RESISTANCE
MAIN SHAFT	• FORGING A-286	• FORGING WASPALLOY HEE PROTECTION	• ELIMINATE PLATING FOR HEE PROTECTION

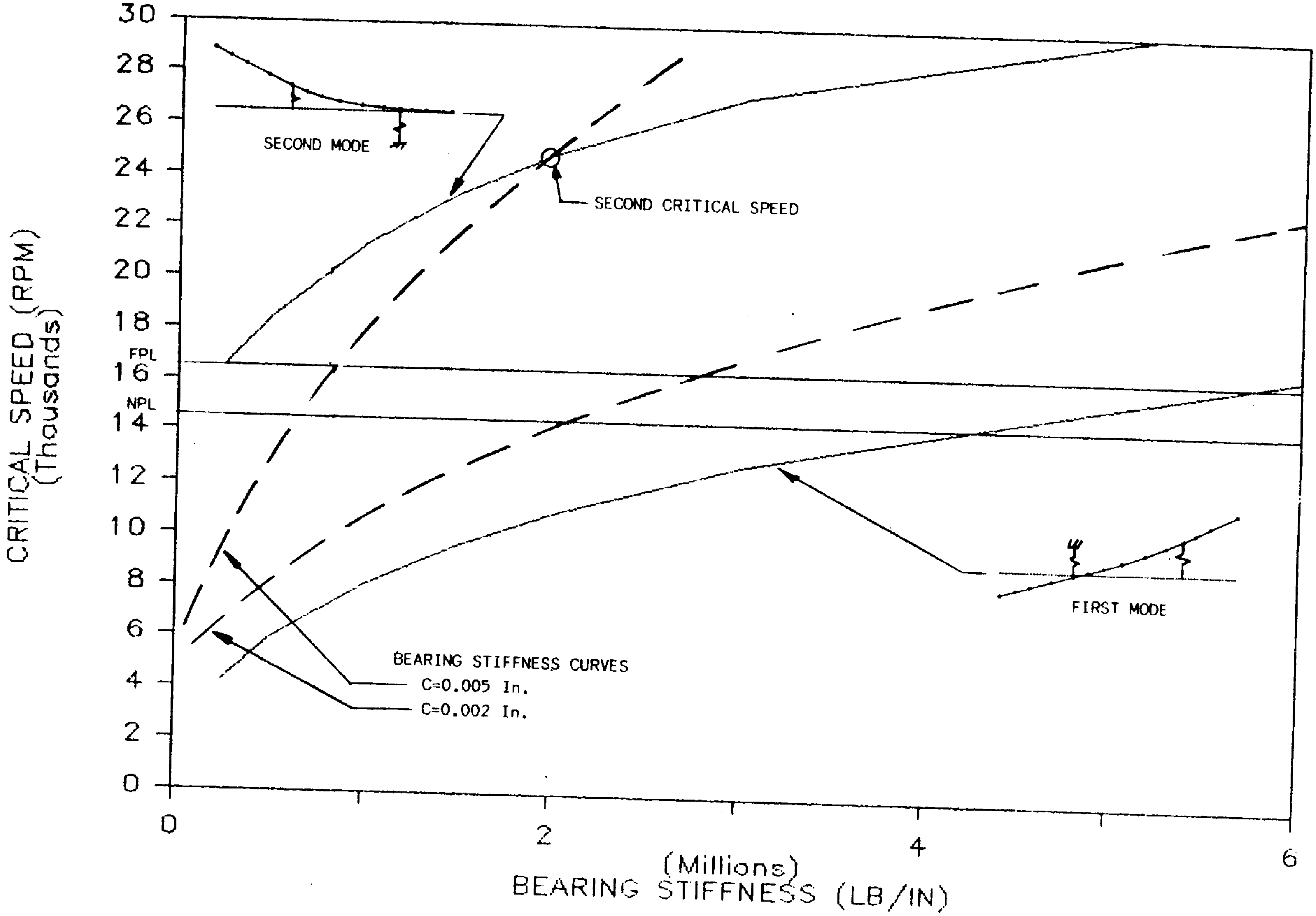

Figure 3-10. STME LO_2 Main Turbopump Critical Speeds--Baseline Configuration

3.4 OXYGEN BOOST TURBOPUMP

3.4.1 Oxygen Boost Pump

The conceptual layout of the LO_2 boost turbopump is given in Figure 3-11. Performance predictions, geometry, and hydrodynamic design parameters for the LO_2 boost pump are summarized in Figures 3-12 through 3-15 and Tables 3-12 through 3-14.

The pump has a single-blade-row axial inducer followed either by an axial diffuser or a volute collector. The axial discharge configuration has a higher efficiency due to the more efficient diffusion/collection system and is considered to be the baseline configuration.

3.4.2 Oxygen Boost Turbine

The STME LO_2 boost pump, with dimensions, is shown in Figure 3-16 with an axial flow discharge. The diameter of the four-stage turbine was dictated by the need to locate the turbine within the discharge diameter of the inducer. The dimensions of the SSME low-pressure oxygen turbopump (LPOTP) layout were used for guidance to produce a turbine mean diameter of 4.1 in. At this diameter, the mean blade speed is 166.3 ft/s and the turbine efficiency is 61%. Table 3-15 describes the basic turbine design parameters, and the turbine design geometry is summarized in Table 3-16. Blade heights are reasonable considering the diameter of the turbine, and the average stage-loading coefficient is acceptable. A summary of pressures and flows along the turbine flow path is presented in Table 3-17. The average pressure drop per stage is 799 psid. Also shown are the seal and bearing leakage flows. Efficiency and head as functions of flow are shown in graphical form in Figures 3-17 and 3-18. Somewhat greater efficiency can be achieved by increasing the number of turbine stages. However, beyond four stages, the efficiency payoff with each additional stage was judged to be too small to justify the added complexity.

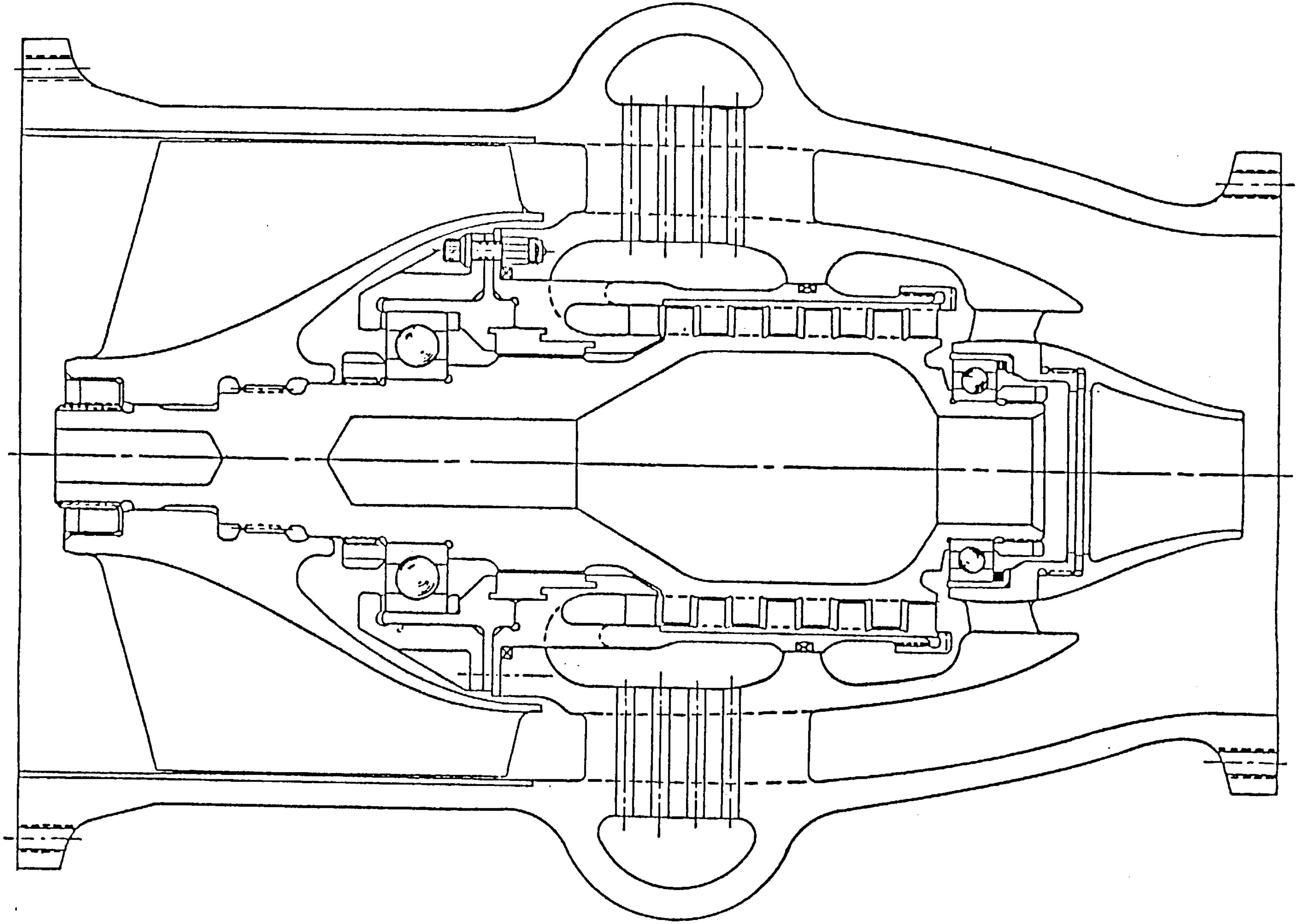

Figure 3-11. STME LO_2 Boost Turbopump

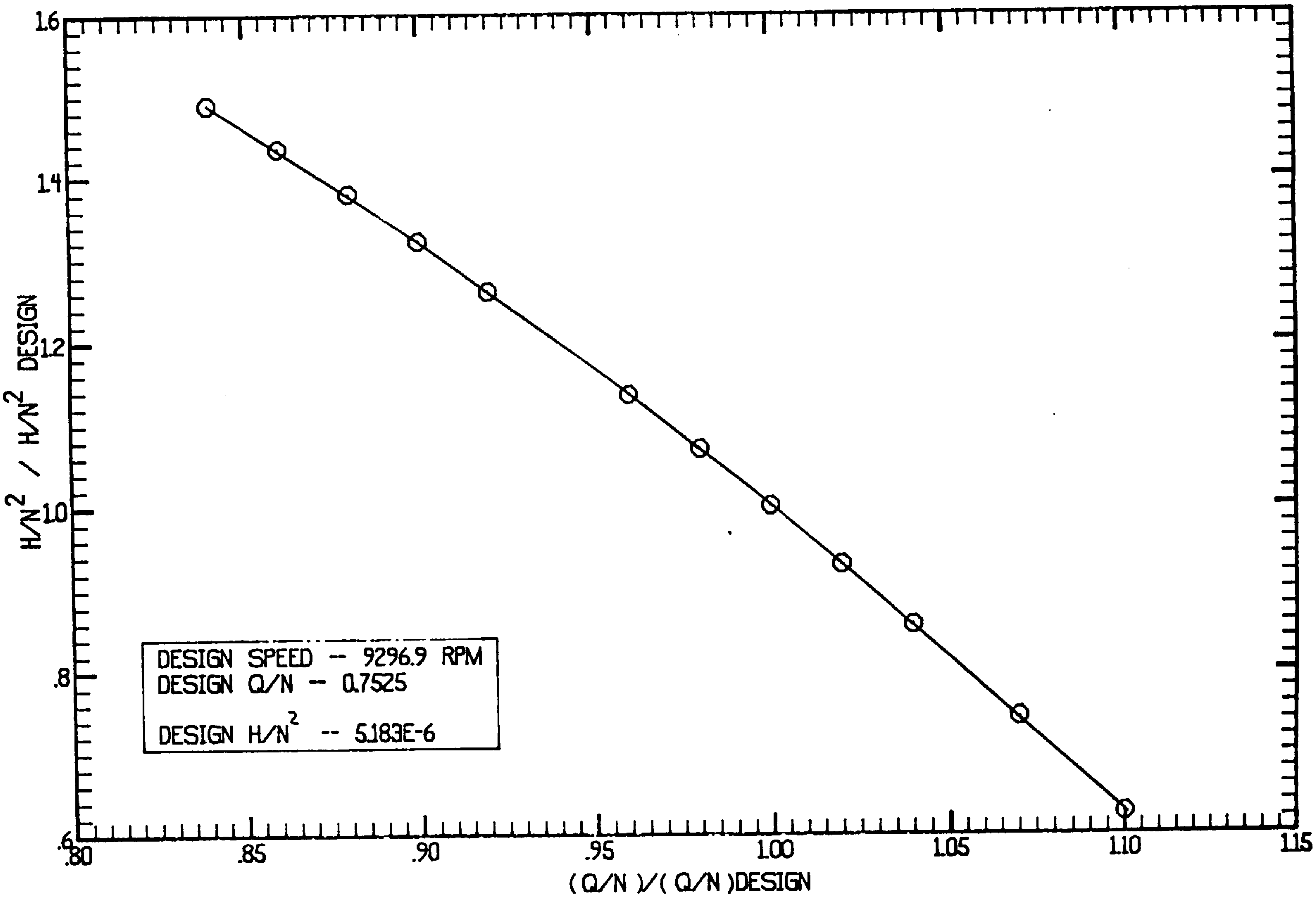

Figure 3-12. STME LO_2 Boost Pump Head Flow Performance with Axial Discharge

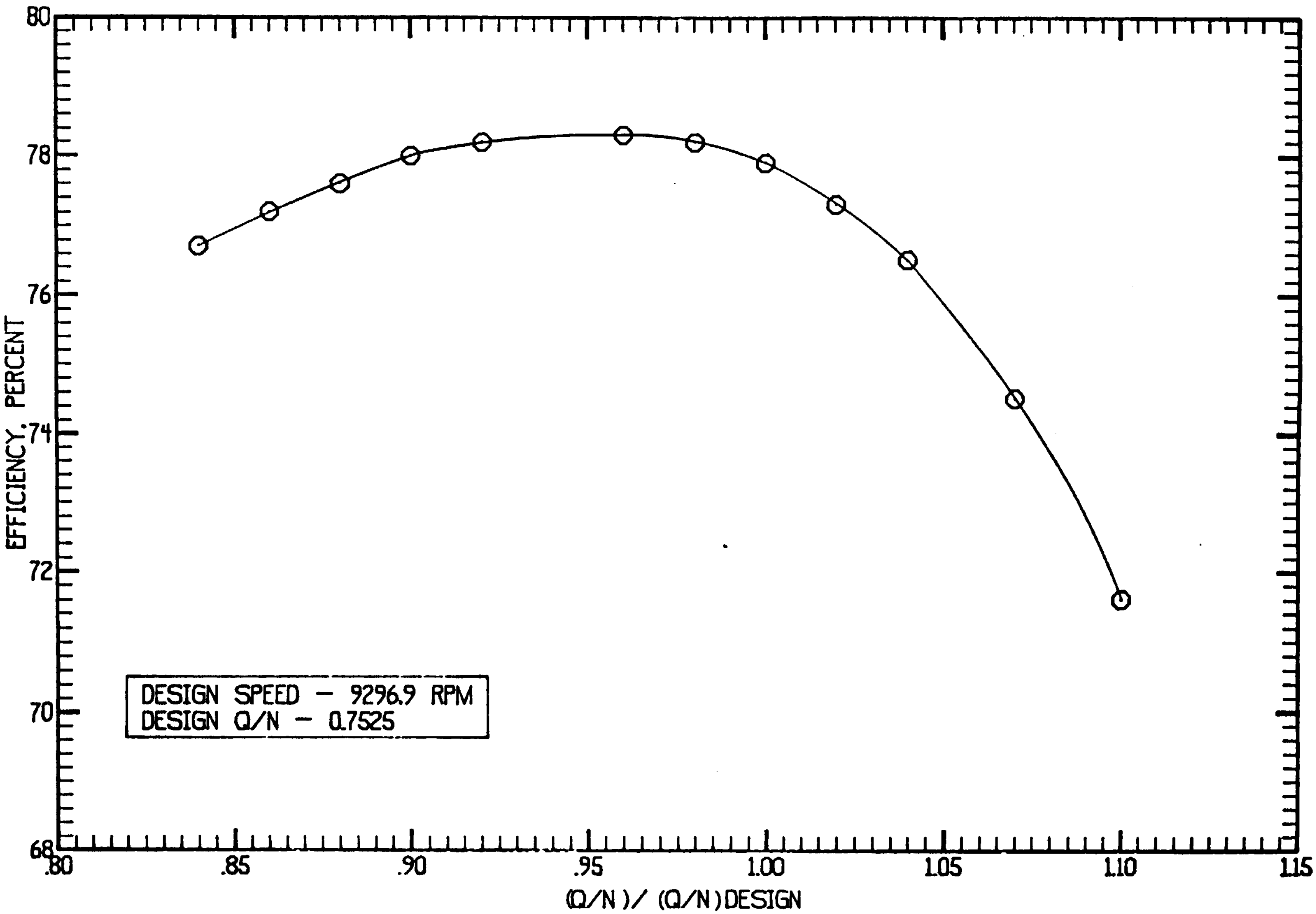

Figure 3-13. STME LO_2 Boost Pump Performance with Axial Discharge

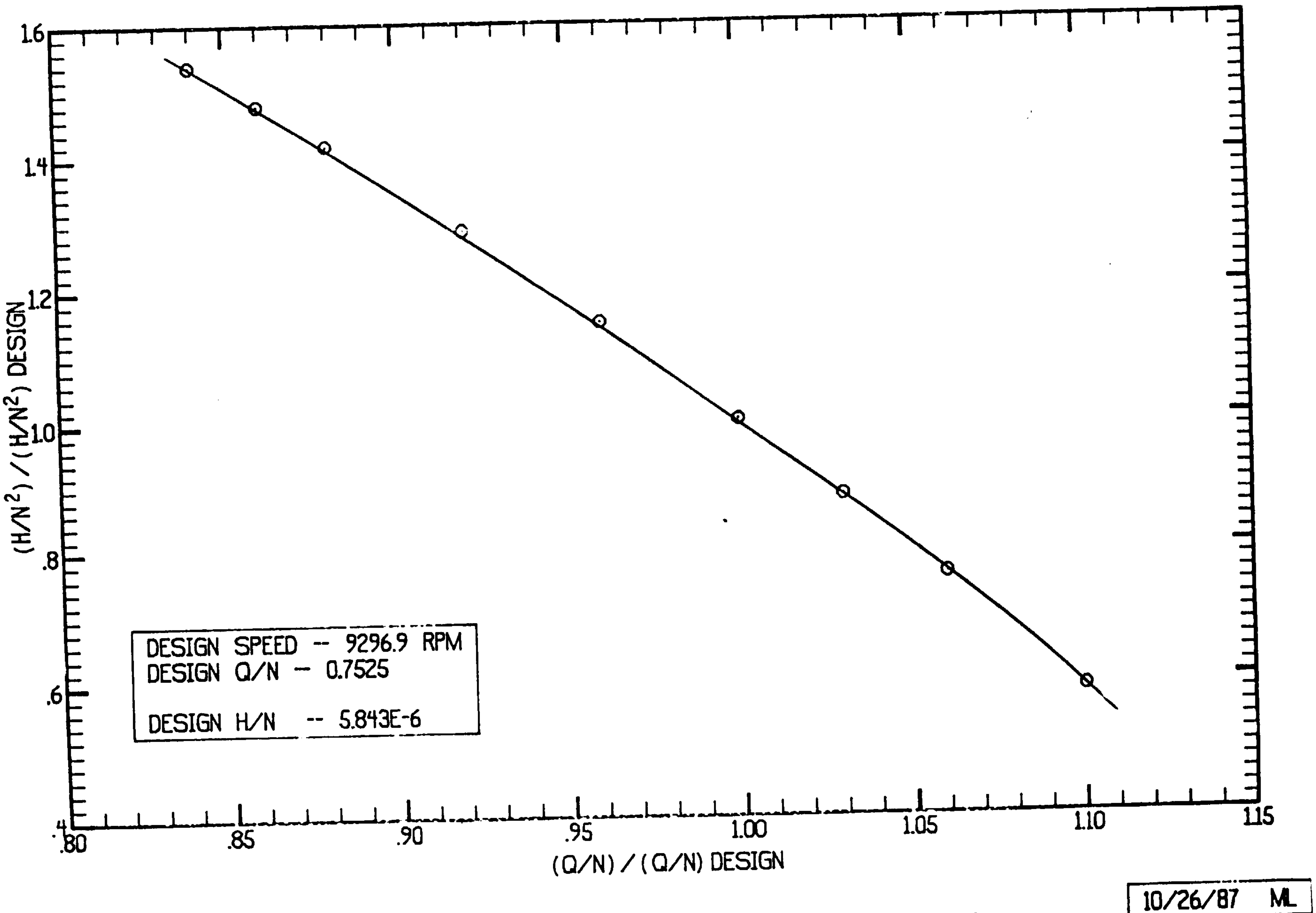

Figure 3-14. STME LO_2 Boost Pump Head Flow Performance with Volute

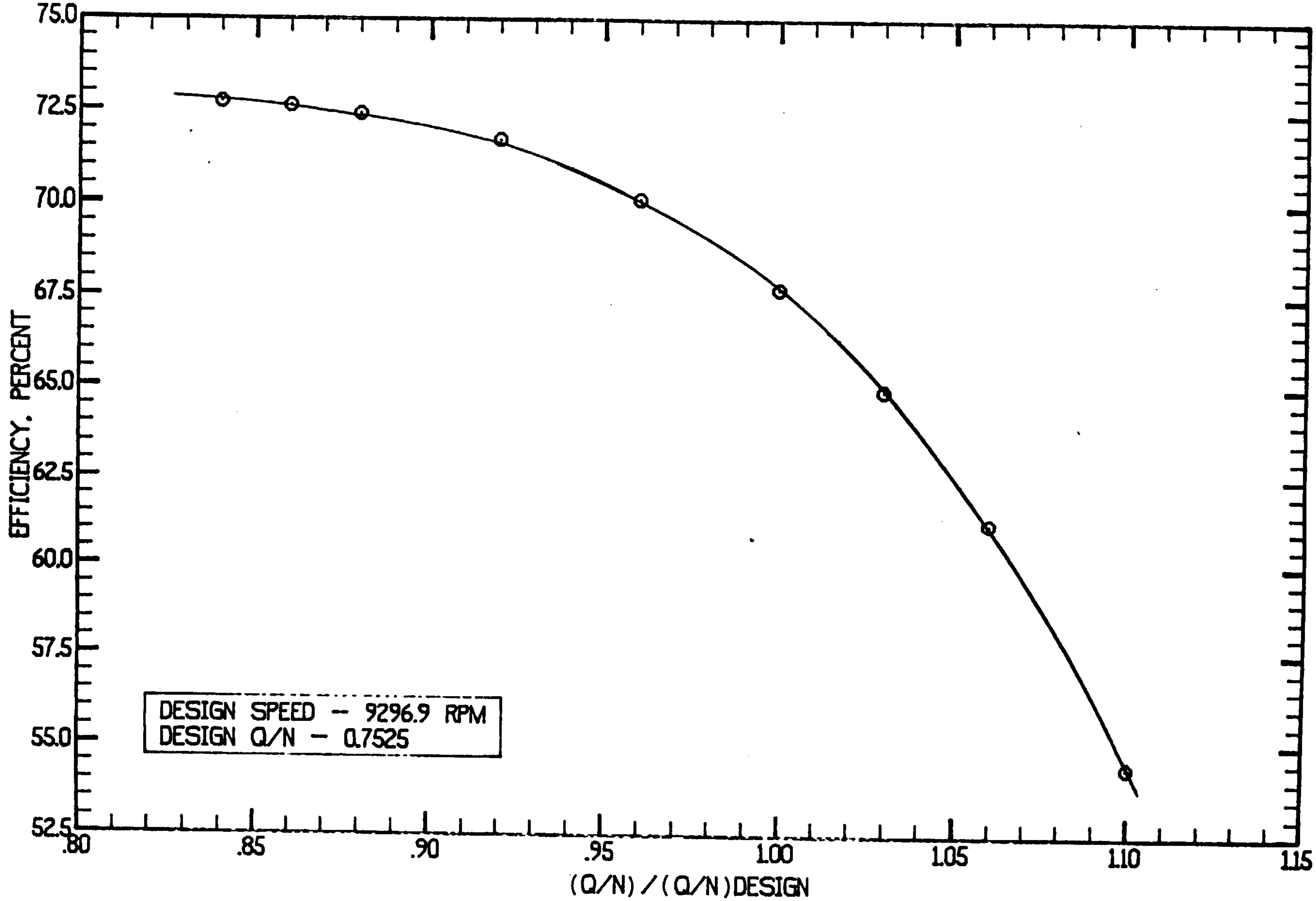

Figure 3-15. STME LO_2 Boost Pump Performance with Volute

10/26/87 ML

Table 3-12. LO_2 Boost Pump Design Conditions

	AXIAL DISCHARGE	VOLUTE DISCHARGE
INLET FLOWRATE, GPM	6996.1	6996.1
HEAD, FT	629.1	619.7
SPEED, RPM	9296.9	9296.9
EFFICIENCY	77.9	67.9
REQUIRED SHAFT POWER, HP	1630.1	1842.3
TURBOPUMP WEIGHT, LB	157.6	169.6
MINIMUM INLET NPSH, FT	60.66	60.66
DISCHARGE PRESSURE, PSIA	358.1	353.5
MAX. OPERATING SUCTION SPECIFIC SPEED	35777	35777

Table 3-13. LO_2 Boost Pump Geometry

	AXIAL DISCHARGE	VOLUTE DISCHARGE
INDUCER:		
TIP DIAMETER, INCH	9.22	9.22
INLET HUB DIAMETER, INCH	2.77	2.77
DISCHARGE HUB DIAMETER, INCH	6.9	6.9
AXIAL LENGTH, INCH	2.85	3.0
INLET HUB TO TIP RATIO	.3	.3
STATOR:		
INLET TIP DIAMETER, INCH	9.22	
DISCHARGE TIP DIAMETER, INCH	8.8	
INLET HUB DIAMETER, INCH	6.9	
DISCHARGE HUB DIAMETER, INCH	6.9	
AXIAL LENGTH, INCH	6.6	
DISCHARGE DUCT DIAMETER, INCH	6.95	6.95

Table 3-14. LO_2 Boost Pump Hydrodynamic Design Parameters

	AXIAL DISCHARGE INDUCER	AXIAL DISCHARGE STATOR	VOLUTE DISCHARGE INDUCER
INLET FLOW COEFF.	.1		.1
DISCHARGE FLOW COEFF.	.218		.219
HEAD COEFF.	.150		.174
TIP SPEED	374.0		374.0
NO. OF BLADES	4	9	4
TIP SOLIDITY	1.53	2.2	1.53
INLET BLADE ANGLE	10.8	46.475	10.8
INCIDENCE	3.09	1.0	3.09
DISCHARGE BLADE ANGLE	21.7	98.4	22.9
DEVIATION	3.76	8.4	4.14
RMS D-FACTOR	.142	.430	.189

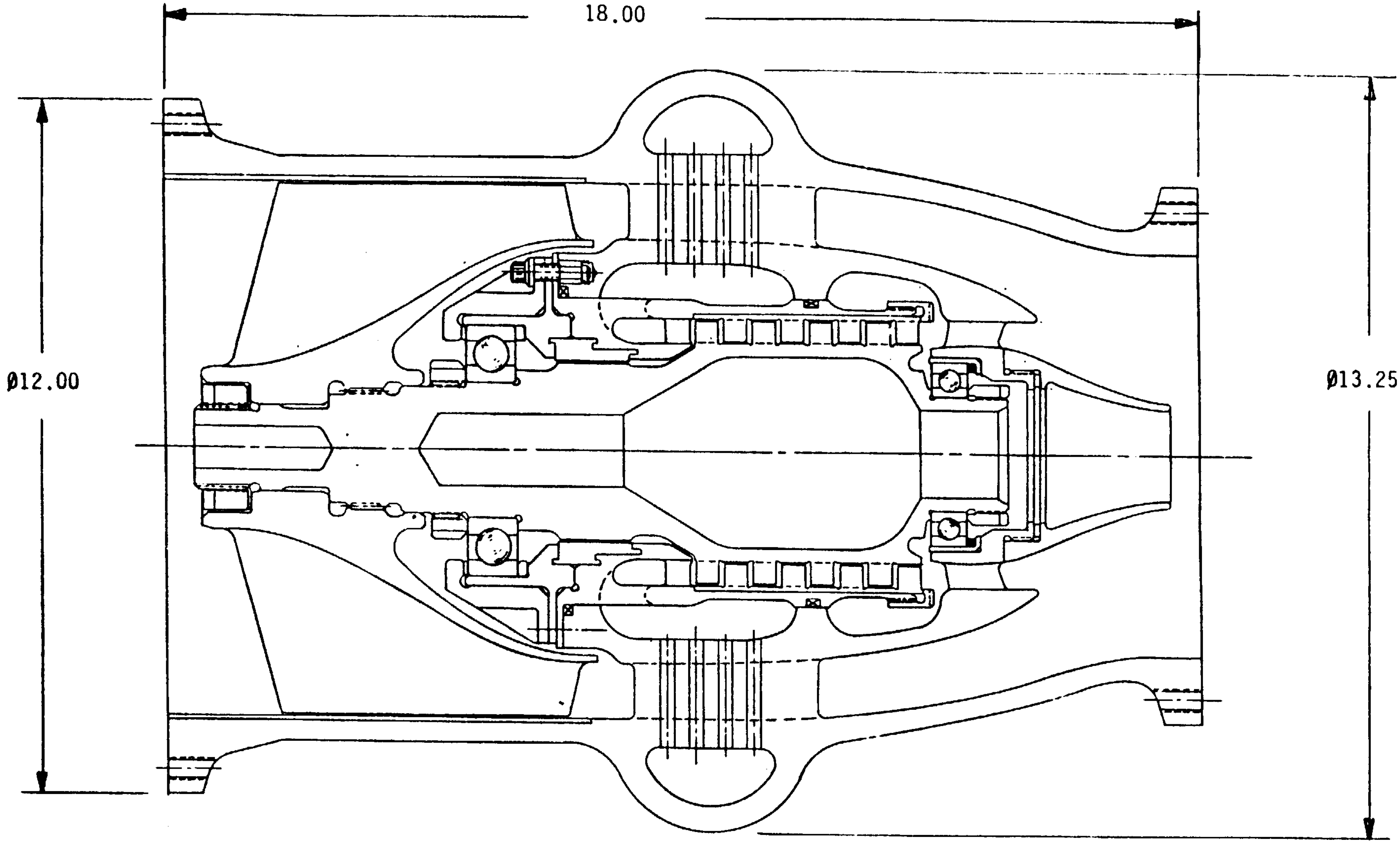

Figure 3-16. LO_2 Boost Turbopump--Baseline Design

Table 3-15. LO_2 Boost Turbopump Turbine Design Parameters (Axial Discharge)

• TURBINE TYPE		
• POWER	1630.1	HP
• SPEED	9296.9	RPM
• FLOW	200.2	LBM/S
• EFFICIENCY	61.0	PERCENT
• P_{TOT} INLET FLANGE	3867	PSIAT
• P_{TOT} OUTLET FLANGE	358.1	PSIAT
• NUMBER OF STAGES	4	
• MEAN DIAMETER	4.1	INCH
• MEAN BLADE SPEED	166.3	FT/S
• OVERALL TURBINE VELOCITY RATIO	0.242	
• AVG STAGE VELOCITY RATIO	0.484	
• STAGE MEAN REACTION (NASA)	0.342	
• AVG STAGE LOADING COEFFICIENT	1.3	

Table 3-16. LO_2 Boost Turbopump Turbine Preliminary Design Geometry (Axial Discharge)

NUMBER OF STAGES	4	
ADMISSION	100	PERCENT
MEAN DIAMETER	4.2	INCH
BLADE HEIGHT	0.4	INCH
BLADE WIDTH	0.4	INCH
AXIAL GAP	0.1	INCH
AVERAGE STAGE LOADING COEFFICIENT	1.3	
MEAN BLADE SPEED	166.3	FT/S

Table 3-17. LO_2 Boost Turbopump Turbine Flow Path Summary (Axial Discharge)

• PRESSURE, INLET FLANGE	3867	PSIAT
• PRESSURE, NOZZLE 1 INLET	3582	PSIAT
• ΔP_{T-T}/STG (AVG)	799	PSID
• PRESSURE, ROTOR 4 DISCHARGE	386	PSIAT
• PRESSURE, DISCHARGE FLANGE	359	PSIAT
• FLOW, INLET FLANGE	200.2	LBM/S
• SEAL LEAKAGE	13.0	LBM/S
• FLOW, TURBINE STAGES	187.2	LBM/S
• BEARING LEAKAGE	7.9	LBM/S
• FLOW, DISCHARGE FLANGE	179.3	LBM/S

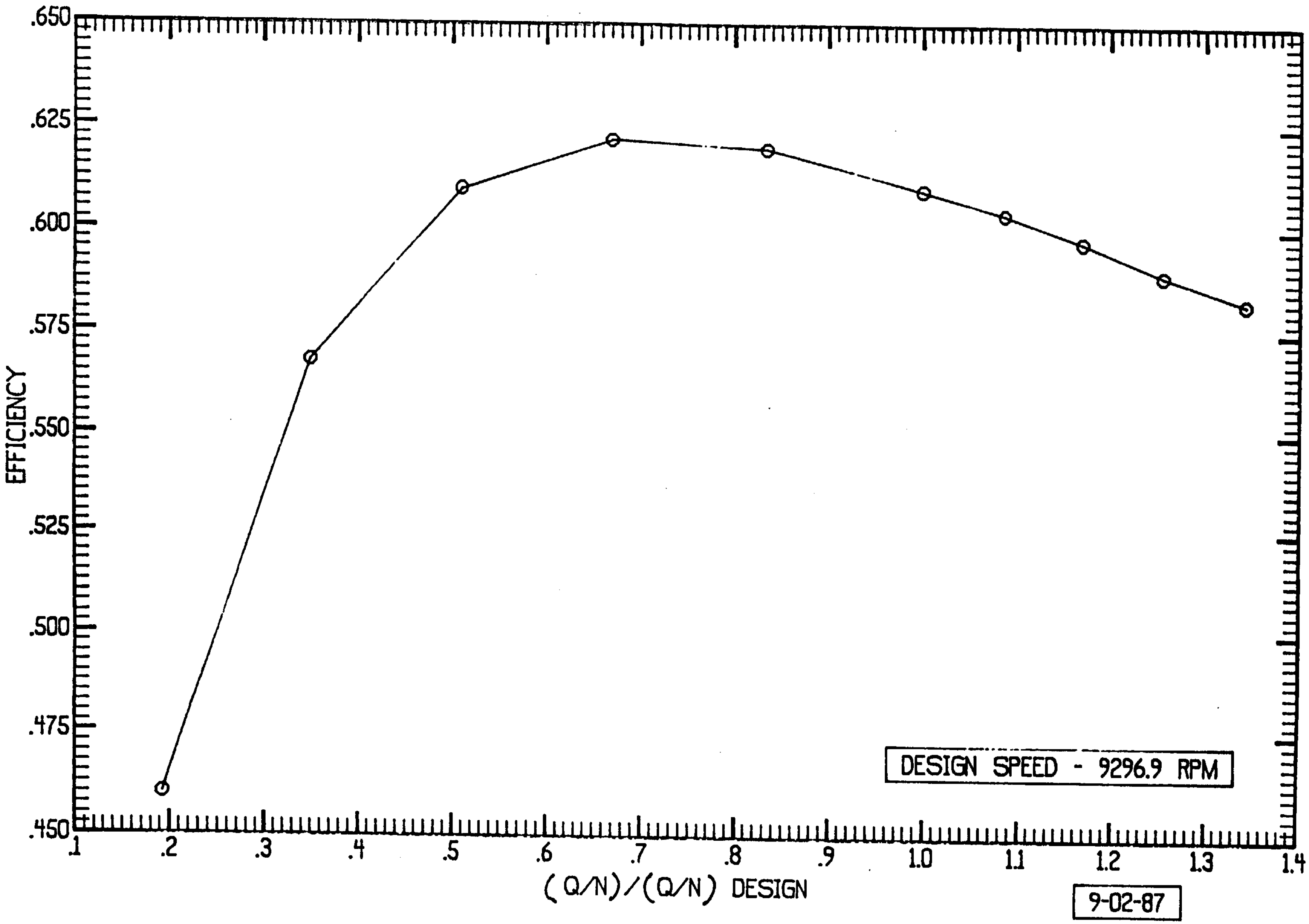

Figure 3-17. STME LO_2 Boost Turbopump Turbine Performance

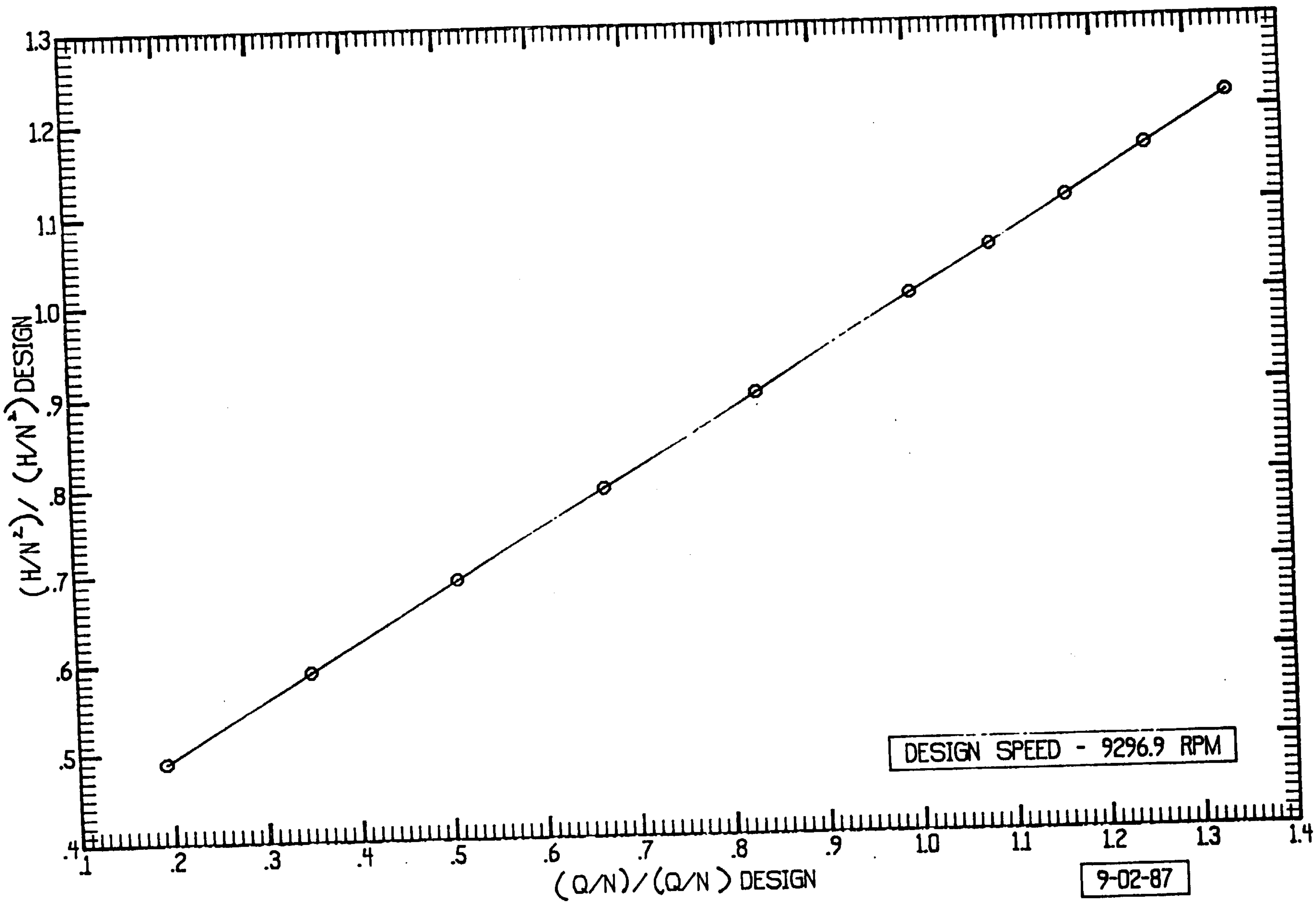

Figure 3-18. STME LO_2 Boost Turbopump Turbine Performance

3.4.3 Oxygen Boost Turbopump Design

The LO_2 boost pump is presented in Figure 3-19. An axial inlet inducer generates the pump head rise followed by axial stator vanes, which efficiently diffuses the whirl component of the LO_2 into the axial discharge. The hydraulic turbine drive using LO_2 supplied from the main LO_2 discharge enters the pump through the pump stator vanes and powers the four-stage axial turbine. The turbine discharge combines with the pump discharge for an axial exit toward the main turbopump. A radial discharge scroll could also be used with some slight performance penalty if required. This low-speed pump operates on ball bearings at DN values of less than 0.6×10^6 mm rpm that have demonstrated long life and high axial thrust capacity in similar designs.

The producibility review of the LO_2 boost pump, when evaluated against SSME hardware, indicated that producibility may not be enhanced by using some different materials, but it also indicates that the simplicity of the design is in keeping with the low-cost objectives of the program. The review results are presented in Table 3-18 and indicate that, for this design, materials for the cast housing, the inducer, and turbine rotor will be similar to the SSME LO_2 boost turbopump. The stator/housing material will be A-357 aluminum, replacing TENS-50 aluminum.

3.4.4 Oxygen Boost Turbopump Rotordynamics

The LO_2 boost turbopump design operates well below its first critical speed with adequate rotordynamic margins, as shown in Figure 3-20. The first mode is a rigid-rotor mode with little rotor bending; its frequency is controlled primarily by pump bearing stiffness and inducer mass. This design was rotordynamically acceptable in its original configuration, and no design iterations were required.

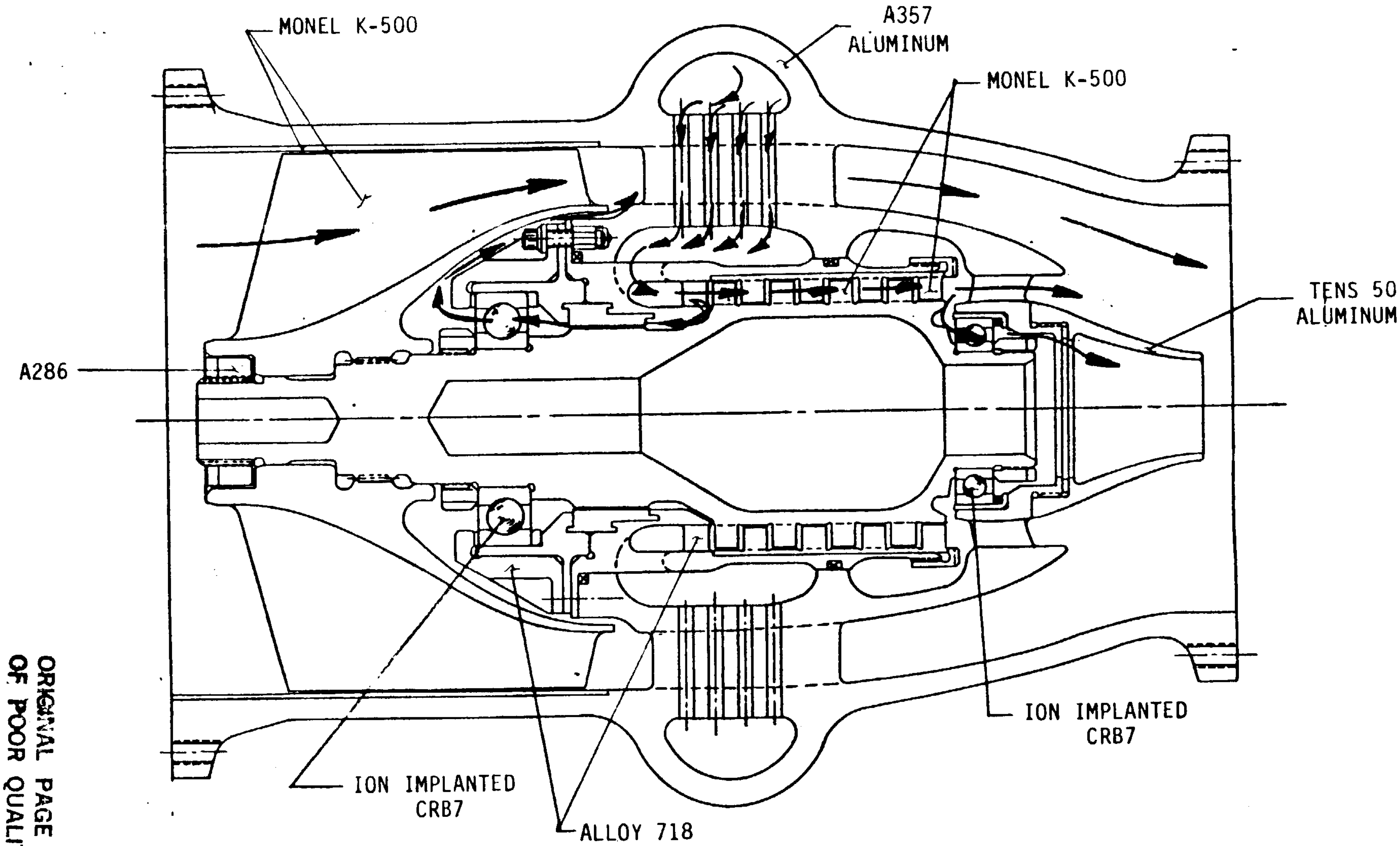

Figure 3-19. LO_2 Boost Turbopump

Table 3-18. Producibility--STME LO_2 Boost Turbopump

Component	Material	SSME Equivalent	Remarks
Pump main housing	• Casting A357 Al alloy	• Casting tens 50 Al alloy	• Improved producibility
Inducer	• Forging Monel K-500	• Forging Monel K-500	• No change in producibility
Turbine rotor	• Forging Monel K-500	• Forging Monel K-500	• No change in producibility
Turbine stator	• Forging Monel K-500	• Casting Monel K-500	• No change in producibility

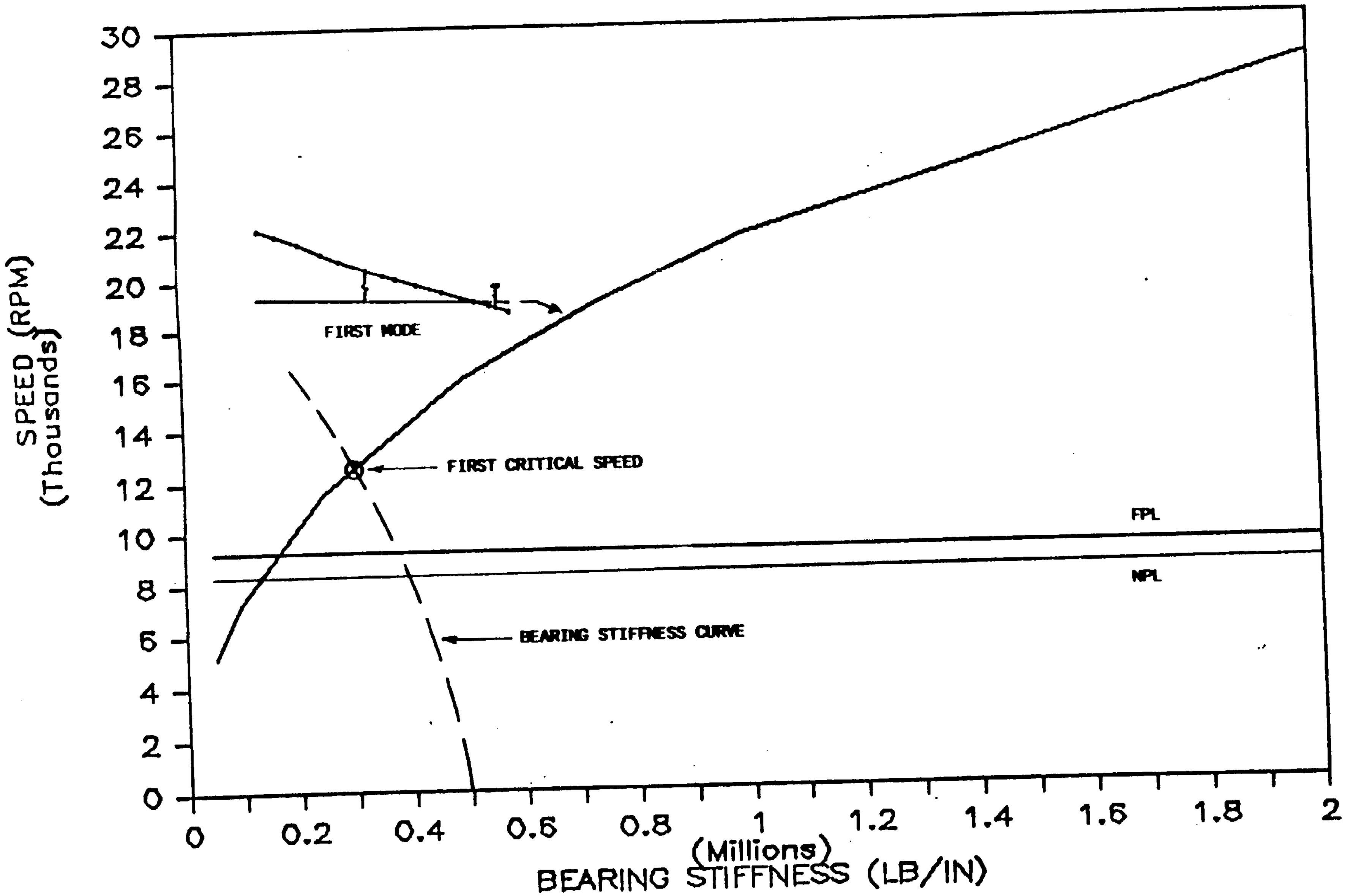

Figure 3-20. STME LO_2 Boost Pump Critical Speeds--
Baseline Configuration

3.5 HYDROGEN TURBOPUMP

3.5.1 Hydrogen Pump

The conceptual layout of the hydrogen turbopump is given in Figure 3-21. Performance predictions, geometry, and hydrodynamic design parameters for the hydrogen pump are presented in Figures 3-22 and 3-23 and Tables 3-19 through 3-21. The pump is a three-stage centrifugal pump with an inducer upstream of the first impeller to maximize suction performance. Unlike the LO_2 pump, this pump has a single-discharge volute as the low density of hydrogen reduces the magnitude of hydrodynamically generated radial loads.

3.5.2 Hydrogen Turbine

Figure 3-24 shows the configuration, with dimensions, of the LH_2 turbopump. A two-stage pressure compounded design is shown. However, with a pressure ratio over 9 and a velocity ratio of 0.18, a velocity compounded design will continue to be evaluated for the baseline design. The mean diameter of 13.528 in. is well matched to the pump impeller diameter, resulting in a well-proportioned pump casing. The mean blade speed is 1,550 ft/s, which corresponds to the limit of the disk material. Approximately 70% of the power is generated in the first stage. The velocity ratio, stage-loading coefficients, and Zwiefel coefficients are all in reasonable ranges. Discharge velocities from the first nozzle are supersonic. Blade heights are reasonable for this turbine and do not approach any experience limits.

Table 3-22 presents the basic turbine parameters for the LH_2 main pump turbine. Table 3-23 describes the turbine geometry, and Table 3-24 summarizes the parameters along the hot gas flow path through the turbine. Figure 3-25 documents the predicted performance of the turbine with a plot of efficiency versus turbine velocity ratio where the throat area of the supersonic first nozzle is shown.

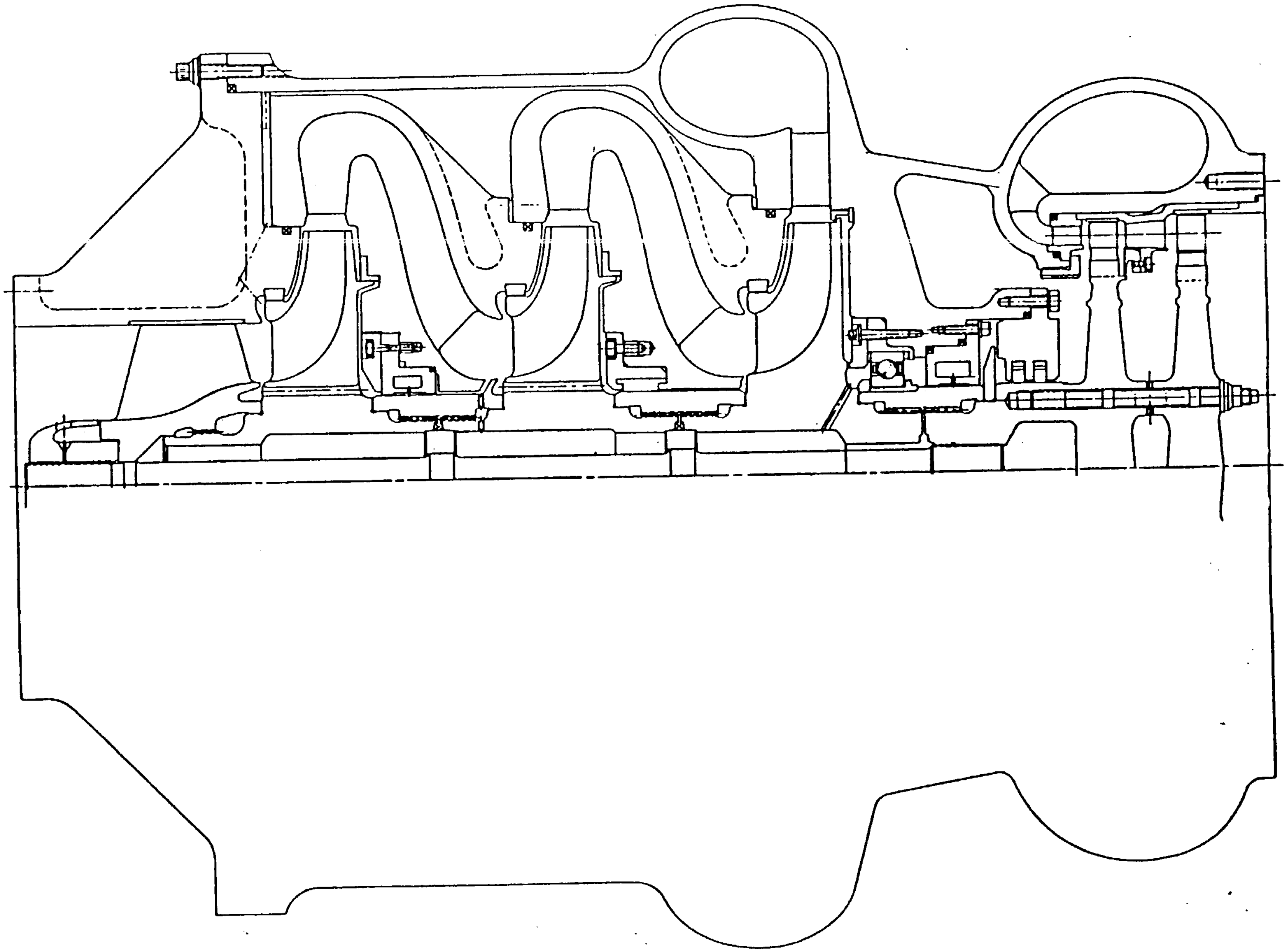

Figure 3-21. STME Hydrogen Main Turbopump

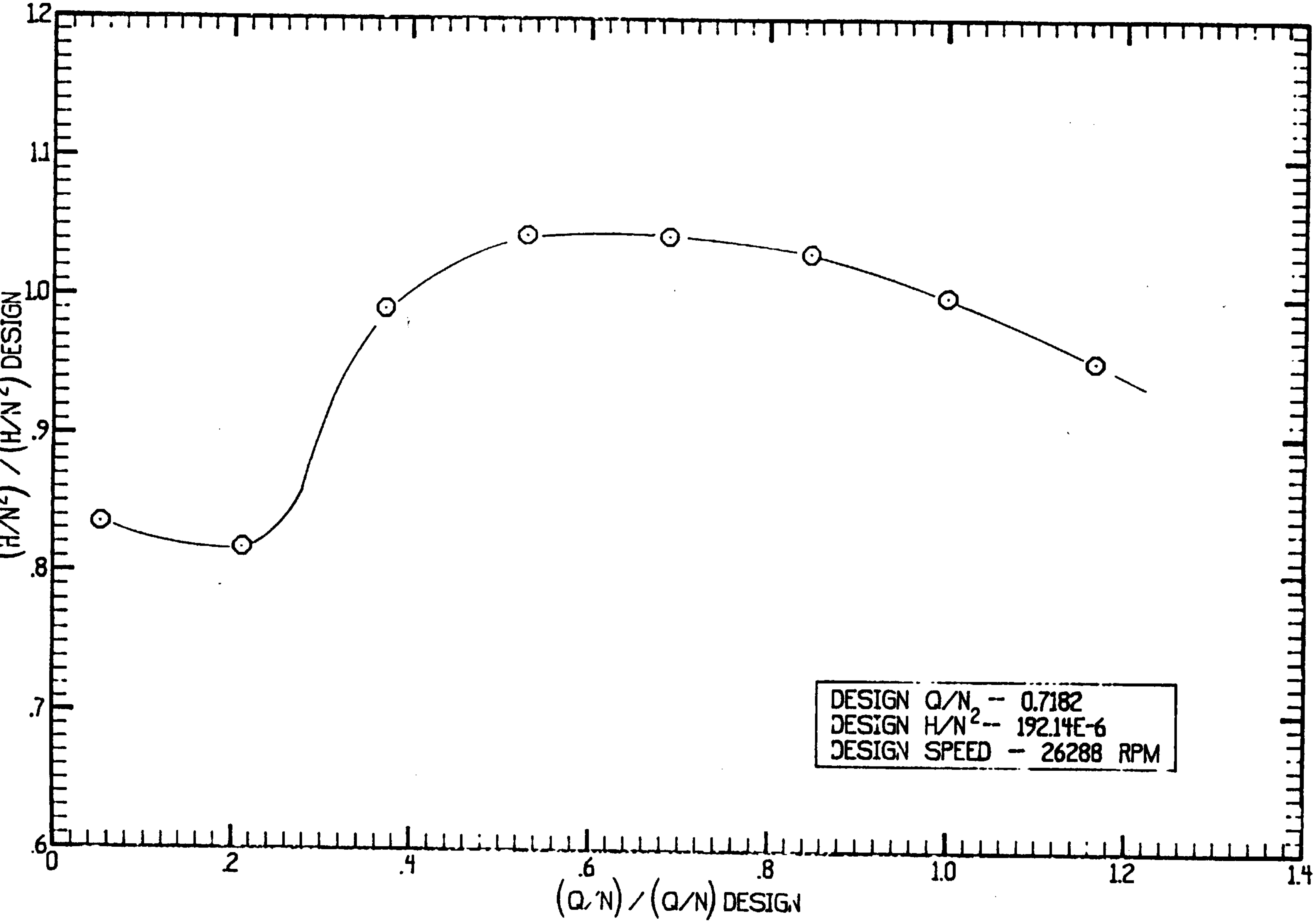

Figure 3-22. STME Main Hydrogen Pump Overall Head Flow Performance

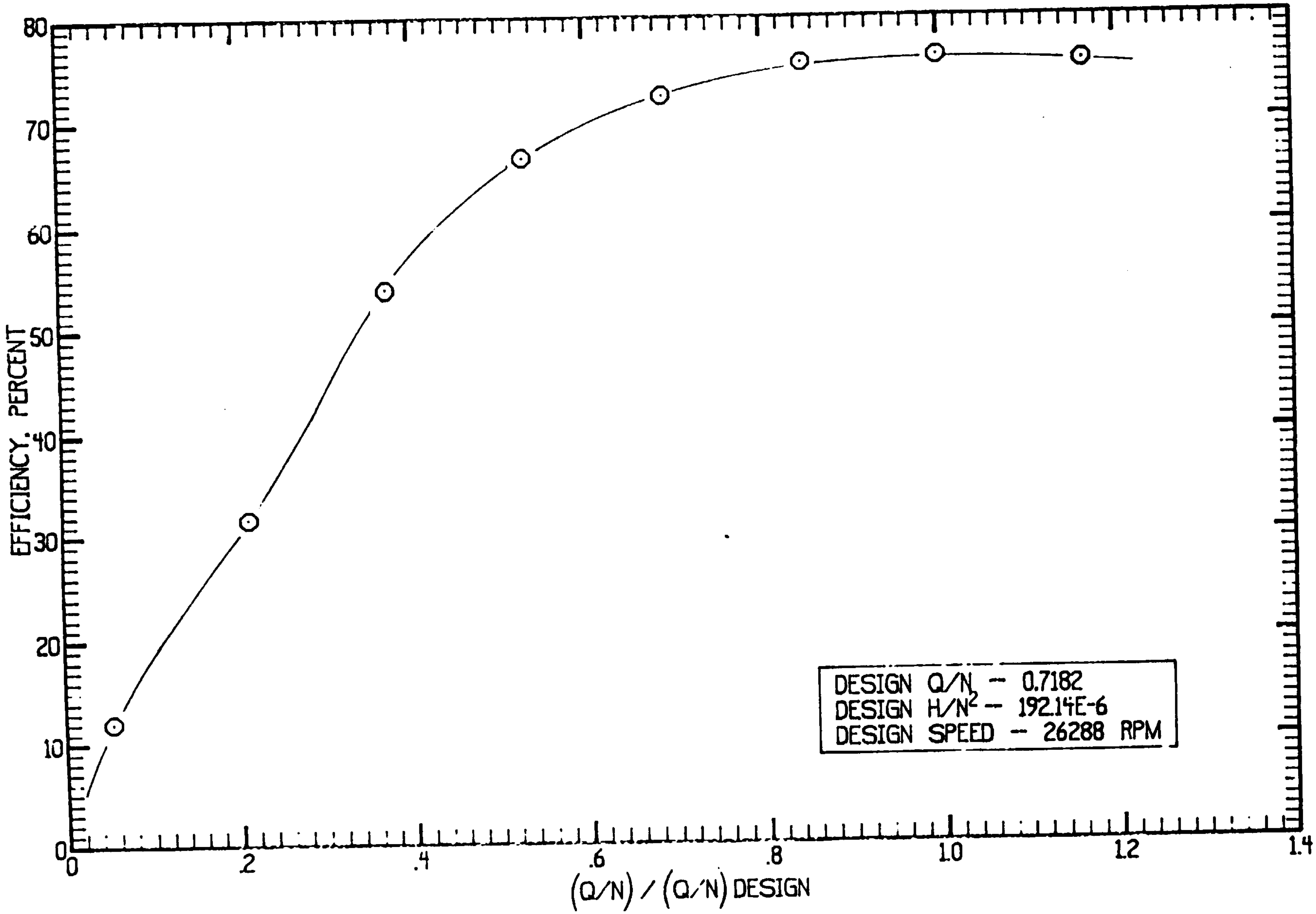

Figure 3-23. STME Main Hydrogen Pump Overall Performance

Table 3-19. STME Hydrogen Main Pump Design Conditions

PUMP TYPE	3 STAGE CENTRIFUGAL
INLET FLOWRATE, GPM	18881
HEAD, FT	132778
SPEED, RPM	26288
EFFICIENCY	76.0
REQUIRED SHAFT POWER, HP	58772
TURBOPUMP WEIGHT, LB	968
MINIMUM INLET NPSH, FT	245
DISCHARGE PRESSURE, PSIA	4544.4
STAGE SPECIFIC SPEED	1126
MAX. OPERATING SUCTION SPECIFIC SPEED	58249
BOOST PUMP TURBINE RECIRC. FLOW	N/A
BEARING DN, 10^6 MM RPM	2.05
SEAL RUBBING SPEED, FPS	441

Table 3-20. STME Hydrogen Main Pump Geometry

INDUCER:	
TIP DIAMETER, INCH	9.285
INLET HUB DIAMETER, INCH	3.71
DISCHARGE HUB DIAMETER, INCH	5.75
INLET HUB TO TIP RATIO	0.4
AXIAL LENGTH, INCH	2.1
IMPELLER:	
TIP DIAMETER, INCH	14.5
TIP WIDTH, INCH	1.036
EYE DIAMETER, INCH	9.35
HUB DIAMETER, INCH	5.75
DIFFUSER:	
INLET DIAMETER, INCH	15.5
DISCHARGE DIAMETER, INCH	18.8

VOLUTE:	
TYPE	SINGLE DISCHARGE
AREA, $INCH^2$	12.01
DIAMETER, INCH	22.3
DISCHARGE DUCT:	
DIAMETER, INCH	4.5

Table 3-21. STME Hydrogen Main Pump Hydrodynamic Design Parameters

	INDUCER	DIFFUSER	IMPELLER
INLET FLOW COEFFICIENT	.10		.132
DISCHARGE FLOW COEFFICIENT	.136		.0853
HEAD COEFFICIENT	.177		.55
TIP SPEED, FT/SEC	1065		1663.2
NO OF BLADES	4		5+5
TIP SOLIDITY	1.5		1.4
INLET BLADE ANGLE, DEG	10		19
INCIDENCE, DEG	2.4		4.5
DISCHARGE BLADE ANGLE, DEG	16		34
DEVIATION, DEG	1.3		17.3
RMS D-FACTOR	.30		
		DIFFUSER	
NO. OF BLADES		11	
THROAT ASPECT RATIO		0.69	
LENGTH/THROAT WIDTH RATIO		2.41	
INLET BLADE ANGLE, DEG		7.7	
INCIDENCE, DEG		0.1	
DISCHARGE FLOW ANGLE, DEG		23	
VELOCITY RATIO		0.825	
		VOLUTE	
DISCHARGE VELOCITY, FT/SEC		504.3	

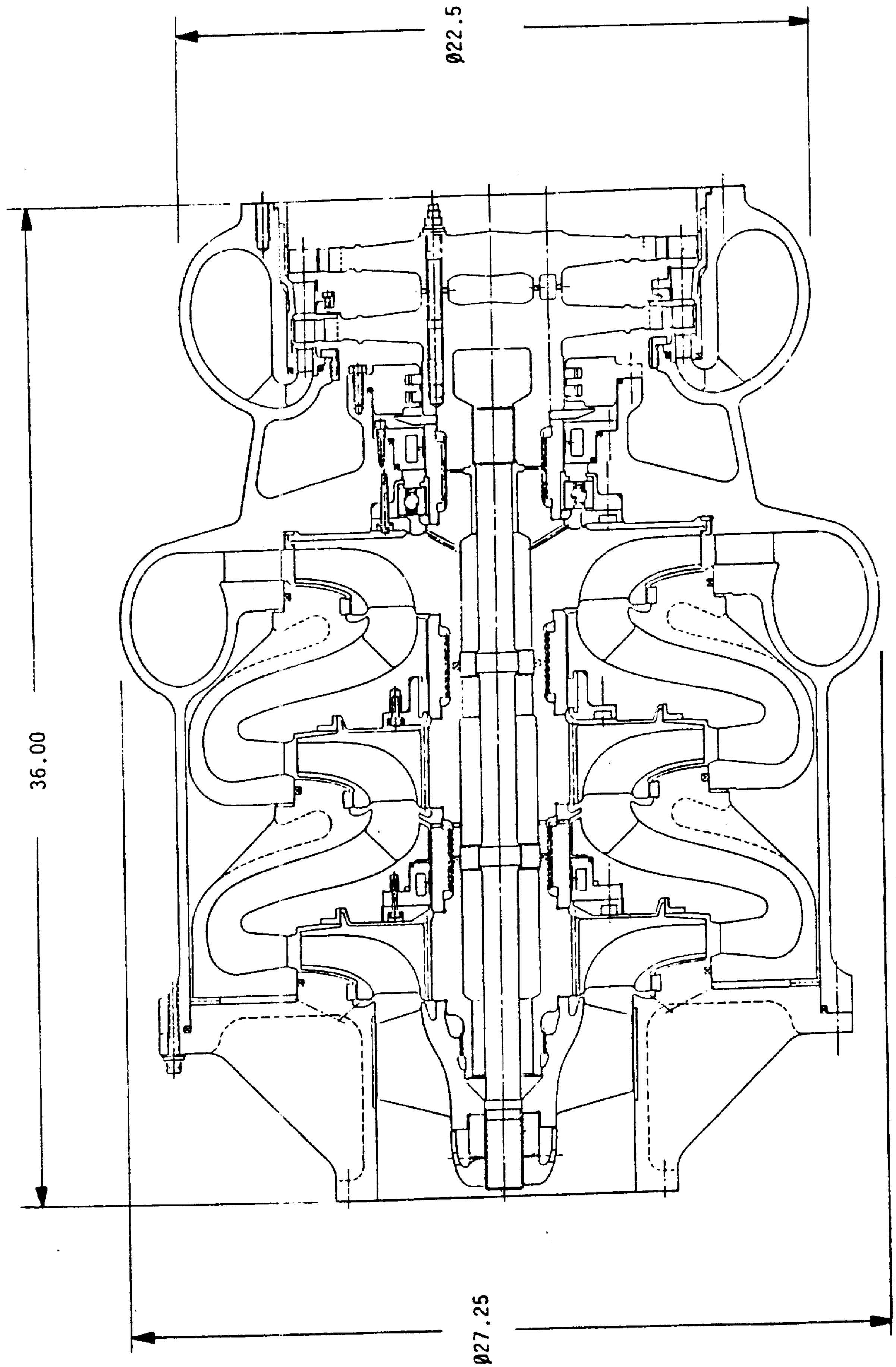

Figure 3-24. STME Hydrogen Main Turbopump

ORIGINAL PAGE IS OF POOR QUALITY

Table 3-22. LH_2 Main Turbopump Turbine Design Parameters (Two-Stage Turbine in LO_2 T/P)

• TURBINE TYPE	2 ROW PRESSURE COMPOUNDED	
• STAGES	2	
• PRESSURE RATIO	9.088	
• FLOW	43.875	LBM/S
• SHAFT POWER	59373	HP
• SPEED	26288	RPM
• EFFICIENCY	61.2	PERCENT
• MEAN DIAMETER	13.528	INCH
• MEAN BLADE SPEED	1550	FT/S
• OVERALL TURBINE VELOCITY RATIO	0.18	
• STAGE VELOCITY RATIO	0.208	T-T STAGE 1
	0.341	T-T STAGE 2
• STAGE LOADING COEFFICIENT	7.18	
	2.99	
• STAGE POWER SPLIT	70.6	PERCENT
	29.4	PERCENT

Table 3-23. LH_2 Main Turbopump Turbine Preliminary Design Geometry (Two-Stage Turbine in LO_2 T/P)

STAGE	1	1	2	2
BLADE ROW	NOZZLE	ROTOR	NOZZLE	ROTOR
NUMBER BLADES	59	83	73	91
% ADMISSION	100	100	100	100
MEAN DIAMETER (INCH)	13.528	13.528	13.528	13.528
BLADE DATA				
HEIGHT (IN)	0.548	0.721	0.824	1.052
WIDTH (IN)	0.80	0.80	0.824	1.052
PITCH (IN)	0.72	0.512	0.582	0.467
AXIAL SOLIDITY	1.111	1.562	1.889	1.713
OUTLET THROAT FLOW AREA (IN^2)	3.7557			
ZWEIFEL COEFFICIENT	0.504	0.913	0.910	0.929
INLET FLANGE AREA (IN^2)	13.908	FOR M = 0.15		
DISCHARGE FLANGE AREA (IN^2)	106.446			

Table 3-24. LH_2 Main Turbopump Turbine GASPATH Summary (Two-Stage Turbine in LO_2 T/P)

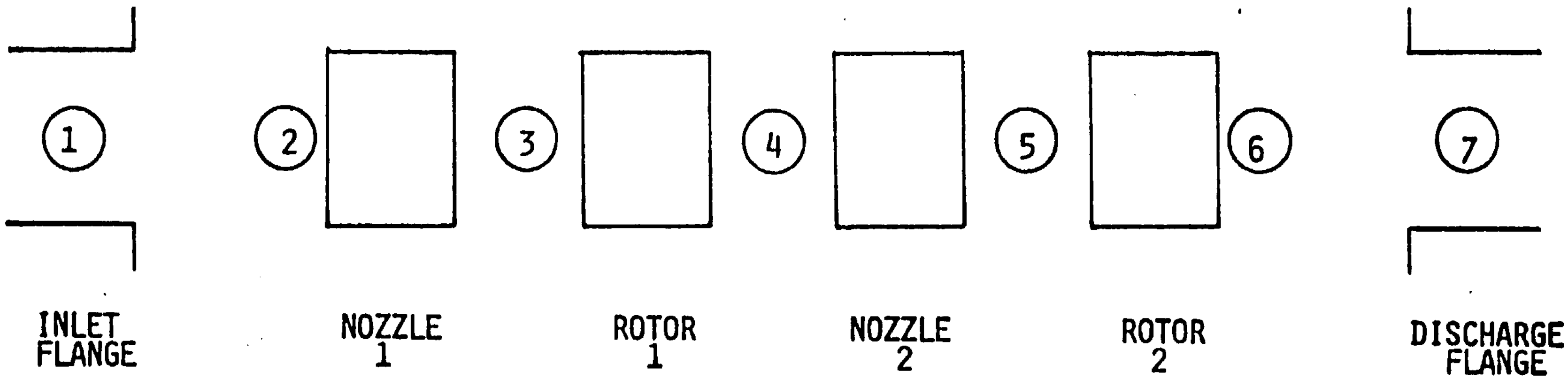

LOCATION			1	2	3	4	5	6	7
T_{TOT}	ABS	°R	1600	1600	1600	1272	1272	1135	1135
T_{TOT}	REL	°R			987		1187		
P_{TOT}	ABS	PSIA	2689	2648	2226	618	540	337	296
P_{TOT}	REL	PSIA			1362		422		
P_{STAT}		PSIA	2648	2648	391	391	325	296	291
DENSITY	LBM/FT^3		0.3037	0.5401	0.5378	0.1133	0.0957	0.0878	0.0838

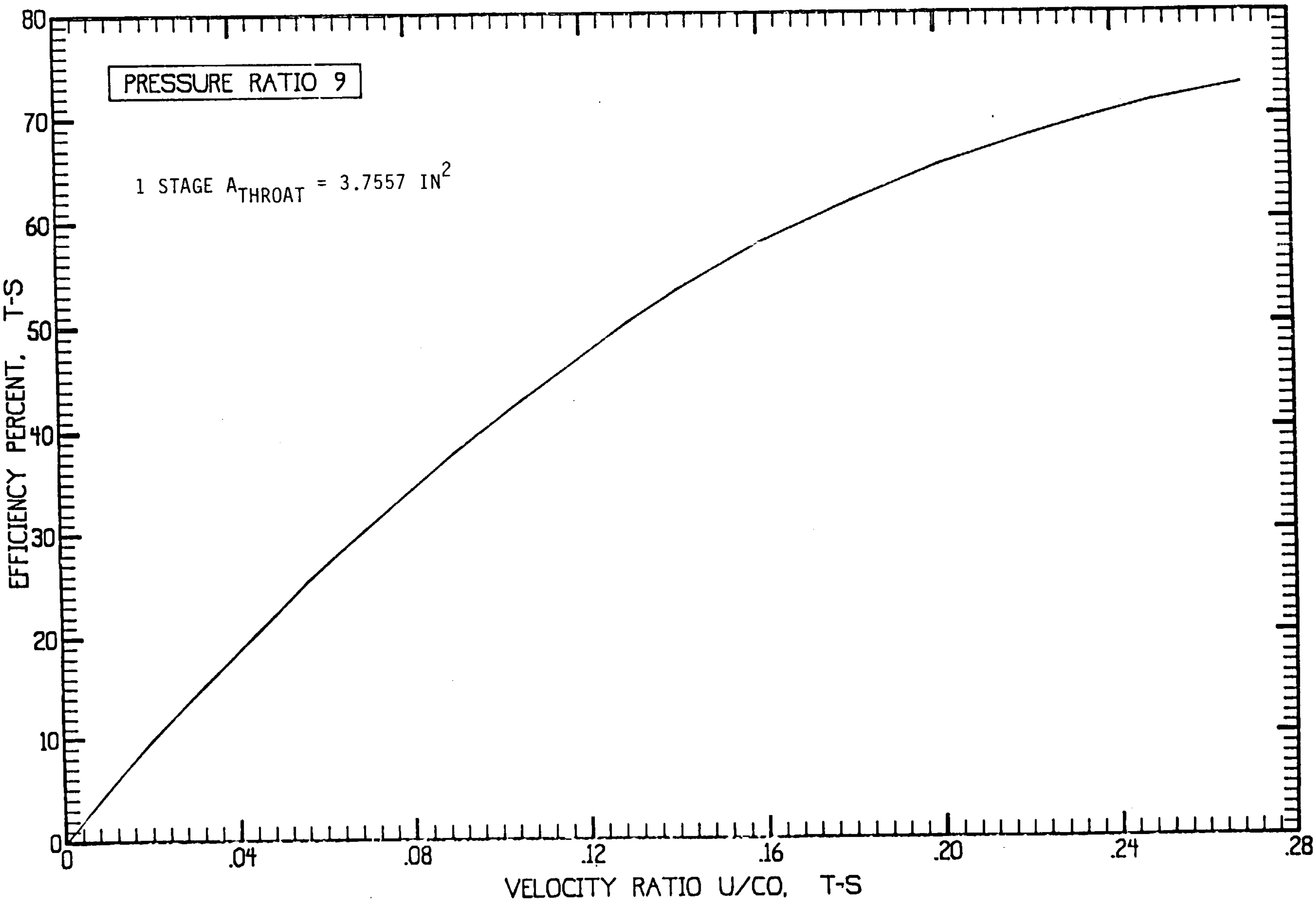

Figure 3-25. STME Hydrogen Main Turbine--Supersonic--Overall Performance

3.5.3 Hydrogen Turbopump Design

The hydrogen pump layout, with flow patterns indicated by arrows, is shown in Figure 3-26 and consists of three impeller stages preceded by an axial inlet and an axial inducer for optimum suction performance margin. The first two impeller stages are followed by diffusing crossovers that efficiently reduce the fluid velocity and present it to the next stage. The third impeller delivers the flow to a radial diffuser which, in turn, discharges into a single-discharge volute folded over to reduce the dimensional envelope. A two-stage pressure compounded turbine drives the turbopump. Hydrostatic bearings control radial shaft position behind the first-stage impeller and near the turbine wheel; the transient axial bearing is located adjacent to the balance piston behind the back face of the impeller third stage.

Historical data were reviewed for the main hydrogen turbopump to avoid the inspection and maintenance problem areas in existing hydrogen turbopump designs in a similar manner to that done on the oxygen turbopump presented earlier. The results are presented in Table 3-25 and indicate that the main areas of concern are bearing wear, balance piston transients, and turbine hot components life. In evaluating these problem areas, design features are incorporated to eliminate any problems previously encountered.

A producibility review of the hydrogen turbopump indicated design improvements necessary to minimize cost and lead time by enhanced producibility. The review results are given in Table 3-26. Again, the emphasis on castings, reduced welding, and improved materials shows the way for cost reductions incorporated in the design phase.

3.5.4 Hydrogen Turbopump Rotordynamics Analysis

The baseline main hydrogen pump operates above its first critical speed as shown in Figure 3-27. It satisfies the rotordynamic margin requirements for the 0.003-in. clearance hydrostatic bearing, but violates the criteria for larger clearance (and therefore softer) bearing designs. Thus, additional

C - 2

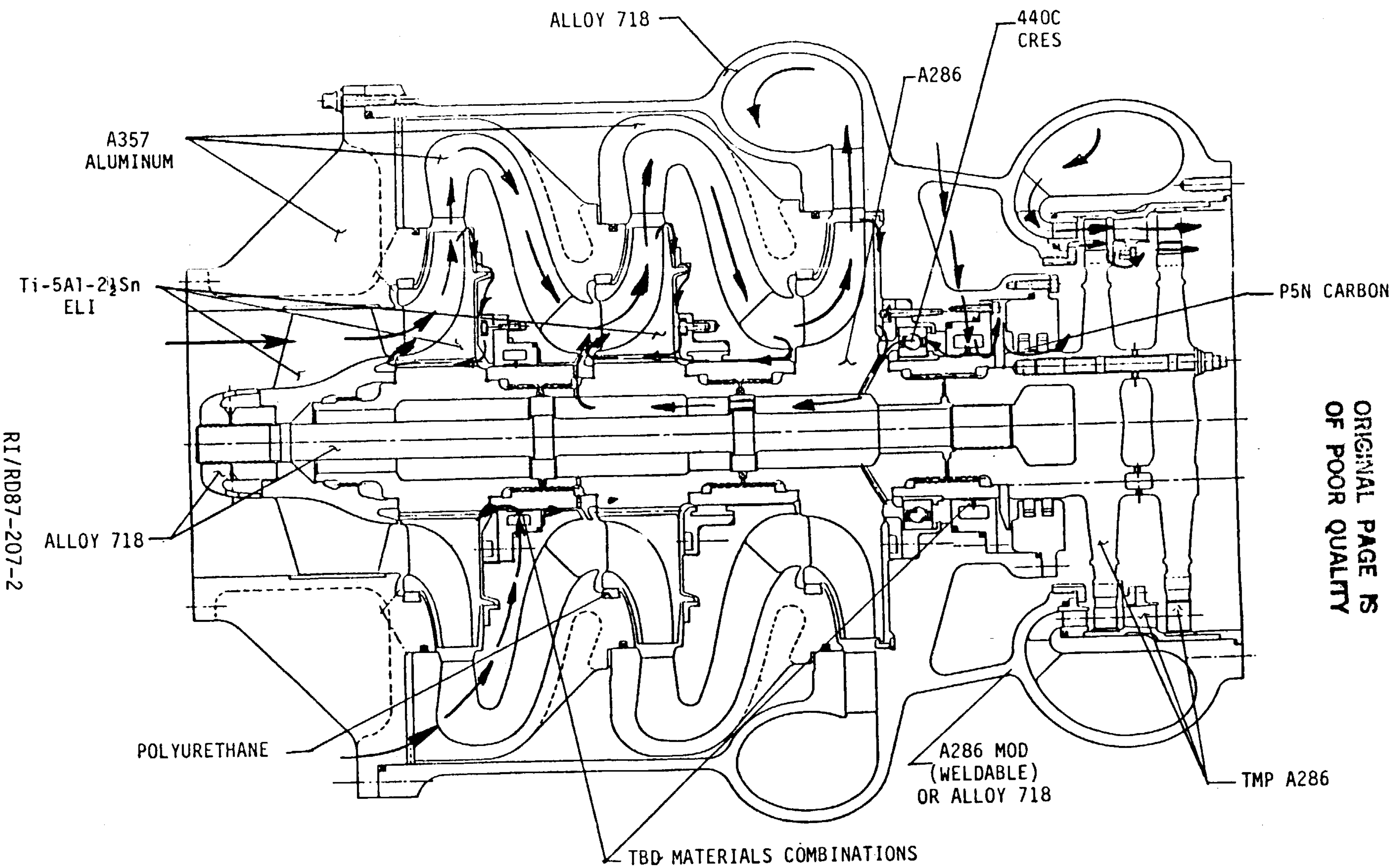

Figure 3-26. STME Hydrogen Main Turbine

ORIGINAL PAGE IS
OF POOR QUALITY

Table 3-25. Reusable Maintenance History Influences STME Designs Hydrogen Turbopump

Inspection Required in Maintenance History	Cause	STME Design Features
Thrust bearing wear	Rubbing wear	Large capacity transient thrust brg.
Radial bearing wear	High loads High speeds	Hydrostatic bearings Minimize radial loads Monitor bearing condition
Moisture in turbine bearings	Stress corrosion limits	No bearing hoop stress
Balance piston wear	Deflections/stack Overlap operation	Thrust control bearing No overlap
Bellows shield cracks	Flow-induced dynamics	Improved design
Turbine blade cracks Turbine sheet metal cracks Tip seal, fish mouth seal cracks Turbine blade erosion Nozzle cracks, erosion	Thermal induced-LCF High temp spikes Cooled blades	GG-cycle controlled start Eliminates temp spikes Lower temp to 1600°R Material changes Segmented nozzles
Blade dampers lost	Fit-tolerance	Improved damper design
Lift-off seal leak checks	Potential leakage	Improved designs
Impeller seal wear	Material durability	Improved material

87D-9-2582

Table 3-26. Producibility--STME Hydrogen Turbopump

Component	Material	SSME Equivalent	Remarks
Pump inlet	• Casting A357 Al alloy	• Weldment 5-2.5T_i	• Eliminate welding • Eliminate complex machining
Pump diffuser and volute	• Casting Inco 718	• Weldment Inco 718	• Eliminate welding • Eliminate complex machining • Axial inlet replaces tangential inlet
Turbine housing	• Forging modified A286	• Forging Inco 718 and 903 HEE protection • Sheet metal liner	• Eliminate HEE protection requirements • Reduce complexity • Eliminate non-inspectable welds • Eliminates need for sheet metal liner
Turbine disc	• Forging TMP A286	• Forging WASPalloy HEE protection	• Eliminate HEE protection requirements
Turbine blades	• Forging TMP A286	• Casting DS MAR-M-246	• Eliminate HEE-assisted cracking
Turbine nozzle and stator	• Forging TMP A286	• Casting MAR-M-246	• Eliminate HEE-assisted cracking
Impellers	• Forging 5-2.5T_i	• Forging Omcp 89	• No change in material
Inducer	• Forging 5-2.5T_i	• Forging 5-2.5T_i (LPFTP)	• No change in material
Inner Stage Crossovers	• Casting A-357 Al alloy	• Casting tens 50 Al alloy	• Improved material

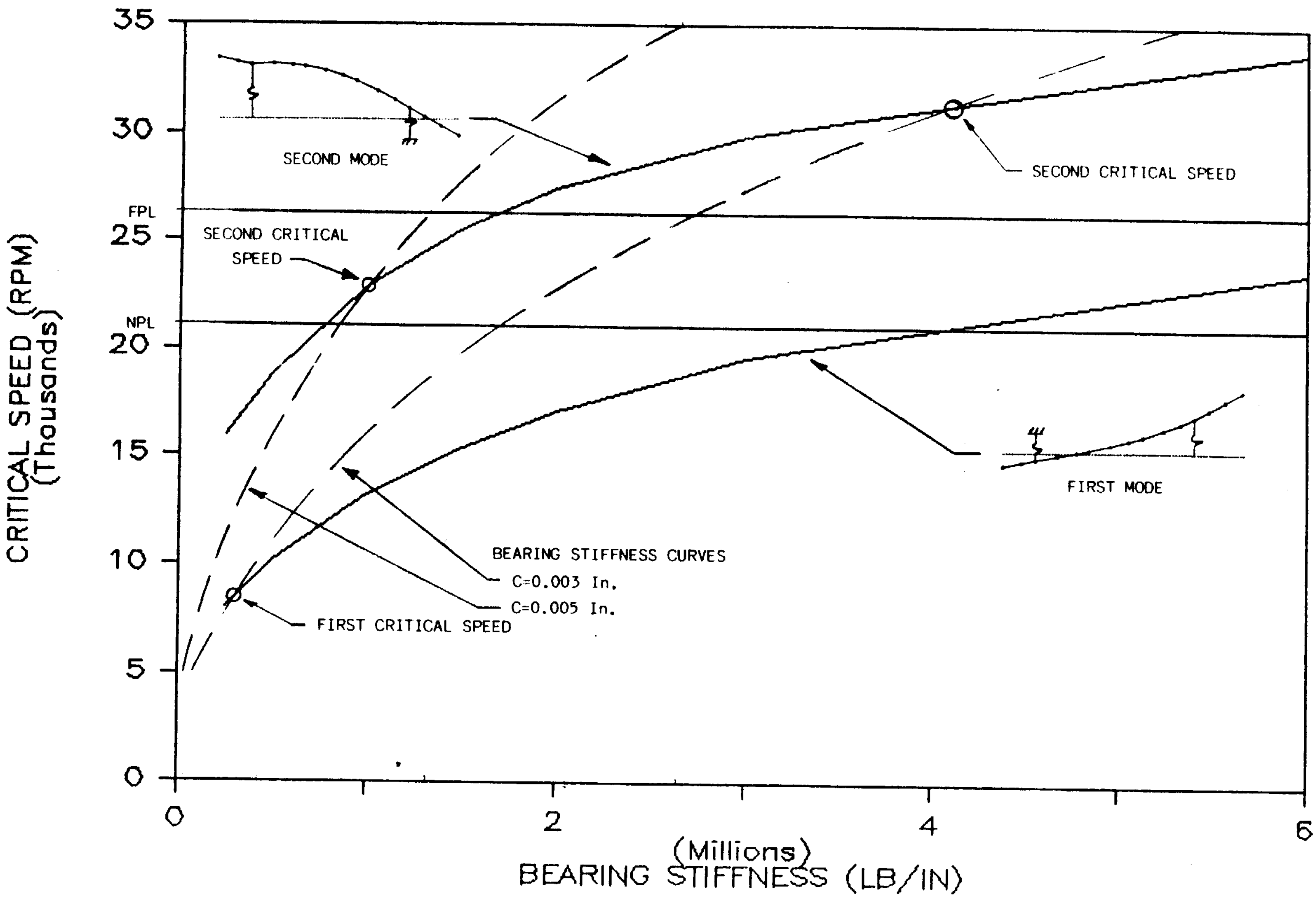

Figure 3-27. STME Hydrogen Turbopump Critical Speeds--Baseline Configuration

design iterations may be required to provide greater natural frequency separation. This will be achieved by reducing pump-end overhangs to increase the frequency of the second mode. The frequency of the first mode violates the stability criteria and can best be controlled by increasing turbine bearing stiffness, if possible, or reducing turbine mass and/or overhang to provide the requisite margin. Operation below the first critical speed is not considered possible given the basic mass distribution and the range of available bearing stiffnesses. Like the main LO_2 pump design, super-critical operation provides the best solution to the design requirements for the main hydrogen pump.

3.5.5 Use of SSME High-Pressure Fuel Turbopump

Using the SSME HPFTP for the STME LH_2 pump was investigated. Table 3-27 compares the pump operating conditions for the SSME full power level (FPL) operating point and the optimum STME operating point at 580,000 thrust. The pump operates at a Q/N higher than the SSME FPL operating point, and is outside our current operating experience. The poor suction performance of the pump at this point (observed in separate component tests) would require a low-pressure or boost pump. The current SSME low-pressure fuel turbopump (LPFTP) could be used, but would require a redesign to the HPFTP to include an inducer upstream of the first stage. Alternatively, a new boost pump could be designed. In either case, significant system modifications would be required to supply warm gas to drive the boost pump.

These issues, combined with the fact that a new turbine design would be required due to the different engine cycle (raising serious questions about axial thrust balance), led to the SSME HPFTP being rejected as a candidate for the STME LH_2 pump.

Table 3-27. Use of SSME HPFTP for STME Fuel Turbopump

	SSME FPL	STME
FLOW, GPM	17000	18737
SPEED, RPM	36352	34500
HEAD, FT	190079	147913
(Q/N)/(Q/N) DESIGN	1.0	1.16

3.6 MATERIAL SELECTION

3.6.1 Introduction

A preliminary evaluation of the materials requirements for the STME turbomachinery was completed. This was done in conjunction with the conceptual design coupled with the producibility evaluations previously cited. The turbopump conceptual layouts have been presented in Figures 3-9 and 3-26, respectively, for the oxygen and hydrogen main turbopumps and in Figure 3-11 for the LO_2 boost turbopump. These figures show a proposed selection of material to be used for the turbopump. The following is a general rationale for the selection of the major materials. Included in the discussion are areas identified where materials technology programs are in place or where they will be required to support the STME program.

3.6.2 Material Selection Rationale

The material choice for the majority of components in the main turbopump turbines is A286, in several forms. This choice is based largely on the material's proven resistance to hydrogen environment embrittlement (HEE) and its ability to be modified for higher strength and improved weldability.

A compositionally modified and thermomechanically processed variant of A286 is being developed at Rocketdyne for improved strength. Room temperature ultimate strength of 185 ksi and yield strength of 140 ksi have been demonstrated on laboratory-scale heats with no degradation of HEE resistance. This is the material of choice for the main pump turbine discs and blades, and interstage nozzle and turning vanes, if these are wrought. Consideration is being given to electrochemically milling blades integral with the disc if unshrouded turbines can be tolerated.

If it should prove more desirable to use cast blades, interstage nozzles, and turning vanes because of design complexity and producibility issues, a number of material choices are available. The most attractive at the moment appears to be 713LC (Hafnium modified) as a fine-grain casting. It has good strength and ductility over the temperature range; the fine grain and small carbide size provide resistance to high-cycle or low-cycle fatigue crack initiation. Conventionally cast material does show degradation in hydrogen (HEE), but data are not available for microcast material. Higher strength alternatives include IN-738, IN-100, and MAR-M-200(DS). A test program would be required to evaluate selected materials produced by up-to-date casting techniques with respect to their mechanical properties and hydrogen behavior.

The main pump turbine housings require a material that is castable and/or weldable. Conventional A286 is not readily weldable. A test program is underway at Rocketdyne to evaluate the gas tungsten arc and electron beam weldability of compositionally modified A286. The program includes variations on postweld heat treatment, mechanical testing, and evaluation of HEE resistance. In anticipation of favorable results, a modified, weldable A286 has been baselined for the main pump turbine housings; however, it may prove desirable to be able to cast the turbine housing. A286 has been investment cast, but few data are available, and no known foundry presently casts the alloy. An alternate, also inherently HEE resistant and also with little characterization, is a cast version of alloy 909. Both of these alloys would need to be the subject of a substantial development program if they were to be used for the application. A third alternate is alloy 625, which is readily cast and welded and well characterized. However, it is easily embrittled by hydrogen and careful design would be necessary to ensure its utility. Conventional A286 has been chosen for various nuts, bolts, and shafts. It has adequate strength, good ductility, and an extensive history of satisfactory performance in a wide variety of Rocketdyne engine hardware.

Alloy 718 has been chosen for a number of major components in all of the pumps where high strength and good cryogenic ductility are important. Again, there is extensive experience with this alloy in a variety of applications in both cast and wrought forms. Recent improvements in casting techniques have eliminated core reaction (rough, contaminated surfaces) on internal passages of castings; e.g., pump volutes. However, some casting development will be necessary for the specific configurations of these pumps' components.

Because of rotordynamic considerations, high specific strength (strength to weight ratio) materials are desirable for rotating elements such as inducers and impellers. Titanium alloys provide the highest specific strength of metallic materials. While titanium alloys cannot be used in LO_2 because of ignition concerns, Ti-5Al-2 1/2 Sn extra-low interstitial (ELI) has been chosen for the hydrogen main pump inducers and impellers. This particular alloy was chosen because, in its ELI form, it has the highest cryogenic toughness of any of the well-characterized titanium alloys. In addition, Rocketdyne has considerable experience with its use in a variety of fuel turbopumps.

Monel-K-500 is used for parts where rubbing may occur in LO_2. While it has good cryogenic properties, its resistance to ignition is the prime reason for selection in these applications.

The main pump bearings see low loads under transient conditions. It is considered, therefore, that 440C, the standard bearing material, will be more than adequate for the job. The booster pump bearings, however, are used more conventionally. In that case, material improvements to reduce wear and extend life are appropriate. There are several ongoing technology programs screening potential bearings materials for use in cryogenic liquids.

Final choice of the bearing material combinations (including, hopefully, a lubricating cage) will depend on the results of these programs. Based on present-day knowledge, the materials of choice would be ion-implanted CRB-7 balls and raceways with a cage material containing teflon.

P5N and G84 carbon materials have been used for seals in numerous turbopumps with excellent results. P5N contains lithium fluoride, which provides some lubrication when working with the nonlubricating cryogenic fluids. G84 is more normally used in the higher temperature environments. Choice is largely based on satisfactory experience.

KEL-F has been used for soft seals in previous turbopump designs. It requires a complicated and expensive machining/stress-relieving sequence and must be mechanically attached. Cast-in-place soft seals of polyurethane have been chosen for the main hydrogen pump to improve producibility and simplify design. Polyurethane has been shown to be thermal shock resistant and chemically compatible with LH_2. Experience with its use in a turbopump environment, however, is limited. For the LO_2 pump, compatibility considerations preclude the use of castable polymerics. As such, a machined seal of Vespel SP211 is recommended. Vespel SP211 has better high-temperature capability than KEL-F and is probably more resistant to internal frictional heating.

No material combinations have yet been selected for the main pumps' hydrostatic bearings and counterfacing shaft sleeves. When operational, these two surfaces are not in contact and so offer few materials challenges. However, during startup and shutdown, when fluid of sufficient pressure is not being delivered to the bearing, there will possibly be quite severe rubbing. Estimates of loads and durations are required before potential material selections can be narrowed down. The materials chosen must be compatible with the propellants and, in the case of the LO_2 pump, LO_2 compatible and ignition resistant. It is believed that low friction will be very important for startup and low wear rate will be essential to preserve geometry. In light of those two requirements, it seems likely that some form of active and replenished lubricant will have to be provided. In addition to tribological properties, selected materials' physical and mechanical properties will have to be considered, as well as such attributes as resistance to thermal shock. Materials combinations for hydrostatic bearings running in LH_2 and LO_2 are being evaluated or are planned for evaluation in technology programs at Rocketdyne. These programs will study both parametrics and materials behavior. These applications may prove necessary should presently available materials not perform well. In that case, additional fundamental materials technology effort will be required.

3.7 COMMONALITY

3.7.1 System Studies for Pump Commonality

Traditional approaches to commonality attempt to design the pump to operate over a wide operating range to accommodate the requirements of the system. In this study, the required thrust ratio of the STBE and STME engines was calculated for totally common MCC and LO_2 pumps. Thrust chamber characteristics were obtained from engine balance studies in the form of ratios of thrust, chamber pressure, and LO_2 flow between the STBE and STME engines for common MCCs. Figure 3-28 shows the results of this study showing that for totally common pumps operating at the same Q/N, the STME to STBE vacuum thrust ratio should be 1.283 and the chamber pressure ratio should be 1.224.

Figures 3-29 and 3-30 can be used with Figure 3-28 to assess the effect of operating the totally common pump at an off-design Q/N. Two of the major issues of off-design operation are addressed by these charts: cavitation damage susceptibility at low Q/N operation and volute-generated radial loads. Figure 3-29 shows a typical suction performance characteristic for 2% head loss and ranges of allowable operation for expendable and reusable applications that avoid excessive cavitation damage on the inducer blades. The dashed line indicates the locus of operating points of the STME LO_2 pump if the pumps and the MCC are completely common (the pump design point must be set for the STBE operating conditions as it has the more stringent suction performance requirements). This shows that, with the current thrust levels, totally common LO_2 pumps are not possible.

Figure 3-30 shows the pump H-Q curve for the totally common pump with lines of constant radial load indicated. Again, the dashed line shows the locus of STME operating points for common MCC and indicates that, for the current thrust levels, the radial loads would be doubled. Although it is planned to minimize steady radial loads through using double-discharge or double-tongue volutes, this plot also indicates the general level of dynamic loads on the rotor and can be used as an operating risk indicator.

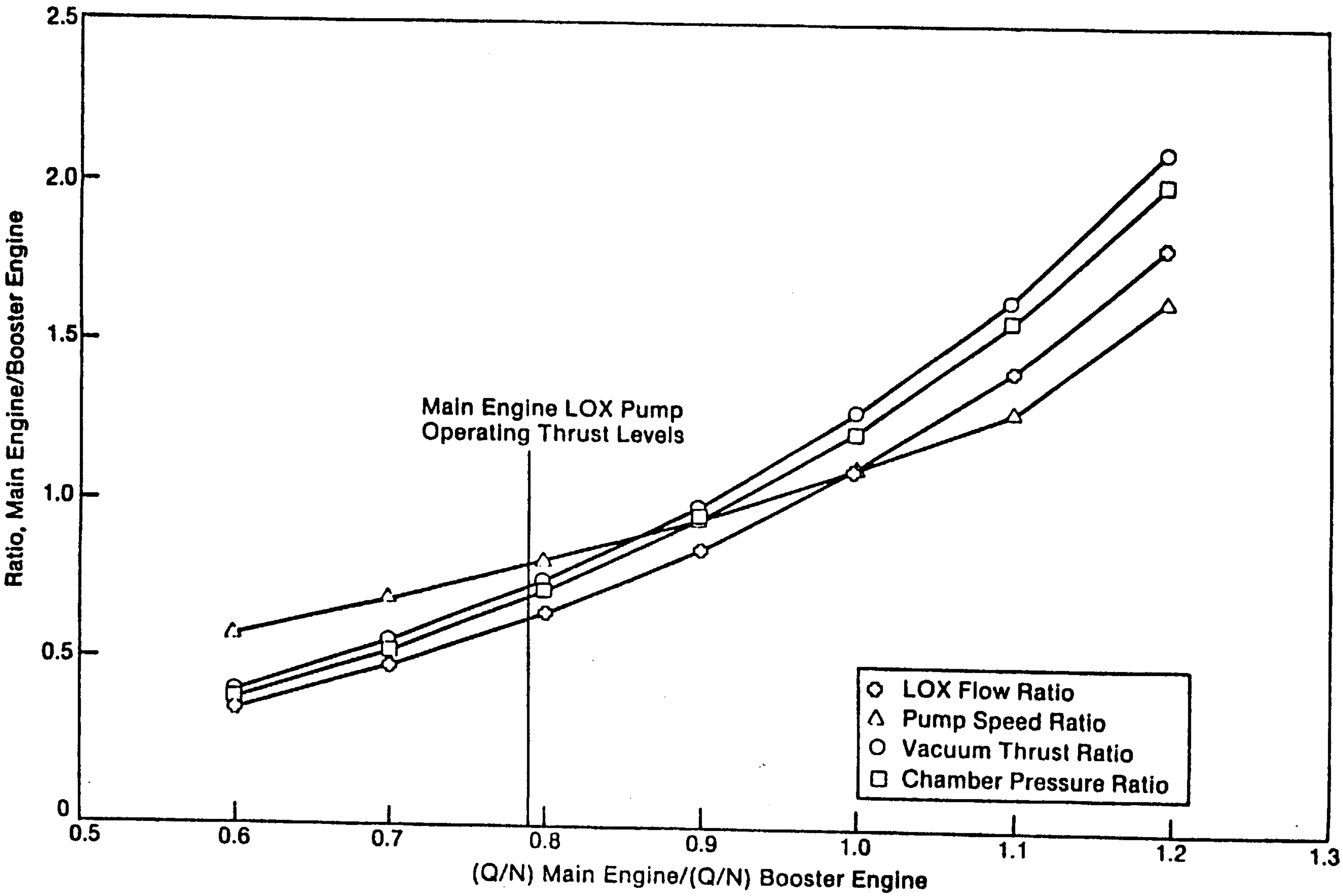

Figure 3-28. System Characteristics with Common LO_2 Pumps

87D-9-3195

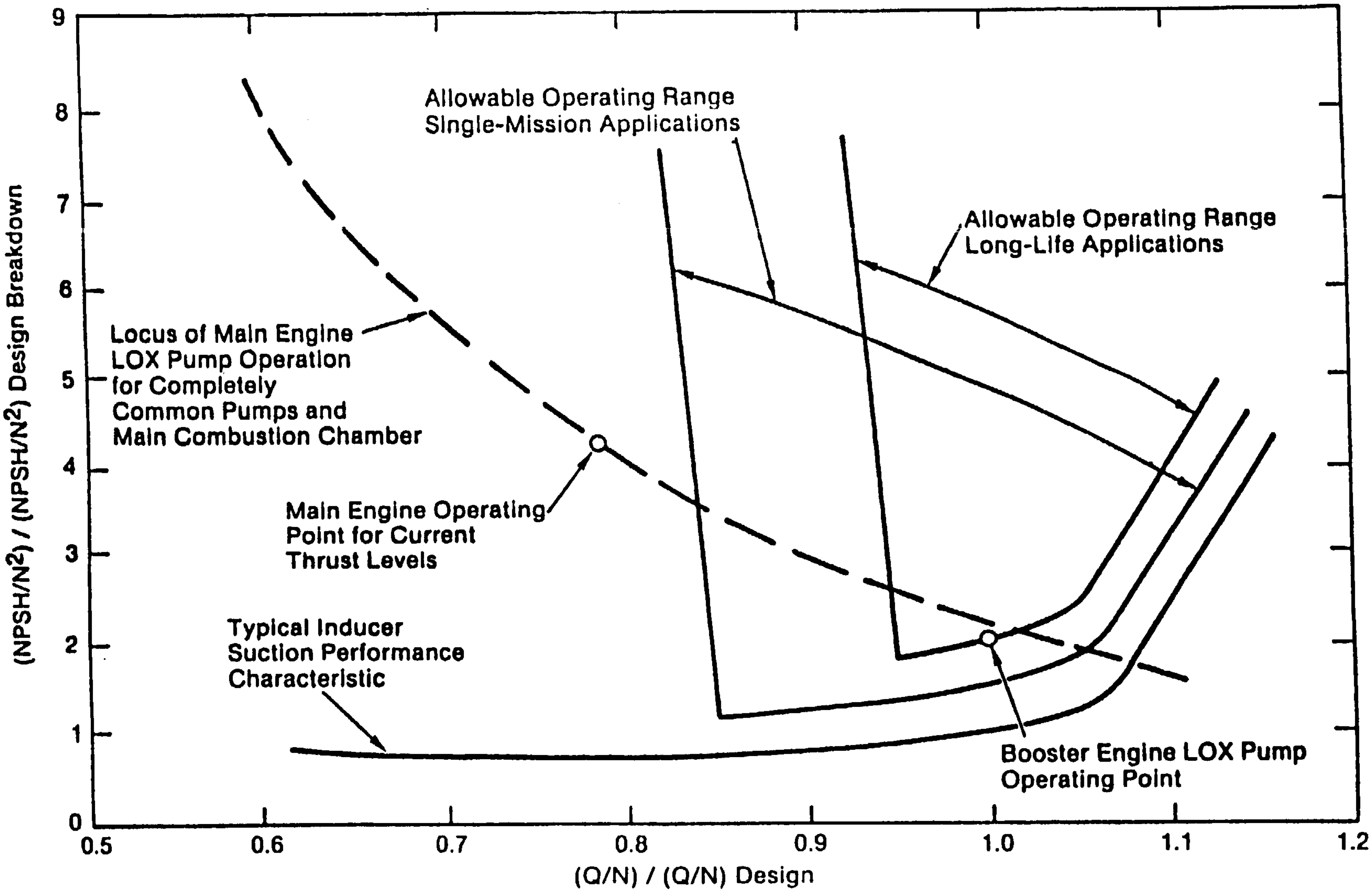

Figure 3-29. Suction Performance Characteristics of Common LO_2 Pumps

87D-9-3193

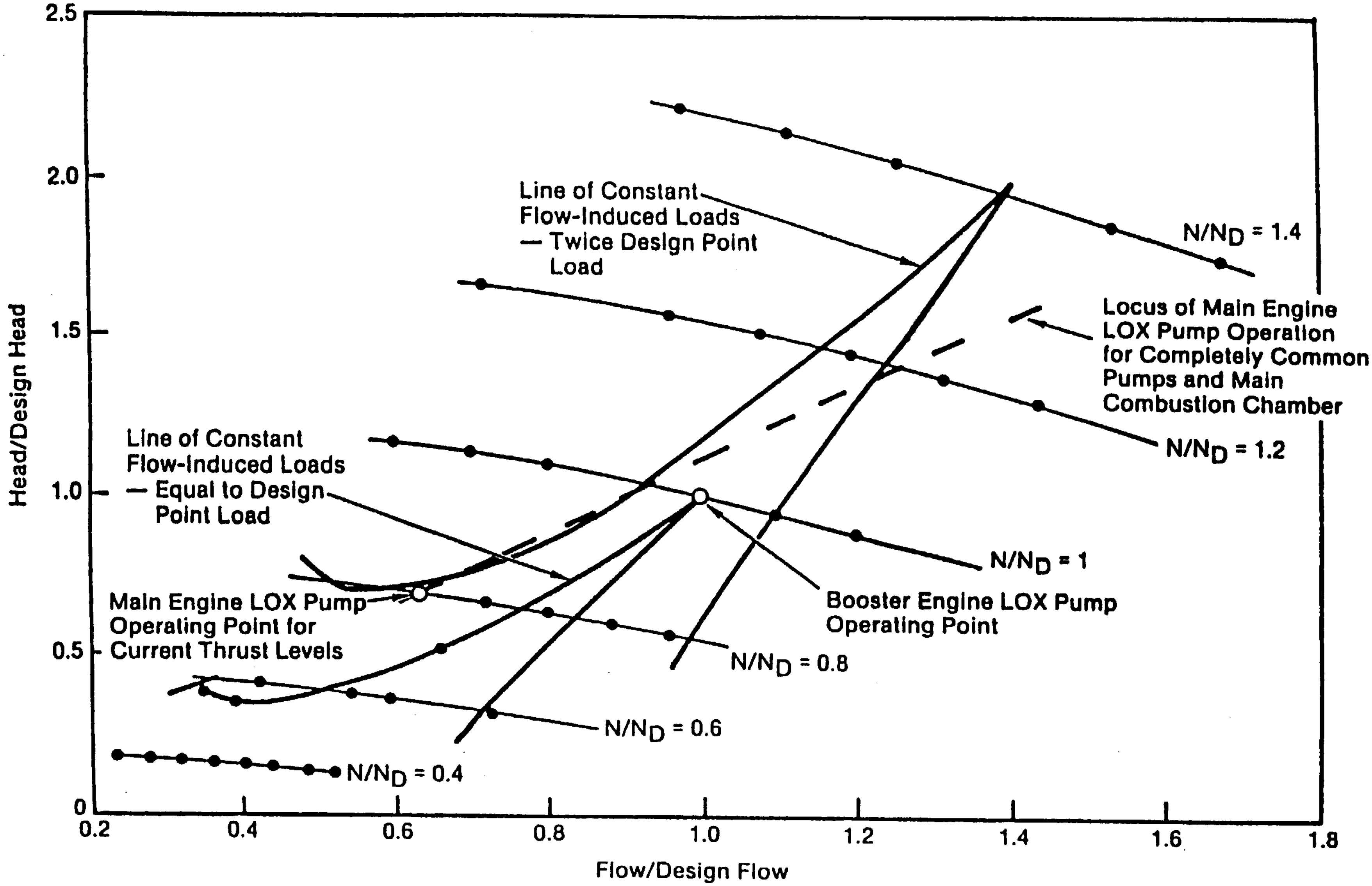

87D-9-3196

Figure 3-30. Operating Characteristics of Common LO_2 Pumps

3.7.2 Pump Commonality with Compromised Turbomachinery

Since it is not possible to design common turbopumps for the current engine thrust levels, the number of pump elements that could be common was investigated. A high priority was placed on making the expensive components common (e.g., housings). Two combinations of common pumps were investigated: STBE LO_2/STME LO_2 and STBE LO_2/STME LO_2/STBE methane. The balances for a common MCC were used, which had a 3,600-psi chamber pressure for the STBE engine, and a 2,464-psi chamber pressure for the STME engine. These compare to 3,000 psi and 2,689 psi, respectively, being used for the optimum engine at this time (see Table 3-1).

It was found that it was possible to use a totally common housing with separate inducers and impellers if a vaned diffuser was not required and a double-discharge or double-tongue volute was used. The double volute reduces the steady radial loads and removing the vaned diffuser eliminates the dynamic loads due to diffuser stall and the severe incidence mismatch that would occur at the off-design conditions. Since diffuser vanes are generally required in a high-pressure turbopump to carry the volute separating loads, configurations with diffuser vanes were also considered. It was found that the incidence range on the diffuser vanes was too large even when the hydrodynamic design of the impellers was severely compromised; thus, the baseline common configuration with vaned diffusers required separate diffuser vanes for each pump.

At this stage of the study, the configuration with separate bladed components (inducer, impeller, and diffuser) was selected pending stress analysis to determine whether diffuser vanes were required and, if they were, whether a bolt-in arrangement could be used. Tables 3-28 and 3-29 show the key parameters for the two common pumps investigated.

Table 3-28. Common LO_2 Pumps with Common MCC

Configuration	STBE		STME	
	Non-Common Turbopump	Common Turbopump	Non-Common Turbopump	Common Turbopump
P_c target (psia)	3.600	3,600	2,689	2,464
Flow (gpm)	12,362	12,362	7,854	7,703
Speed (rpm)	14,400	14,400	16,500	11,500
Efficiency (%)	79	79	81	76
Power (hp)	47,735	47,735	22,595	21,089
Weight (lb)	1,247	1,247	721	1,247
Impeller tip diameter (in.)	13.65	13.65	10.6	13.65
Impeller tip width (in.)	0.91	0.91	0.93	0.83
Diffuser width (in.)	1.00	1.00	0.98	1.00

Table 3-29. LO_2 Pump for LO_2/LO_2/Methane Commonality

CONFIGURATION	NON-COMMON TURBOPUMP	COMMON TURBOPUMP
Pc TARGET, PSIA	2689	2464
FLOW, GPM	7854	7652
SPEED, RPM	16500	9850
EFFICIENCY	81	77
POWER, HP	22595	20970
WEIGHT, LB	721	1329
IMPELLER TIP DIAM., INCH	10.6	15.9
IMPELLER TIP WIDTH, INCH	.93	.83
DIFFUSER WIDTH, INCH	.98	.89

3.7.3 Turbine Commonality Studies

In contrast to the historical trend of emphasizing maximum performance and minimum weight, the design of the STME and STBE engines has introduced minimum cost as a major consideration spanning both initial cost and life-cycle costs. For the turbines, this has meant that some compromise on turbine performance would be acceptable if lower cost could be achieved through commonality of turbine components. A wide range of possible actions has been considered with initial effort focused on the approaches that alter the optimized configurations the least. Much of the turbine commonality work has been focused on the STBE turbines, but the following turbine commonality cases have been completed for the STME and are reported in the following:

- STBE LO_2 main--STME LO_2 main
- STBE LO_2 and CH_4 main--STME LO_2 main.

Table 3-30 summarizes the approach taken in the turbine commonality studies. To minimize cost, the investigation held housings and other castings, inlets, inlet volutes, and turbine discs common across the turbines under consideration. Turbine speeds and powers were hard constraints based on pump requirements. Turbine inlet gas conditions were established by the gas generator and were held as hard constraints. Hard constraints were not modified in this study regardless of impact. Soft constraints were those that were highly desirable but that could be violated when necessary. Soft constraints were the gas conditions at the discharge of the STME LO_2 turbine and the geometry of the first nozzle of the "common" turbines.

To achieve commonality in the turbines, the following parameters were varied: admission, discharge gas conditions, number of stages, and blade geometry (in approximately the order given). Turbine flow area is set by the turbine flow necessary to generate the required power. Turbine diameter is set under the conflicting demands of increasing diameter to achieve greater velocity ratios (and thereby efficiencies) and decreasing diameter to meet tip speed limits. Partial admission is used to maintain reasonable blade heights

Table 3-30. STBE/STME Turbine Commonality Approach

- HARDWARE COMMON TO TURBINES
  - HOUSING, CASTINGS
  - INLETS, INLET VOLUTES
  - TURBINE DISKS
- CONSTRAINED TURBINE PARAMETERS
  - FROM PUMPS
    - SPEED (HARD)
    - POWER (HARD)
  - INLET GAS CONDITIONS (HARD)
  - DISCHARGE GAS CONDITIONS (SOFT)
  - FIRST NOZZLE GEOMETRY (SOFT)
- VARIABLES TO ACHIEVE COMMONALITY (APPROXIMATE ORDER)
  - ADMISSION
  - DISCHARGE GAS CONDITIONS
  - NUMBER OF STAGES
  - BLADE GEOMETRY (PROFILES, HEIGHT)
- CONSEQUENCES
  - EFFICIENCY, FLOW, SIZE, WEIGHT
  - NEED SYSTEM & VEHICLE ASSESSMENT

when turbine diameter and required flow area would combine to produce very short blades. For small low-power turbines, partial admission has often been successfully used at Rocketdyne. However, for high-power turbines, the increased blade loads that are generated as the rotor blades pass in and out of the arc of admission could cause significant reductions in turbine blade life and margin. In addition, the operating characteristics of high-power turbines with partial admission have not been established.

The alternative method of providing the appropriate turbine flow area at a given turbine diameter is variation in blade height. With this option, turbine commonality is sacrificed. With a liner at the tip, however, commonality in the housings and turbine discs can be maintained. A possibility still exists of common blade profiles for the common turbines, but for the turbine with the smaller blade heights, the turbine blades would be machined to the appropriate height.

3.7.4 Common STME LO_2/STBE Tri-Propellant LO_2 Turbines

Table 3-31 shows the results of a study of commonality for the turbines for the LO_2 pumps for the STBE tri-propellant and the STME engines. In this case, full admission is used and the blade heights are varied to achieve the required flow area. The performance was established for optimized turbines so that both the turbine heights and the turbine blade profile shapes vary. Thus, different blading would be required for the two turbines. Inlet and discharge flange areas have been set by the STME LO_2 turbine. The mean diameter of 17.5 in. is, of course, common to both turbines, but has been reduced from the 21.65-in. value for the optimized STME LO_2 turbopump to provide a better match to the pump-end dimensions. Because of the resultant lower velocity ratios, the turbine efficiencies are lower and the turbine flow rates higher. The configuration of the hot gas flow path has been retained; this configuration uses a pressure ratio of 20.2 for the STBE LO_2 turbine and 2.49 for the STME LO_2 turbine. Such large differences in inlet pressure and in pressure ratios pose severe problems for turbine commonality. Because of the lower inlet pressures, the blade heights for the STME LO_2 turbine are

Table 3-31. STBE/STME LO_2-LO_2 Turbine Commonality--
Turbine Arrangement of Baseline Retained

	STBE(1)			STME	
	LOX(2,3)	CH4	LH2	LOX(2)	LH2
POWER, HP	47735	34098	20931	21370	56511
SPEED, RPM	14000	20724	44000	11500	24431
TURBINE TYPE	2RVC	2RVC	IMPULSE	2RVC	2RVC
MEAN DIAMETER, INCHES	17.5	17.0	8.05	17.5	14.5
PRESSURE RATIO	20.2	6.2	3.2	2.49	7.46
ADMISSION, PERCENT	100	100	100	100	100
FLOW, LBM/S	42.62	35.09	35.09	45.97	45.97
MEAN BLADE SPEED, FT/S	1069	1537	1545	878	1546
EFFICIENCY, PERCENT	40.1	58.1	43.7	61	62
VELOCITY RATIO	0.108	0.200	0.224	0.17	0.19
BLADE HEIGHT/MEAN DIAMETER					
NOZZLE 1	0.030	0.041	0.037	0.080	0.038
ROTOR 1	0.051	0.056	0.046	0.091	0.049
NOZZLE 2	0.063	0.061	-	0.099	0.056
ROTOR 2	0.072	0.060	-	0.102	0.059
INLET FLANGE AREA, IN^2	108.3	25.6	8.49	108.3	15.9
DISCH FLANGE AREA, IN^2	255.1	136.5	25.12	255.1	101.7

1. IDENTICAL TO STBE "OPTIMIZED" TURBINES EXCEPT FOR (3) BELOW
2. BLADE PROFILES AND HEIGHTS DIFFERENT
3. FLANGE AREAS SET BY STME LOX

much larger than those of the STBE. In this case, absolutely common turbine blading is not feasible.

3.7.5 Common STME LO_2/STBE Tri-Propellant LO_2 and Methane Turbines

Table 3-32 presents the results of a turbine commonality study for the turbines for the STBE LO_2 and CH_4 main pumps and for the STME LO_2 main pump. The results are very similar to those presented in Table 3-31, and the main drivers in each figure have been the same. The small differences arise principally from the different power and speed requirements in the baseline configurations at the time the different studies were conducted. The principal new conclusion from Table 3-32 is that the turbine commonality is not significantly affected when the STBE CH_4 turbopump is included.

These studies of turbine commonality held fixed several parameters that could maximize the potential for turbine commonality. For example, the layout of the hot gas flow system was not changed. The baseline layouts give a series turbine flow path for the STME and a parallel flow path for the STBE. System changes that resulted in decreased pressure ratio across the turbine for the STBE LO_2 pump potentially could make common blade profiles and height possible. In addition, design concepts that are marginal for optimized turbines and, therefore, have been historically neglected might be attractive for turbine commonality. The potential for turbine commonality will be continued in the next reporting period by expanding the range of allowable configurations for the hot gas flow system and for the turbine blading itself.

3.7.6 Common LO_2 STME/STBE Turbopump

The main LO_2 pump design described previously has been optimized for operation with the STME engine system. Significant cost savings could be realized if turbopumps were designed that could be used in both the STME and STBE applications. The design of such a common turbopump would be strongly influenced by the more severe requirements of the larger STBE engine system. Thus, although specific common STBE/STME LO_2 pump designs were not analyzed

Table 3-32. STME/STBE LO_2-LO_2 CH_4 Turbine Commonality--
Turbine Arrangement of Baseline Retained

	STBE			STME	
	LOX	CH4	LH2	LOX	LH2
POWER, HP (RQMNT)	46270	36630	24483	20970	56511
SPEED, RPM (RQMNT)	12200	19530	38770	9850	24431
TURBINE TYPE	2RVC	2RVC	2RPC	2RVC	2RVC
MEAN DIAMETER, INCHES	17.0	17.0	9.0	17.0	14.5
PRESSURE RATIO	20.2	7.7	2.5	2.9	6.4
ADMISSION, PERCENT	100	100	100	100	100
FLOW, LBM/S	46.6	36.1	36.1	47.8	47.8
BLADE SPEED, FT/S	905	1450	1522	731	1546
EFFICIENCY, PERCENT	36	56	59	50	63
VELOCITY RATIO	0.091	0.181	0.25	0.132	0.190
BLADE HEIGHT/MEAN DIAMETER					
NOZZLE 1	0.034	0.041	0.037	0.073	0.037
ROTOR 1	0.057	0.057	0.043	0.084	0.047
NOZZLE 2	0.073	0.057	0.045	0.084	0.054
ROTOR 2	0.084	0.057	0.050	0.084	0.056
INLET FLANGE AREA, IN^2	98.4	98.4	8.75	98.4	16.6
DISCH FLANGE AREA, IN^2	268.6	268.6	20.64	268.6	93.2

by rotordynamics during the reporting period, general rotordynamic trends can be inferred from STBE LO_2 pump designs. The common designs will have identical impeller and turbine diameters, which will provide rotor-dynamically similar rotating assemblies. Hydrostatic bearing properties will also be similar, since propellant properties are not a major influence on bearing stiffness. The common pump will operate at a lower speed in the STME application than in the STBE. Thus, a common LO_2 turbopump design that is subcritical in an STBE application will probably be subcritical with increased margins when used on the STME. Specific designs will be reviewed and the results discussed for common STBE/STME applications in subsequent reports.

3.7.7 Commonality Issues

Several issues remain to be addressed in the commonality study. From a system standpoint, the possibility of having common pumps and MCC at the currently specified thrust levels with one engine orificed to allow the pumps to operate at the same specific speed should be investigated. For the option with the compromised turbomachinery, the diffuser vane issue must be resolved. If stress requirements show that not only are diffuser vanes required, but that they must be cast integrally with the housing, options to prevent separate casting inserts for the two different diffuser vane shapes must be investigated. Further, as can be seen in Tables 3-28 and 3-29, since the width of the diffuser must be set for the highest flow rate pump, there will be a large expansion at the impeller discharge for the other pumps; the effect of this on the dynamic loads imposed on the rotor and the rotordynamic coefficients associated with the impeller/diffuser interaction is unknown and could only be completely investigated through a test program.

5355e/sjv

4.0 COMBUSTION DEVICES

4.1 INTRODUCTION

As a result of the in-depth subsystem studies and engine evaluations conducted in Phase A, a GG cycle engine configuration was selected that uses LO_2 and hydrogen propellants in the main combustor, with LH_2 for MCC and nozzle cooling and also for fuel-rich GG fuel. The engine balance generated and the resultant parameter values were used to establish the pertinent MCC, nozzle, and GG operating requirements as well as some of the main injector, combustion chamber, and nozzle geometry. In addition, trade studies were used to select the two-position nozzle contour and cooling approach.

Pertinent main-injector/chamber operating conditions and geometry and the GG operating conditions and geometry were used to support preparation of conceptual design drawings for the injector, MCC, nozzle, and GG. A detailed description of these concepts is presented in the Design Definition Document (DDD).

During Phase A', additional trade studies were conducted on select combustion devices to investigate (1) commonality potential between the STME and STBE components and (2) alternative nozzle design approaches in order to simplify the nozzle and reduced costs. Results of these trade studies are described in the following sections.

4.2 SUMMARY

In-depth trade studies were conducted to evaluate the potential commonality of the STME and STBE combustion devices components, including the main injector, MCC, nozzle, and GG. Results of these studies indicated that the main injector can be common with some reasonable LO_2 ΔP compromises and "kitting" of the coaxial injector element fuel sleeves (replaceable sleeves) for fuel ΔP control. Common MCCs, common STBE nozzle and STME primary nozzle, and common GG combustors/injectors are very feasible with only minor adjustments to coolant flow rate and pressure drop parameters. Each of these common components must be further analyzed to establish actual pressure loss and coolant flow characteristics. Also, each of these components must be designed for the higher pressure stresses resulting from the STBE operation.

Several nozzle concepts were evaluated and compared relative to performance, weight cost, and reusability, versus expendability. An extendable/ retractable RAO optimum contour would produce the highest performance of the candidate nozzles including the baseline retractable dual bell nozzle; however, the RAO would be highest cost of the candidates studies. The baseline reusable dual bell concept with a dump cooled extension (secondary nozzle) was compared to an expendable fixed dual bell nozzle with a turbine exhaust gas-cooled solid wall secondary nozzle. The expendable version would be considerably cheaper, lighter weight, slightly higher performance, and less complex. This is primarily due to the elimination of the retraction mechanism and dynamic seals and due to replacement of the dump cooling with the turbine exhaust gas cooling of the solid wall secondary nozzle. Further engine and vehicle studies are required to support the nozzle selection process.

4.3 RESULTS

4.3.1 Commonality

Commonality of combustion devices components between the STME and STBE is highly desirable since they represent a major part of the engine cost. If one design can serve two functions, STME or STBE, then a significant development and production cost reduction can be realized. Consequently, in-depth trade studies were conducted to investigate commonality potential for the main injector, MCC, nozzle, and GG.

Results from the main injector commonality studies are presented in Figures 4-1 and 4-2. Figure 4-1 shows the baseline design and operating parameters for both engines at full power with the STME operating at 2,700 psia

Engine	STME	STBE
Elements	**700**	**1100**
P_C psia	2700	3600
W_O (lb/sec)	1090	1753
ΔP_O (psi)	675	864
$\Delta P_O / P_C$	.25	.24
W_F (lb/sec)	157	501
ΔP_F (psi)	284	720
$\Delta P_F / P_C$	.11	.20

- **Baseline injectors unsuitable for other engine**

STBE/STME Coaxial Injector Element Design

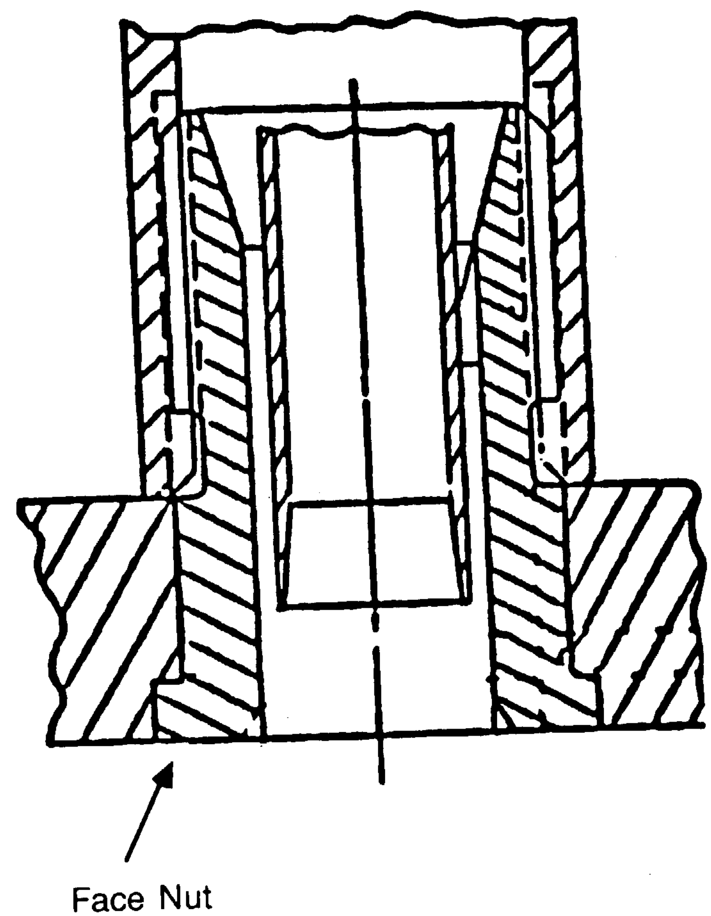

88CA-0518-1

Figure 4-1. STME/STBE Commonality--Baseline Design MCC Injectors

Design Approach

- STME oxidizer $\Delta P/P_C$ at nominal power level reduced. Baseline is 25%
- STBE oxidizer $\Delta P/P_C$ at maximum power level increased. Baseline is 24%
- 0.011 in. fuel annulus used for STBE
- 0.020 in. fuel annulus used for STME

	STME	STBE
Elements	1100	1100
P_C	2700	3600
W_O	1090	1753
ΔP_O	409	1058
$\Delta P_O/P_C$	.15	.29
W_F	157	501
ΔP_F	284	720
$\Delta P_F/P_C$	.11	.20

88CA-0518-2

Figure 4-2. STME/STBE Commonality--Compromise Main Injector Design chamber pressure and the STBE at 2,700 psia. Approximately 700 coaxial injector elements were selected for the STME and 1,100 elements for the STBE. Flow rates and injection pressure drop characteristics are also shown (Figure 4-1) for the selected injector elements for each baseline engine.

It was assumed, for this commonality study, that the STBE injector with 1,100 elements would retain most of its injection features and thereby preserve the STBE and most likely the STME performance. An increased STBE LO_2 injection pressure was selected and $\Delta P/P_c$ increased from 24% to 29% in order to obtain a reasonable 15% $\Delta P/P_c$ for the STME at full power and 11% at reduced power. This STME and STBE LO_2 ΔP relationship would be accomplished with a fixed oxidized element and control orifice geometry using the 1,100 elements. Figure 4-2 shows the flow rates and ΔP relationships with the 1,100 element common LO_2 injector. Replaceable fuel face nuts were selected for the common injector and these face nuts can be used to control the fuel injection area and ΔP. Consequently, the STME fuel ΔP can be maintained at the same level as the baseline design even though the number of elements has changed from 700 to 1,100. The STME fuel annulus gap would change from about 0.030 in. for the baseline to 0.020 in. for the common injector. The STME gap would remain unchanged at about 0.011 in. The common injector would require face nut "kiting" to generate the 0.011 gap for the STBE or 0.020 gap for the STME.

Commonality studies were conducted for the STME and STBE MCC where full power level operation was assumed with the STME at 2,702 psia pressure chamber and the STBE at 3,600 psia. An STBE at 3,000 psia pressure chamber is also shown in Table 4-1 for comparison. The tri-propellant STBE engine uses hydrogen for the MCC coolant, as does the STME; this enhances the commonality. Table 4-1 shows some of the pertinent operating parameters and geometry for the baseline MCC concepts. It can be seen from Table 4-1 that the sizes of the STME MCC and STBE MCC at 3,600 pressure chamber are very similar. Figure 4-3 also shows the size relationship and Figure 4-4 shows the maximum (throat) heat flux comparison at the baseline conditions; e.g., about 76 Btu/in^2-sec for the STBE and 86 for the STME. The baseline STBE MCC uses about 41 lb/sec

Table 4-1. STME/STBE Compatibility Combustor

	STME	STBE Tri-Prop	STBE Tri-Prop
P_c psia	2702	3000	3600
Diameter (in.)	19.98	21.96	19.93
Throat diameter (in.)	11.62	13.37	12.13
Throat area (in.^{2})	105.90	140.30	115.60
Contraction Ratio	2.96	2.70	2.70
Length (in.)	13.45	15.03	13.92

- **Compromise combustor possible**
- **Increasing STBE P_c to 3600 psia helps**

88CA-0518-3

changed from 700 to 1,100. The STME fuel annulus gap would change from about 0.030 in. for the baseline to 0.020 in. for the common injector. The STME gap would remain unchanged at about 0.011 in. The common injector would require face nut "kiting" to generate the 0.011 gap for the STBE or 0.020 gap for the STME.

Commonality studies were conducted for the STME and STBE MCC where full power level operation was assumed with the STME at 2,702 psia pressure chamber and the STBE at 3,600 psia. An STBE at 3,000 psia pressure chamber is also shown in Table 4-1 for comparison. The tri-propellant STBE engine uses hydrogen for the MCC coolant, as does the STME; this enhances the commonality. Table 4-1 shows some of the pertinent operating parameters and geometry for the baseline MCC concepts. It can be seen from Table 4-1 that the sizes of the STME MCC and STBE MCC at 3,600 pressure chamber are very similar. Figure 4-3 also shows the size relationship and Figure 4-4 shows the maximum (throat) heat flux comparison at the baseline conditions; e.g., about 76 Btu/in^2-sec for the STBE and 86 for the STME. The baseline STBE MCC uses about 41 lb/sec

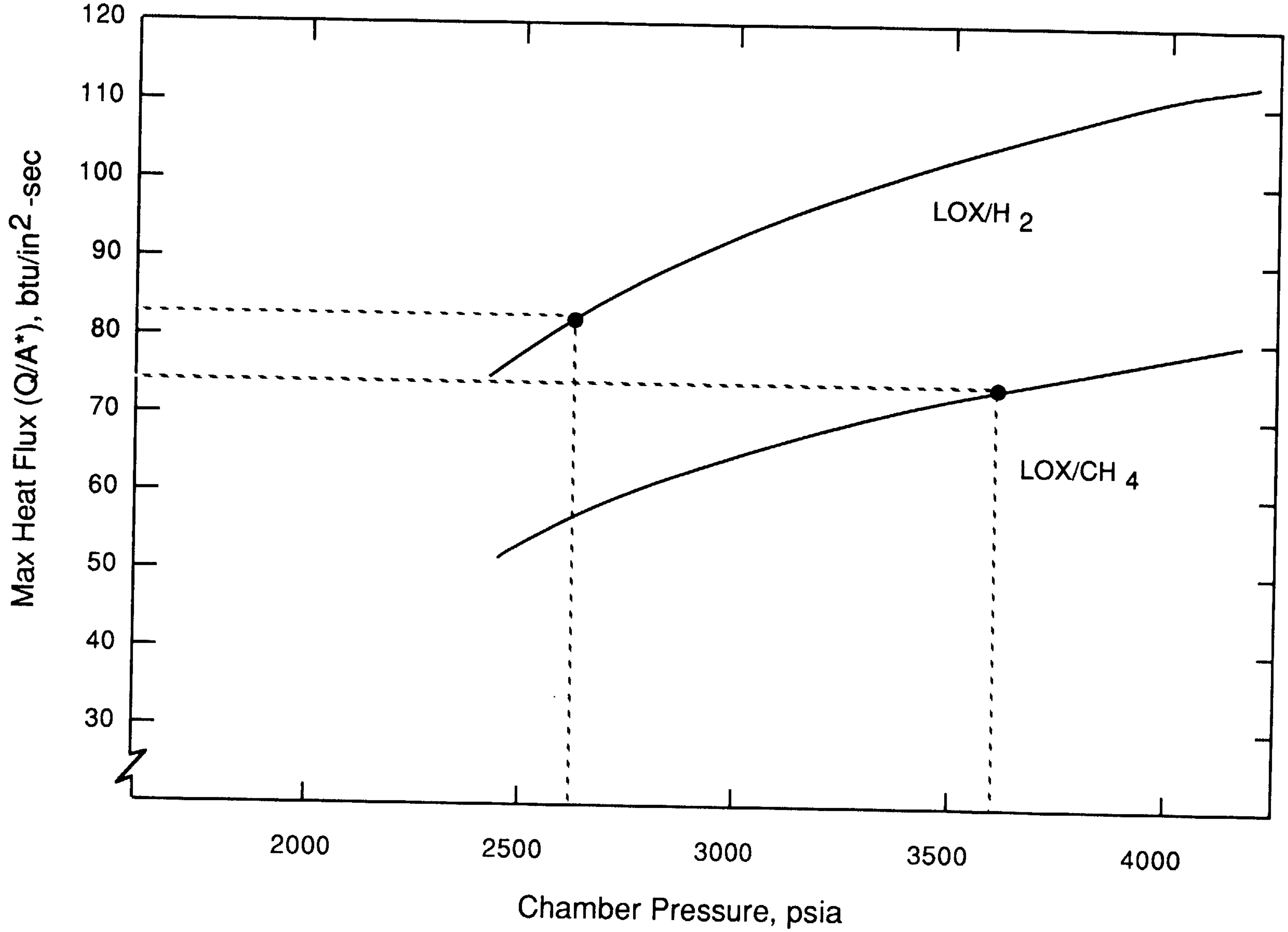

88CA-0518-5

Figure 4-4. STBE/STME MCC Compatibility

of H_2 for cooling and subsequently for GG operations. Slightly more H_2 could be used to adequately cool this MCC at the higher STME heat flux conditions using the same coolant passages and chamber geometry. The actual coolant flow rates and pressure losses remain to be established for the common MCC. A common MCC would also result in minor changes to the thrust or pressure chamber for either or both of the engines depending primarily on throat size selection.

Figure 4-3 shows the MCC/nozzle attach point to be at a 7:1 area ratio and about 31 to 32 in. diameter. The exit area ratio and exit diameter of the STBE nozzle and the primary section exit diameter of the STME nozzle are also very similar as indicated in Figure 4-5. In addition, total heat transfer to these nozzles are similar for the baseline engines ranging from around 87,000 Btu/s for the STBE to 102,000 Btu/s for the STME (primary nozzle). Preliminary heat transfer analyses indicates that a common nozzle coolant passage size could be used for the STME with H_2 cooling or the STBE with CH_4 cooling. The actual coolant passage geometry, flow rates, and pressure loss characteristics are to be determined. The common nozzle coolant passages must be designed for the higher STBE pressure stresses and for slightly higher STME heat loads. Interface requirements at the forward and aft ends may also require compromises for either or both engine nozzles.

The baseline operating parameters for the STME and STBE GGs are presented by Table 4-2. Two STBE chamber pressure levels are shown for comparison. The STME GG and the 3,000 psia pressure chamber STBE GG matched very closely in pressure, gas temperature, flow rate, and size. Consequently, the same GG can be used for both engines. A greater difference is evident between the STME and the 3,600 psia STBE GG; however, the difference could be readily accommodated by compromises in injection pressure losses. The compromise GG would result in lower injection ΔP for the STME or higher ΔPs for the STBE or some of both. Further refinement of a common GG remains to be accomplished after the engine requirements are fixed.

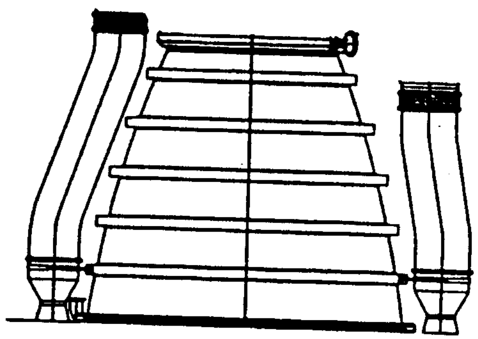

STBE		STME
3600	P_c	2785
ϵ =7	Attach Point	ϵ =7
50	ϵ	50/138
LCH_4	Coolant	LH_2
86.4	Exit dia.	86.1 (prim)

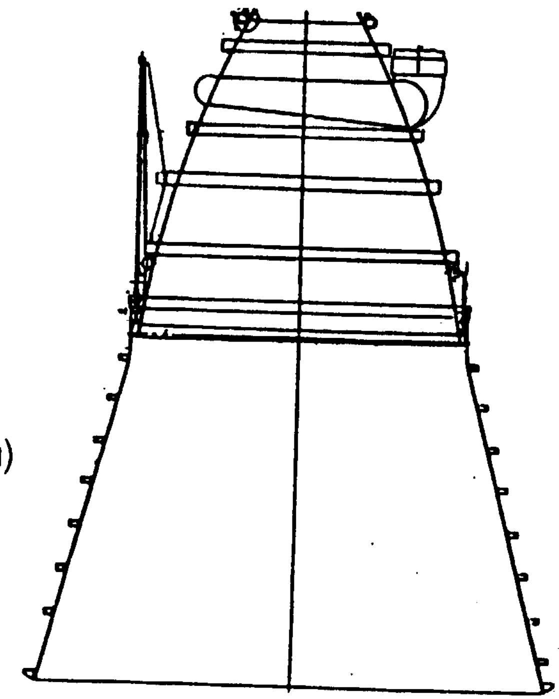

88CA-0518-6

Figure 4-5. STME/STBE Nozzle Commonality

Table 4-2. STME/STBE Compatibility Gas Generator

	STME	STBE Tri-Prop	STBE Tri-Prop
	LOX/H_2	LOX/H_2	LOX/H_2
Pressure (psia)	2702	3000	3600
Temperature (°R)	1600	1600	1600
MR	0.730	0.601	0.655
$\dot{W}$ (lb/sec)	47.70	50.20	67.20
Diameter (in.)	5.60	5.70	6.60

- **Compromise GG possible**
- **Lowering STBE P_c helps**

88CA-0518-7

4.3.2 Nozzle Alternatives

Several nozzle concepts were evaluated during this phase of the program and these evaluations were related to performance, weight, cost, and reusability/expendability. Table 4-3 and Figure 4-6 show the comparison between the reusable baseline retractable dual bell contour, the extendable/retractable Rao contour, and a fixed Rao contour with a smaller area ratio. As shown, the extendable/retractable Rao has the best vacuum performance and the highest payload capability to low earth orbit (LEO). This concept would have a more complex extension mechanism than the retractable dual bell and weigh more than the fixed Rao.

A fixed dual bell concept was investigated primarily for expendable engine use. This dual bell could be operated at sea level where gas separation would occur at the end of the primary nozzle at $\varepsilon = 50$. At some altitude, the gases would attach to the secondary nozzle, which expands to an $\varepsilon = 138$. Figure 4-7 shows this fixed dual bell contour and compares some of its design features with the reusable design. The major differences and advantages of the candidate expendable concept would be:

- Turbine exhaust cooled versus propellant dump cooled
- Elimination of retraction mechanism
- Elimination of dynamic seals
- Reduced cost and weight
- Improved reliability
- Elimination of dump cooling and improved performance.

Design studies were conducted to evaluate the turbine exhaust cooled secondary nozzle feature. Figures 4-8 and 4-9 show two different approaches to the turbine exhaust gas manifolding. In Figure 4-8, gussets are used to support the overhanging wall adjacent to the gas flow and to direct the turbine exhaust. Figure 4-9 is similar except the support structure and exhaust gas flow path is constructed by electrical discharge machining (EDM). Further work is required to determine the best concept.

Table 4-3. STME Nozzle Alternatives

Nozzle Type	Area Ratio	I_s sec SL/Vac	Engine Weight, lb	Payload to Leo	
				Percent	ΔKlb
Retractable dual-bell controur	55/138	367.7/447.4	7550	REF*	REF*
Extendable/retractable RAO contour	55/138	356.5/449.9	7350	101.4	2.3
Fixed RAO contour	72	353.0/438.9	7050	94.4	-9.1

* 163 Klb payload reference

88CA-0518-8

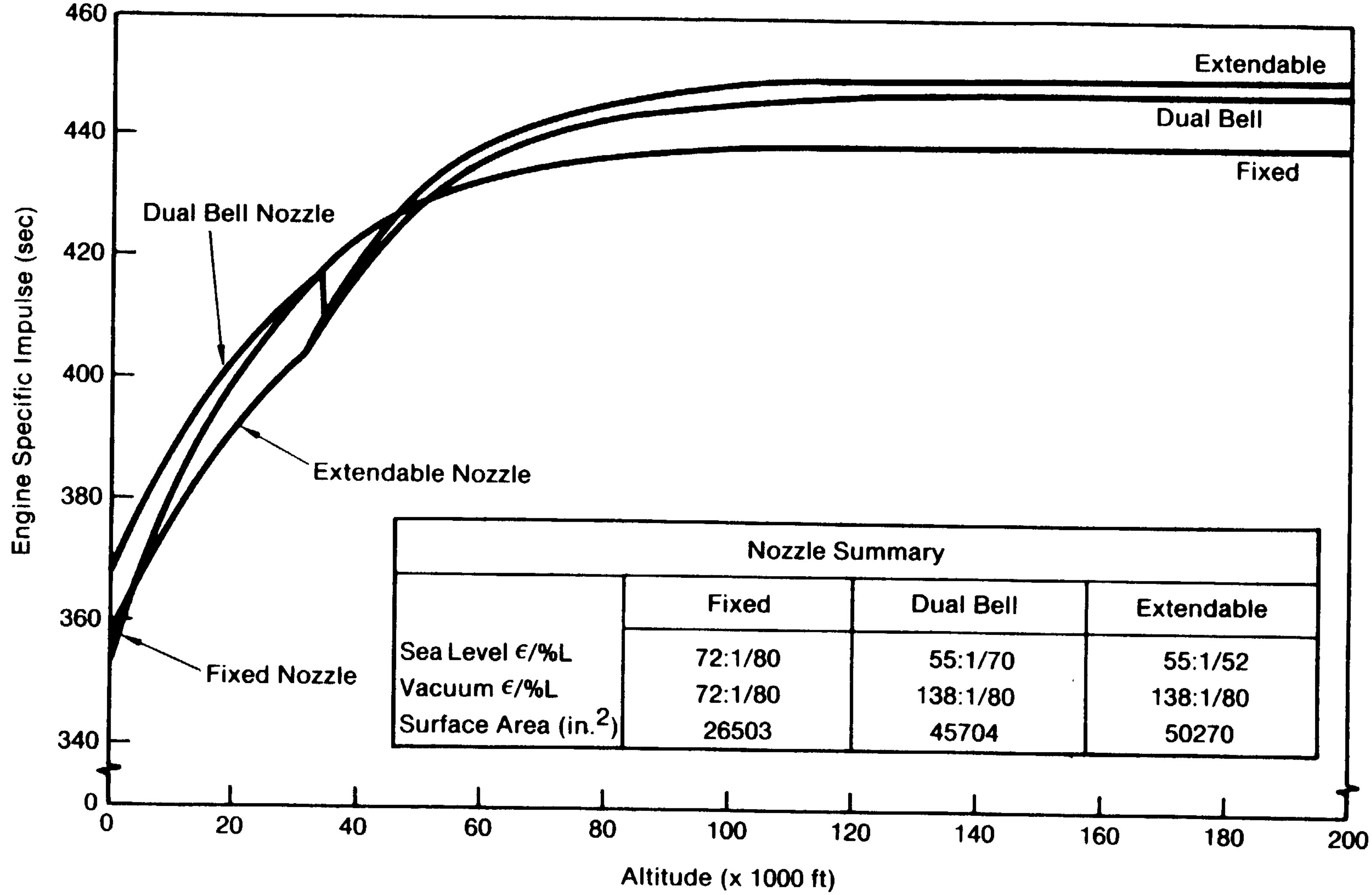

Nozzle Summary	Fixed	Dual Bell	Extendable
Sea Level ε/%L	72:1/80	55:1/70	55:1/52
Vacuum ε/%L	72:1/80	138:1/80	138:1/80
Surface Area (in.^{2})	26503	45704	50270

Figure 4-6. Nozzle Performance Comparison

87D-9-2487

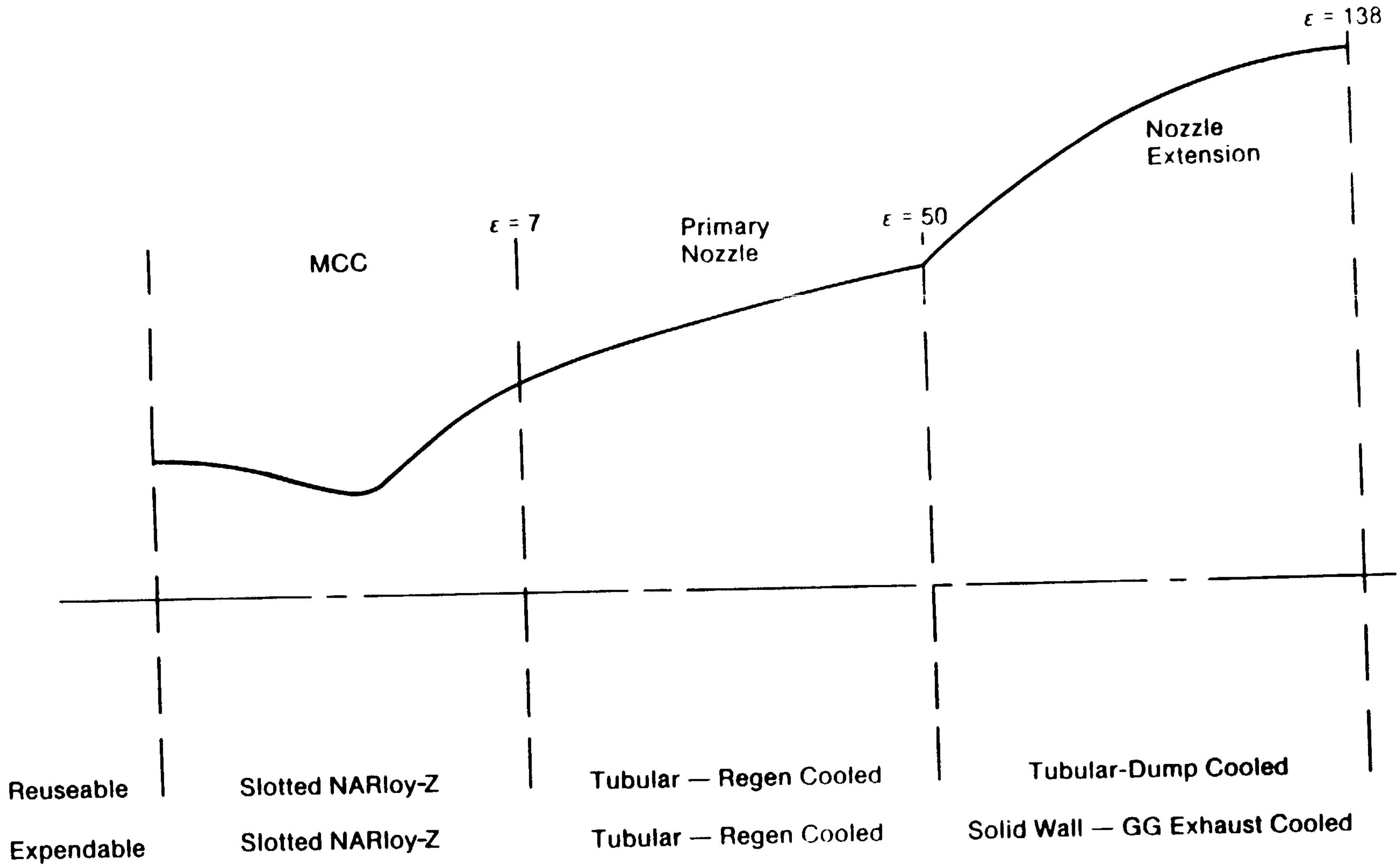

Figure 4-7. STME MCC/Nozzle Comparison

87D-9-3092

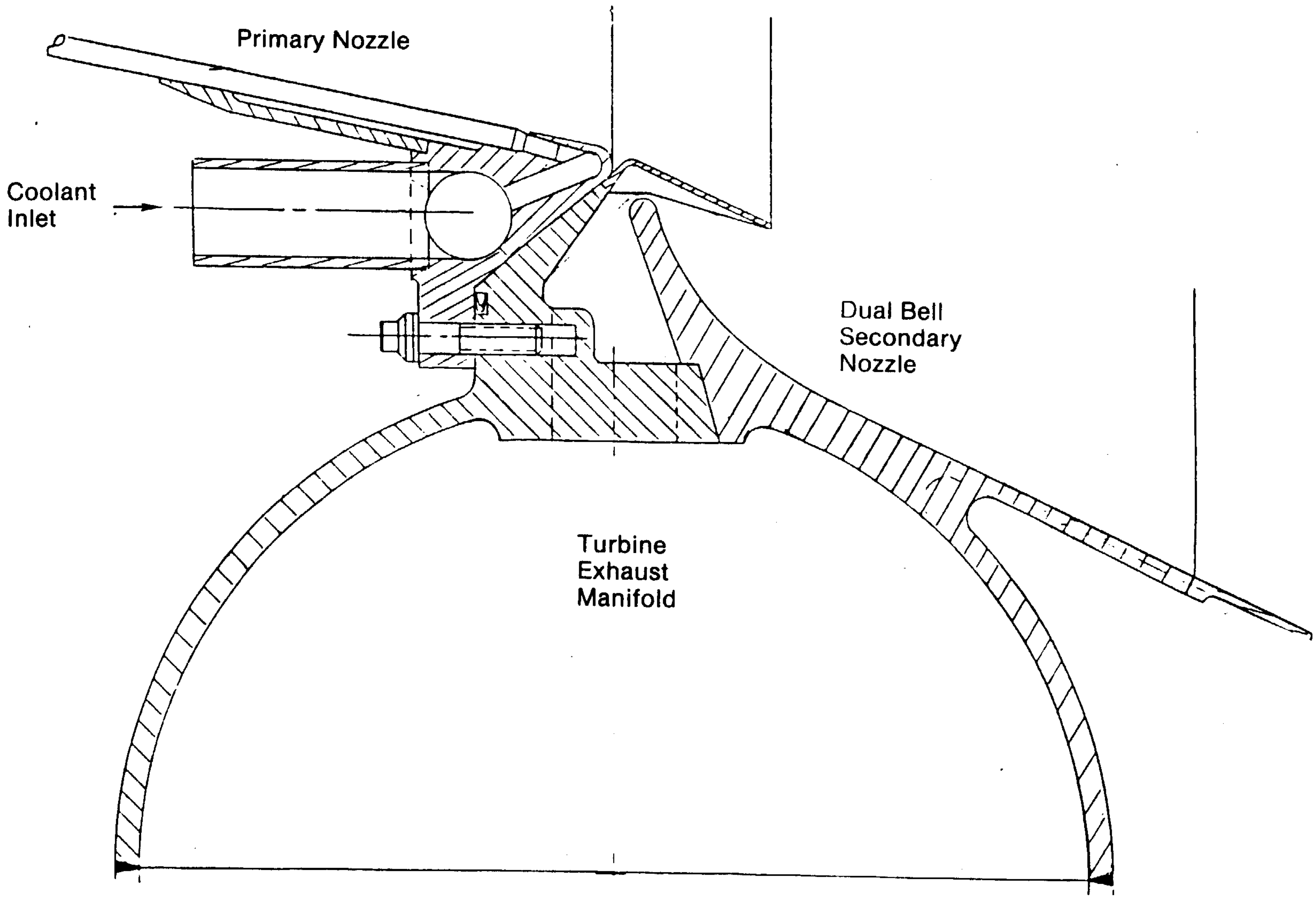

Figure 4-8. Turbine Exhaust Cooled Nozzle Gusset--Configuration

87D-9-3094

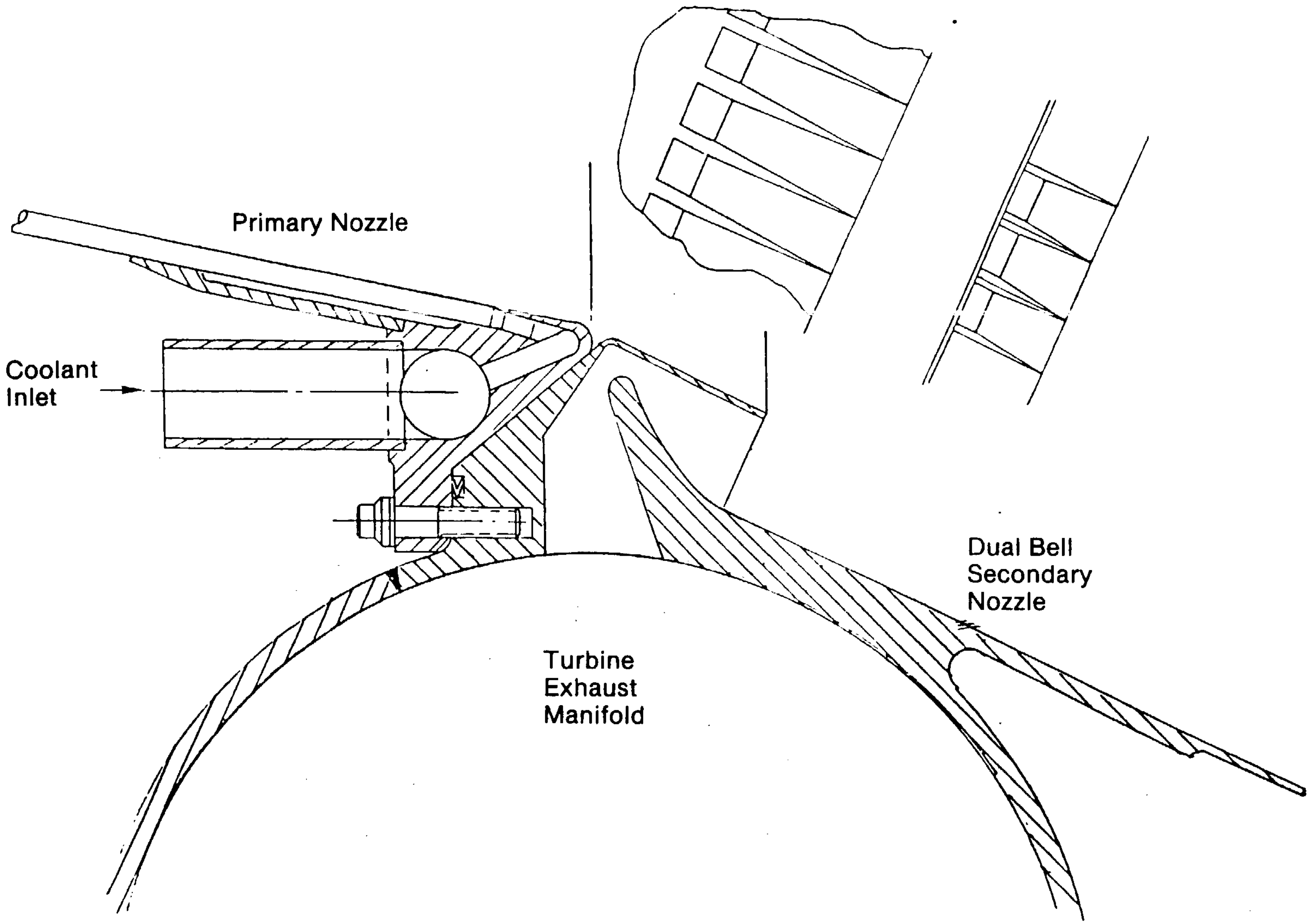

87D-9-3095

Figure 4-9. Turbine Exhaust Cooled Nozzle--EDM Support Configuration

Table 4-4 presents a nozzle cost comparison between the expendable and reusable dual bell nozzles and also between a fixed area ratio, smaller ε nozzle. As shown, the cost and weight are lower and the performance is equal for the expendable dual bell compared to the reusable concept. As anticipated, the cost and weight for the fixed area ratio 60:1 nozzle are lower than either dual bell; however, the vacuum performance is 11 sec lower. Further engine and vehicle trade studies are required to help select the best nozzle concept.

5351e/rmr

Table 4-4. Nozzle Cost Evaluation

Configuration	Reusable Baseline Retractable Dual Bell	Expendable Baseline Fixed Dual Bell	Alternate concept Fixed Area Ratio
Exit area ratio	138	138	60
Cost ($M)	3.43	2.57	1.75
Δ Cost ($M)	--	-0.86	-1.68
Δ Cost (%)	--	25.0	49.0
Ivac (sec) (FPL)	447	447	436
Δ Ivac (sec)	--	--	-11
Δ Weight (lb)	--	-150	-1000

88CA-0518-13

5.0 CONTROL SYSTEM STUDIES

5.1 INTRODUCTION

The objective of this reporting period was to investigate generic control approaches that satisfied the STME requirements at minimum cost. Three candidate control systems were considered using the baseline engine. Each system was examined on the basis of cost, weight, reliability, and performance for hydraulic, electric, and in the open-loop system, pneumatic-actuated valves.

5.2 SUMMARY AND RESULTS

After defining the approach, generic control system baseline requirements were generated. The requirements were (1) reusable engine, (2) closed-loop thrust and mixture ratio control, (3) up-thrust capability for engine out, (4) fail operational/fail safe, and (5) self-contained monitoring to allow redline shutdown. These are similar to the basic SSME requirements. Alternative approaches were then considered. These were, fail degraded/fail safe, fail safe, and open-loop control. Table 5-1 shows a summary of the control systems evaluated.

Schematics for each of the three control systems were generated (Figures 5-1, 5-2, and 5-3) once the approach and requirements were determined. The redundancy management scheme for the three control systems was then defined (Figure 5-4) and the control system features identified (Table 5-2). A control system performance comparison was made based on past Rocketdyne built engines (Table 5-3).

An in-depth cost analysis was conducted for the three systems using SSME control system costs as a point of reference. A review of the components (effectors, sensors, harnesses, and controller) for the three systems was made and the appropriate costs, referenced to the current SSME control system, were determined. Control system 1 (hydraulic) was the most expensive system at $5.09 million. Choosing this system as unity, the cost of the other systems

Table 5-1. Control System Alternatives Assessed

	Control					Redundancy		
	Closed Loop	Open Loop	Hydraulic	Electric	Pneumatic	Fail Operational	Fail Lock	Fail Safe
• System 1	X		X	X		X	X	X
• System 2	X		X	X			X	X
• System 3		X	X	X	X			X

87D-9-3168

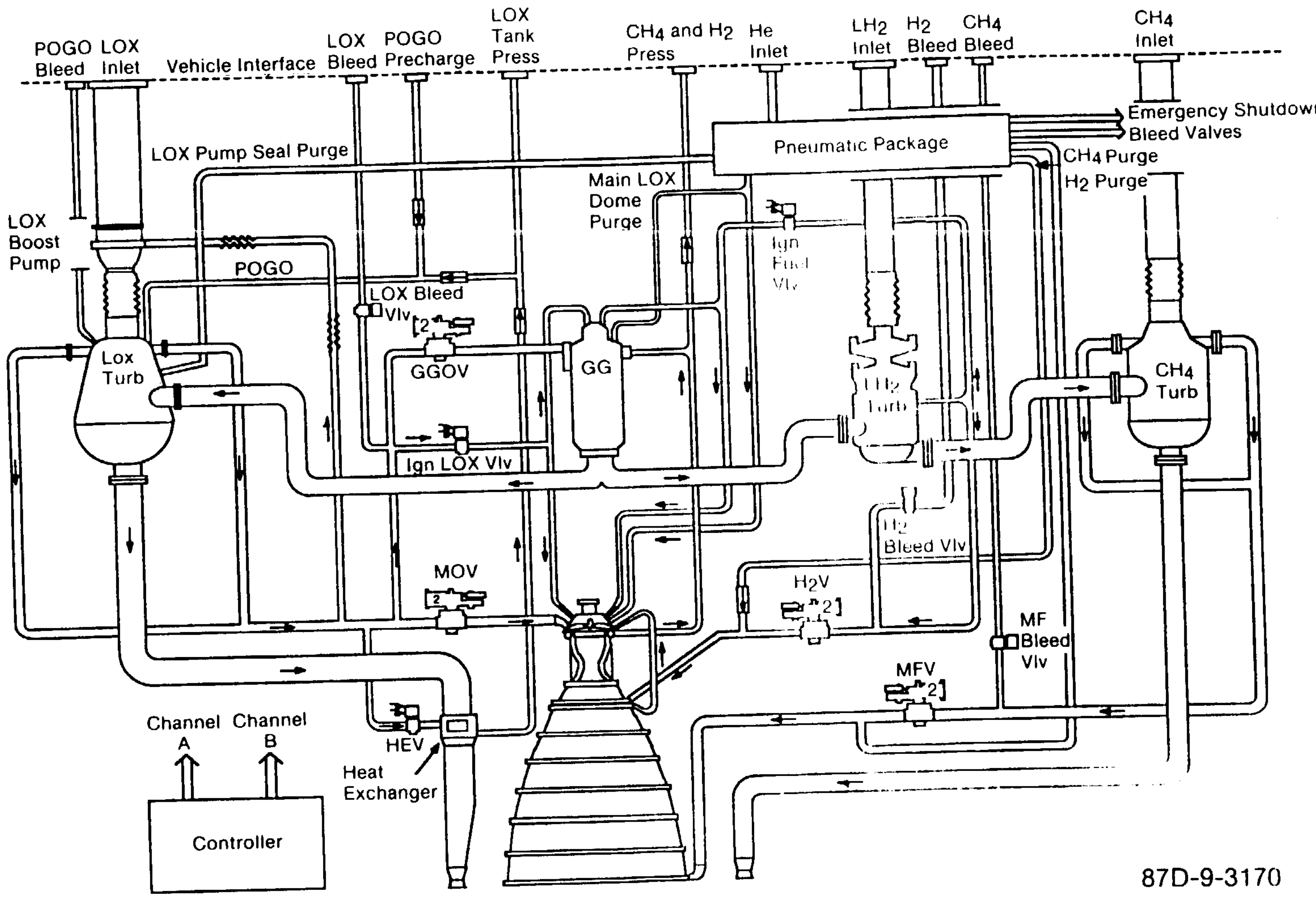

Figure 5-1. STBE Control System 1--Fail Operational/Fail Lock/Fail Safe

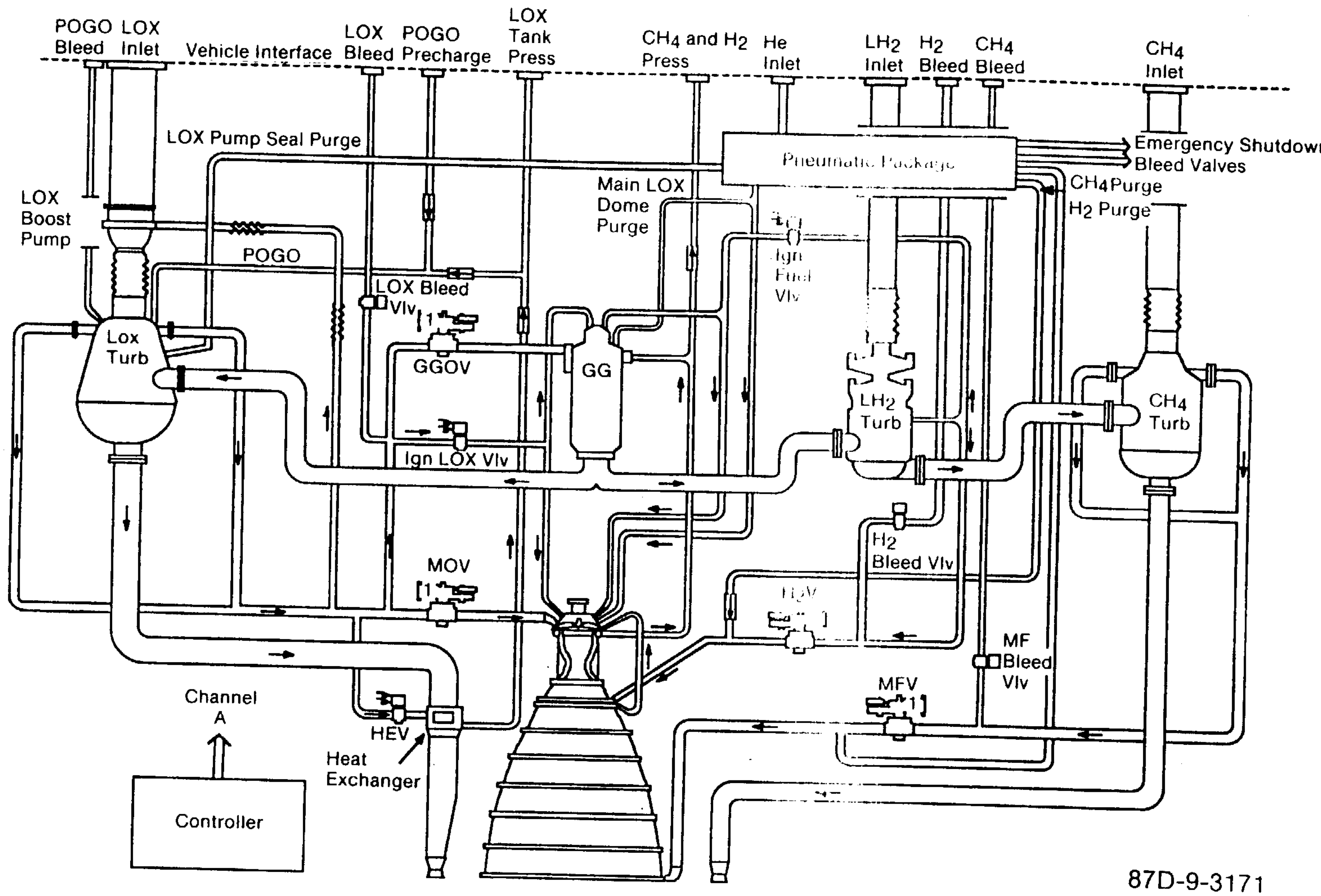

Figure 5-2. STBE Control System 2--Fail Lock/Fail Safe

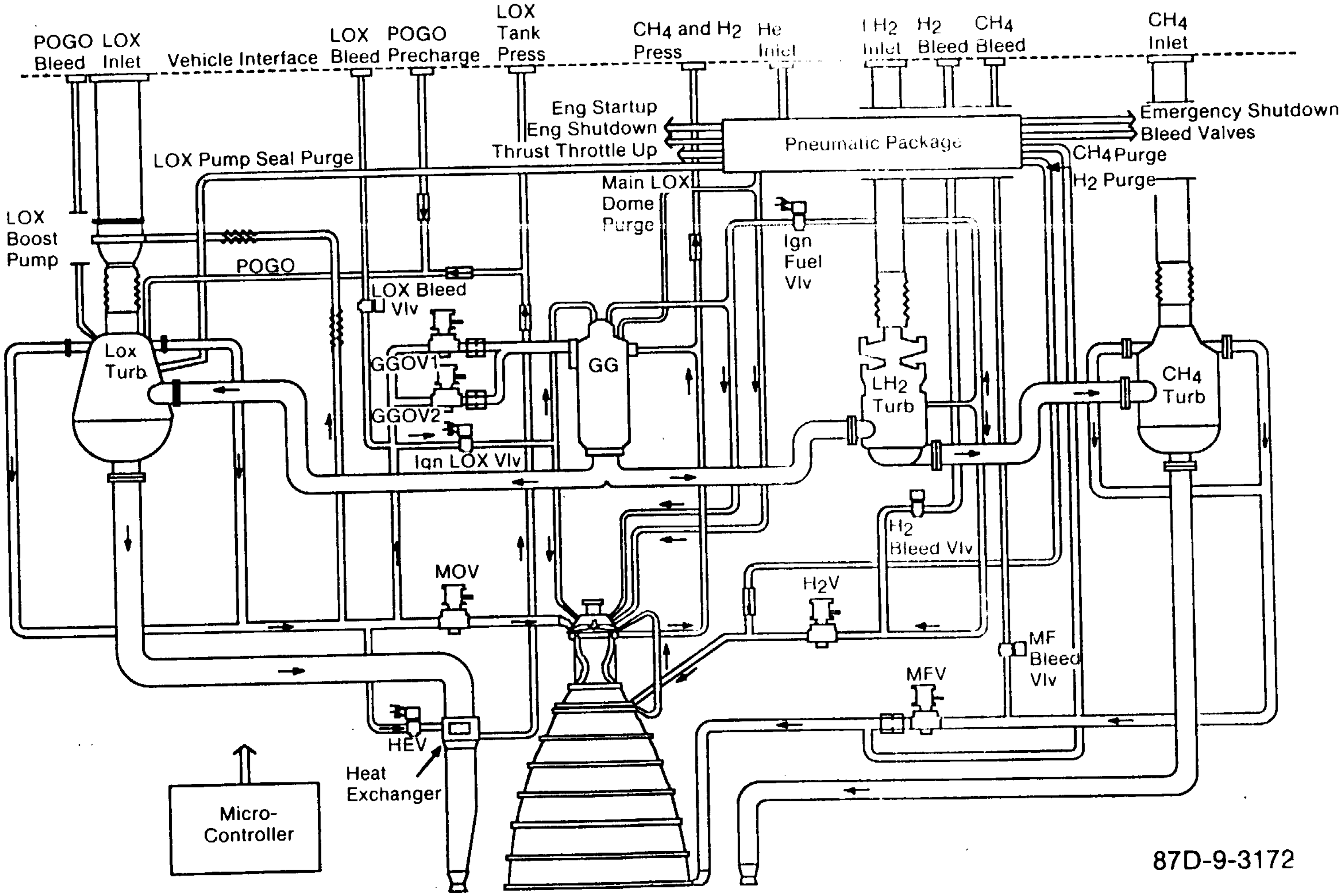

Figure 5-3. STBE Control System 3
Fail Safe

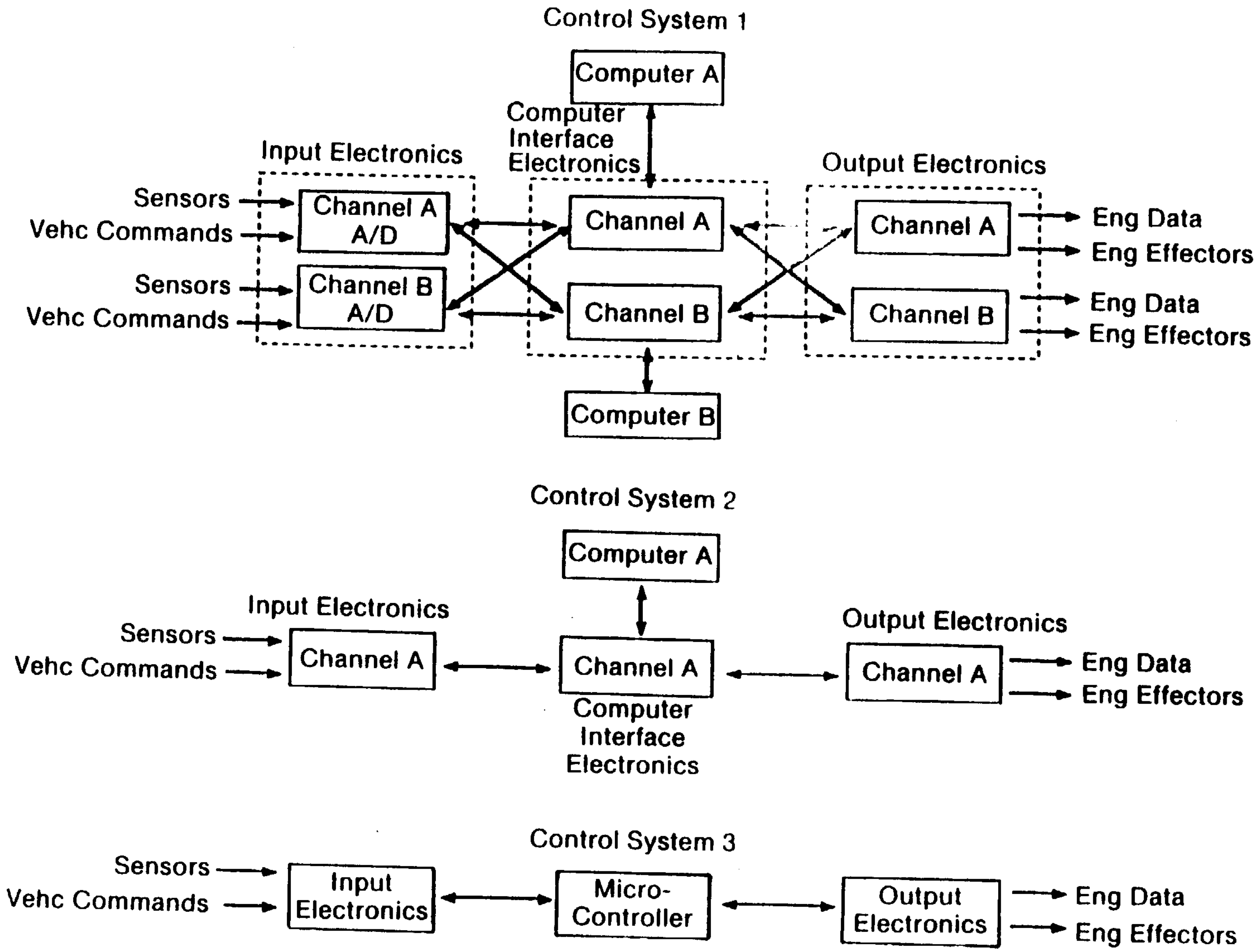

Figure 5-4. Control System Redundancy Management

87D-9-3169

Table 5-2. Control System Features

Feature	System 1	System 2	System 3
Controller Functions			
• Closed loop control	X	X	
• Redundancy management	X		
• Self-test	X	X	X
• Safety monitoring	X	X	X
• Health monitoring	X	X	X
Control Hardware			
• Propellant valve actuators			
• Electric	4	4	0
• Pneumatic	0	0	5
• Solenoids	9	9	13
• Pressure actuated valves	8	8	14

87D-9-3186
2-151-0

Table 5-3. Control System Performance Comparison

Control Accuracy*	Engine Thrust (%)	Mixture Ratio (%)	Propellant Utilization	Data Source
System 1				Based on SSME
Engine-to-engine	±0.61	±0.25		
Run-to-run	±0.46	±0.45		
System 2				Same as System 1
Engine-to-engine	±0.61	±0.25		
Run-to-run	±0.46	±0.45		
System 3				Based on F-1, H-1, J-2, and RS-27
Engine-to-engine	±1.84	±1.59		
Run-to-run	±1.15	±0.88		

*Propellant inlet flight variations not included

87D-9-3177

were compared against it (Figure 5-5). Table 5-4 shows the same data in percentage form.

In summarizing the three control systems studied, several important conclusions are apparent.

1. Control system 1 offers the greatest operational flexibility and its redundancy management allows tolerance of multiple failures. The system gives SSME-type control accuracy, however it is the most costly of the three systems.

2. Control system 2 tolerates single failures by locking-up thrust on the failed engine and up-thrusting the remaining engines if required. Like system 1, this system gives SSME-type control accuracy and is of medium cost compared to systems 1 and 3.

3. Control system 3 tolerates single-point failures by shutting down the failed engine and up-thrusting the remaining engines. The system has less control accuracy than systems 1 and 2, however it is the lowest cost.

Figure 5-6 shows a comparison of the controls systems operational flexibility.

Based on the previously discussed information, control system 2 (electric) is recommended as the new baseline. It tolerates single failures with a fail-lock mode and provides a high probability of mission success with an engine out. The system also offers closed-loop control capability with approximately a 50% cost reduction over system 1. However, it is also recommended to pursue control system 3 for a low-cost expendable STME. This makes an additional 20% cost reduction possible.

5351e/rmr

Table 5-4. Component Percentage of Control System Cost

	CONTROL SYSTEM 1		CONTROL SYSTEM 2		CONTROL SYSTEM 3		
COMPONENT	HYDRAULIC	ELECTRIC	HYDRAULIC	ELECTRIC	HYDRAULIC	ELECTRIC	PNEUMATIC
CONTROLLER	59	59	27	27	8	8	8
HARNESSES	7	7	3	3	3	3	3
SENSORS	6	6	6	6	2	2	2
EFFECTORS	28	18	24	16	26	17	16
TOTAL	**100**	**90**	**60**	**52**	**39**	**30**	**29**

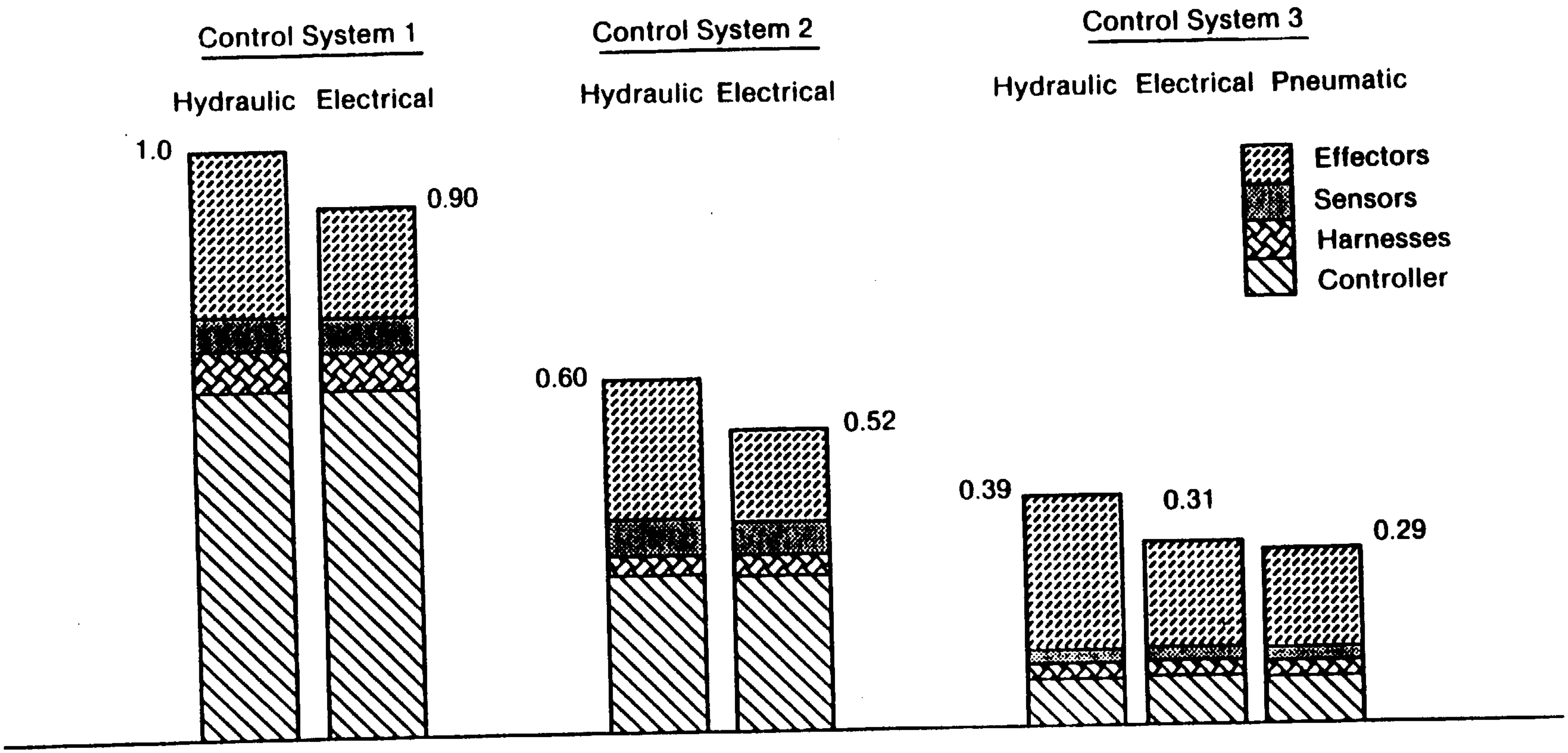

87D-9-3173

Figure 5-5. Comparison of Control System Costs

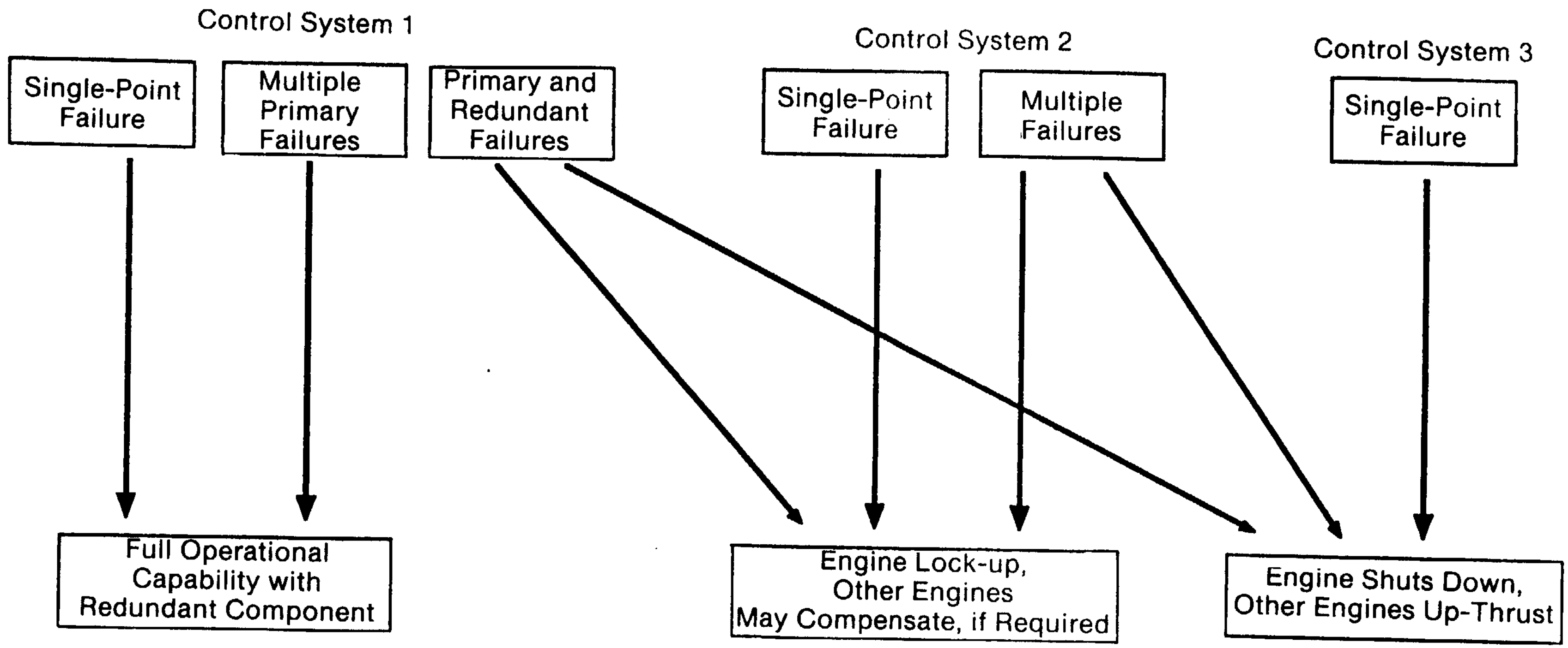

Figure 5-6. Control System Operational Flexibility Comparison

87D-9-3179

6.0 START TRANSIENT ANALYSIS

6.1 INTRODUCTION

The Phase A' start transient analysis assessed two start sequences for the STME. A tank head start and a helium spin start were evaluated with the transient model. Turbopump characteristics were updated in the model to reflect increased moments of inertia and improved performance modeling. Additionally, control gains were modified and inlet pressures were assumed with LH_2 at 51.5 psia and LO_2 at 83 psia.

6.2 SUMMARY AND RESULTS

Both the tank head start and the helium spin start were evaluated with the updated model. The most notable conclusion to be drawn from the evaluations was that the tank head start required approximately 8 sec to achieve the MCC operating pressure compared with 5 sec for the helium spin start. Further, the start simulations showed the helium spin start to be more repeatable than the tank head start.

Comparison of the two starts reveals similar valve position profiles, as shown in Figures 6-1 and 6-2. Figures 6-3 and 6-4 show similar profiles in the MCC pressure buildup, except for the aforementioned time difference. The GG temperature profiles, on the other hand, yield noticeable differences. The tank head start depicts a temperature surge influenced by dome prime while the helium spin shows a faster and smoother buildup, as shown in Figures 6-5 and 6-6. Figures 6-7 through 6-10 show LO_2 and fuel pump speed profiles which are smooth but with slower buildup rates for the tank head start.

The helium start, though it is quicker and more repeatable than the tank heat start, constitutes greater engine hardware complexity. Figure 6-11 shows the helium flow rate necessary for start. The required helium spin system can either be ground based or vehicle based, as shown in Figure 6-12.

5351e/rmr

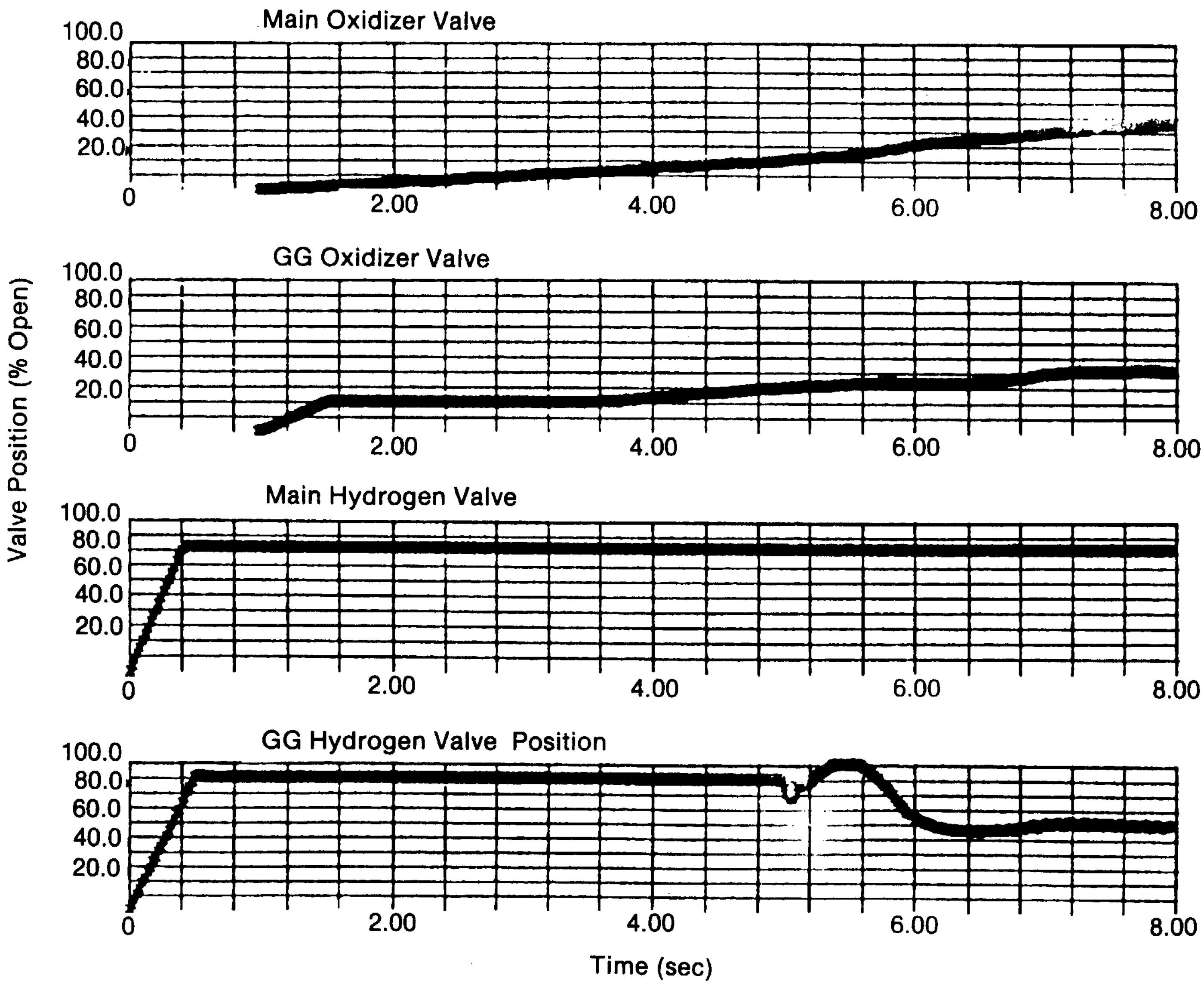

87D-9-3073

Figure 6-1. STME Tank Head Start--Valve Positions

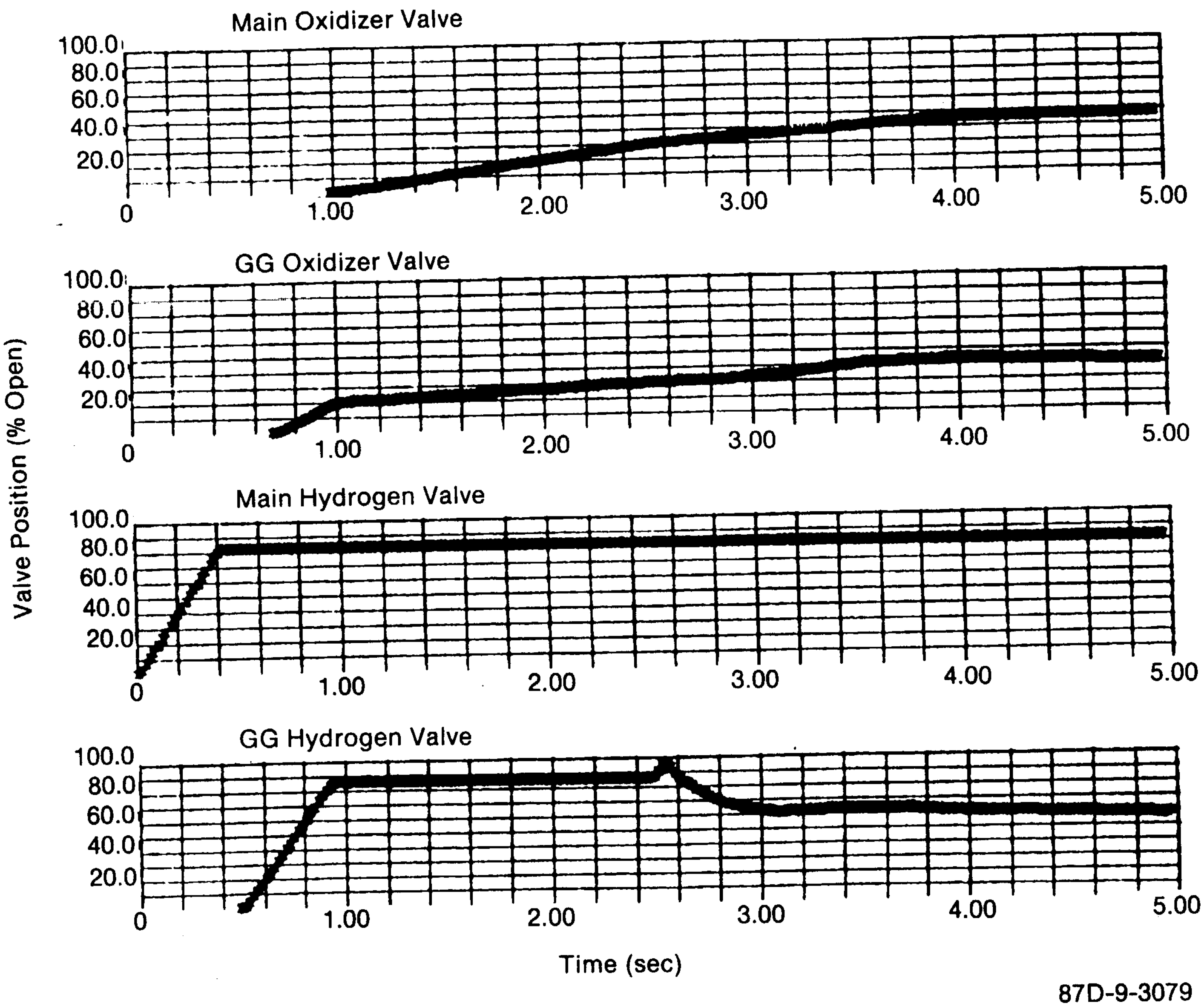

Figure 6-2. STME Helium Spin Start--Valve Positions

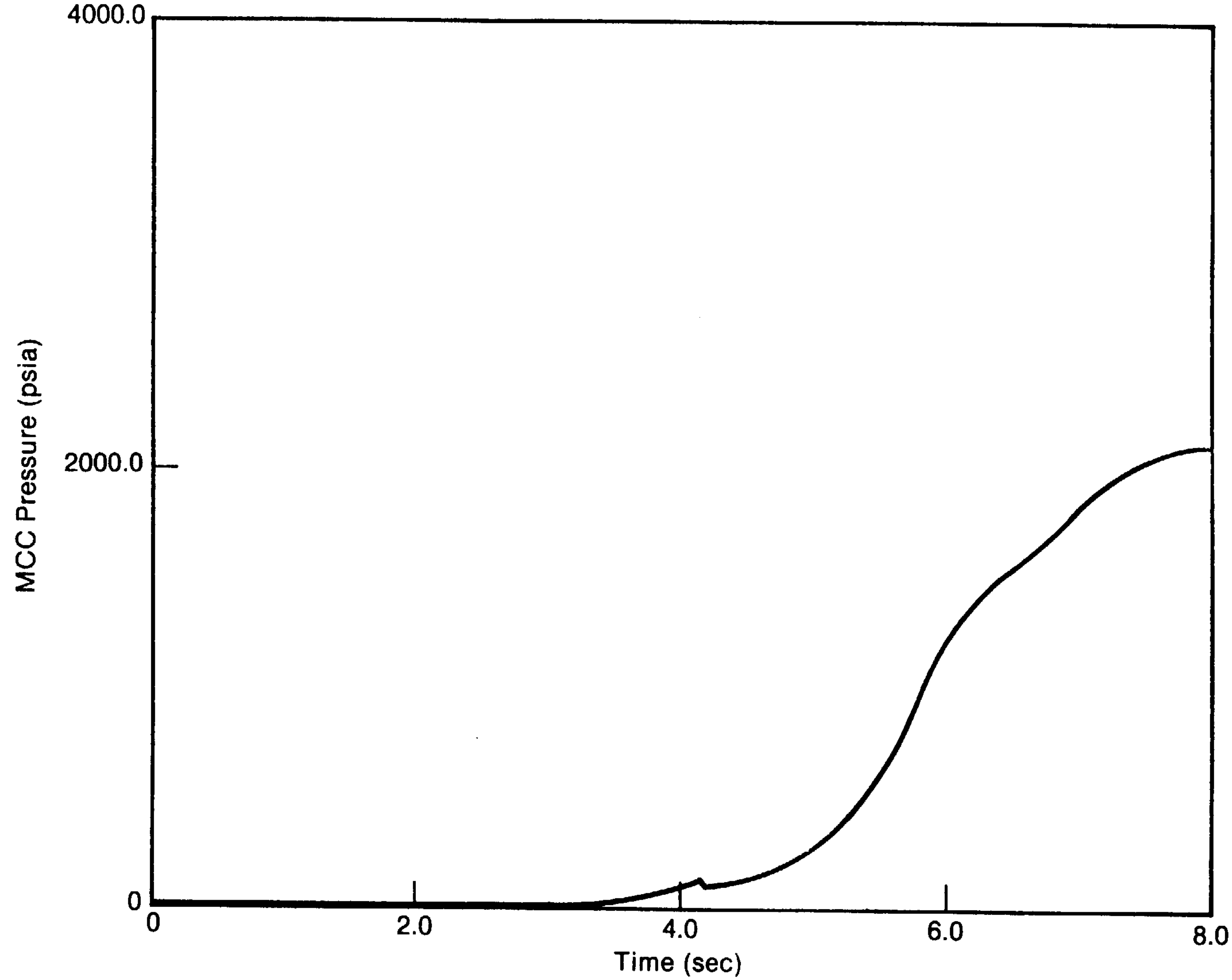

87D-9-3074

Figure 6-3. STME Tank Head Start--Main Chamber Pressure

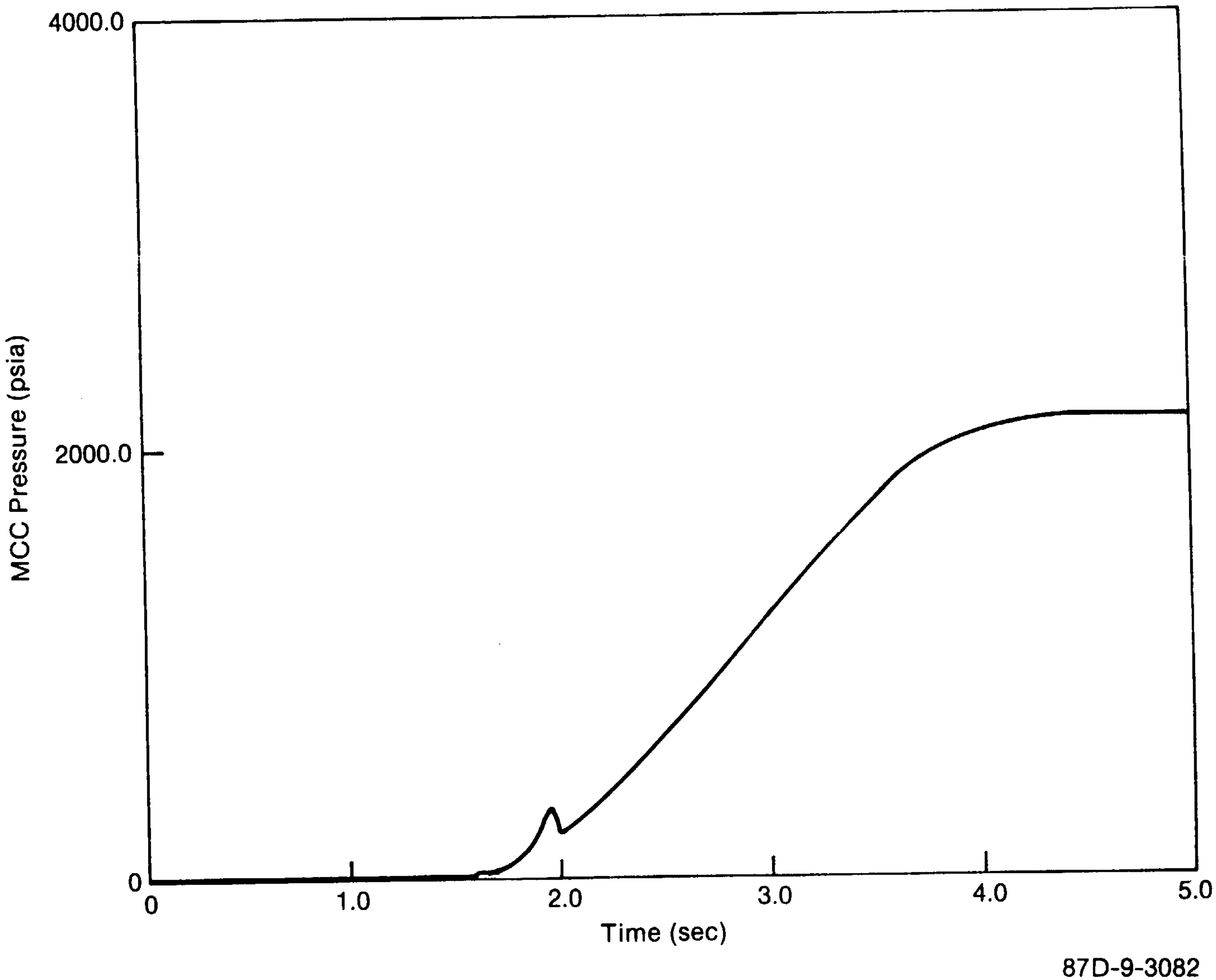

Figure 6-4. STME Helium Spin Start--Main Chamber Pressure

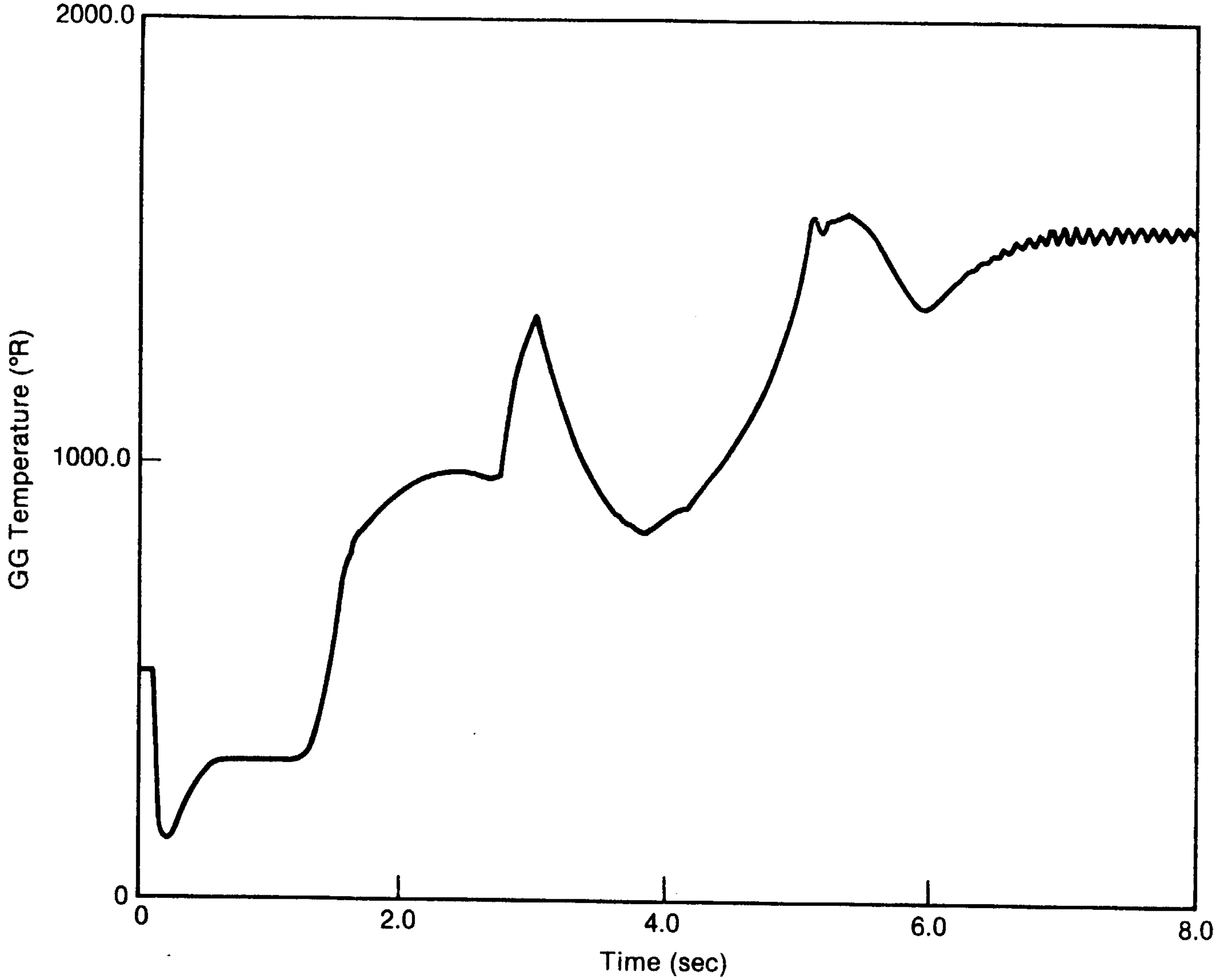

87D-9-3075

Figure 6-5. STME Tank Head Start--GG Temperature

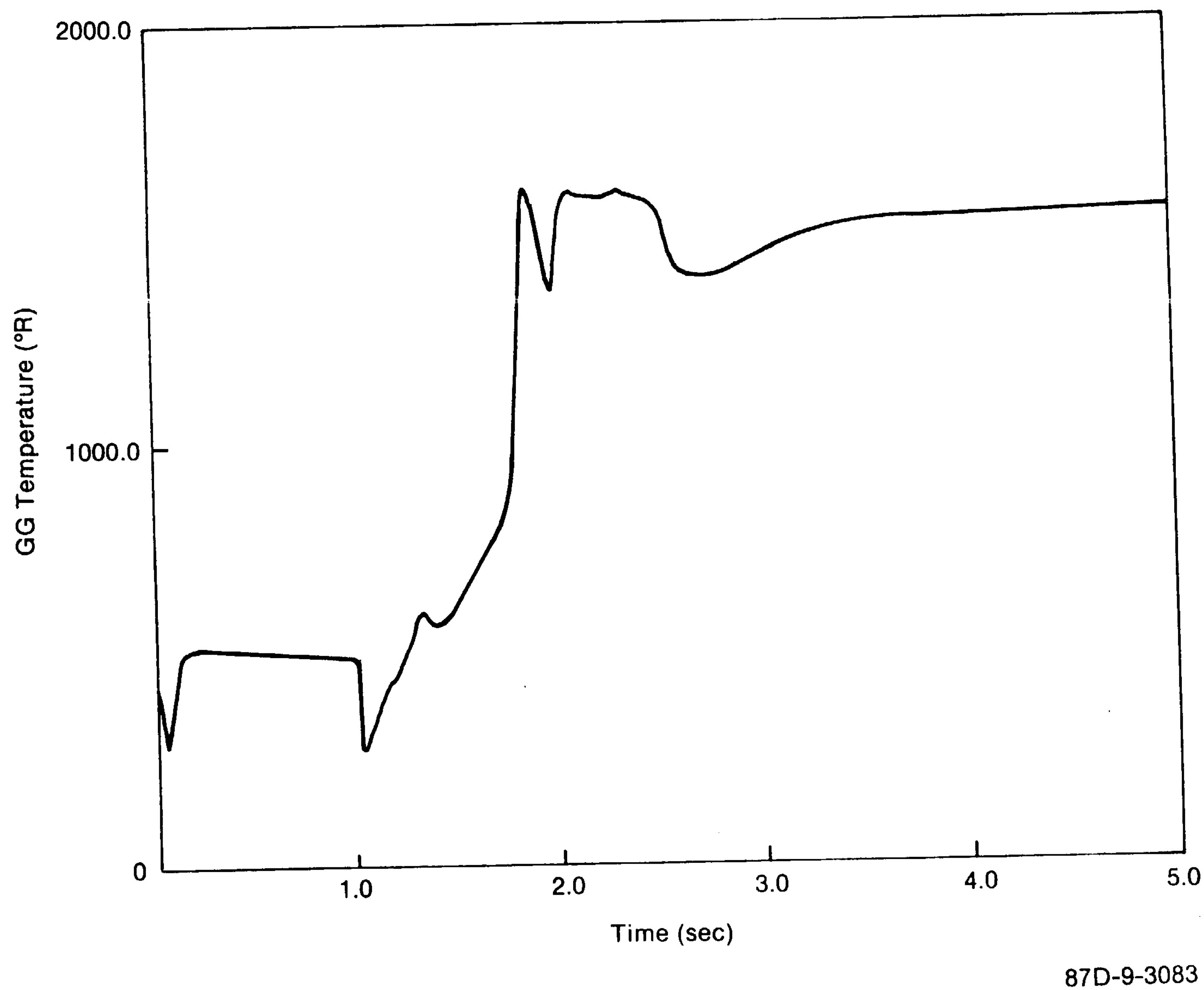

Figure 6-6. STME Helium Spin Start--GG Temperature

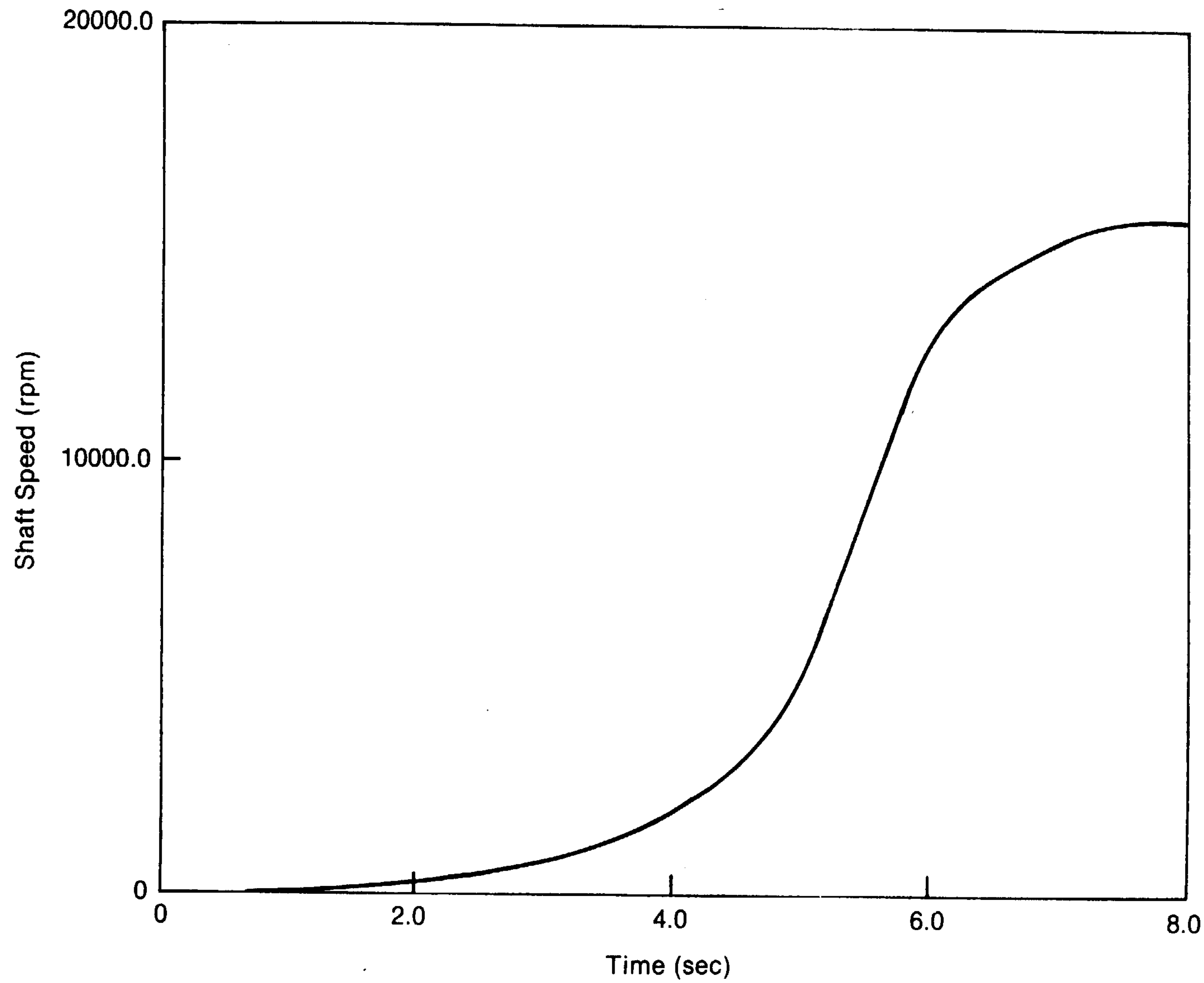

87D-9-3077

Figure 6-7. STME Tank Head Start--LO_2 Pump Speed

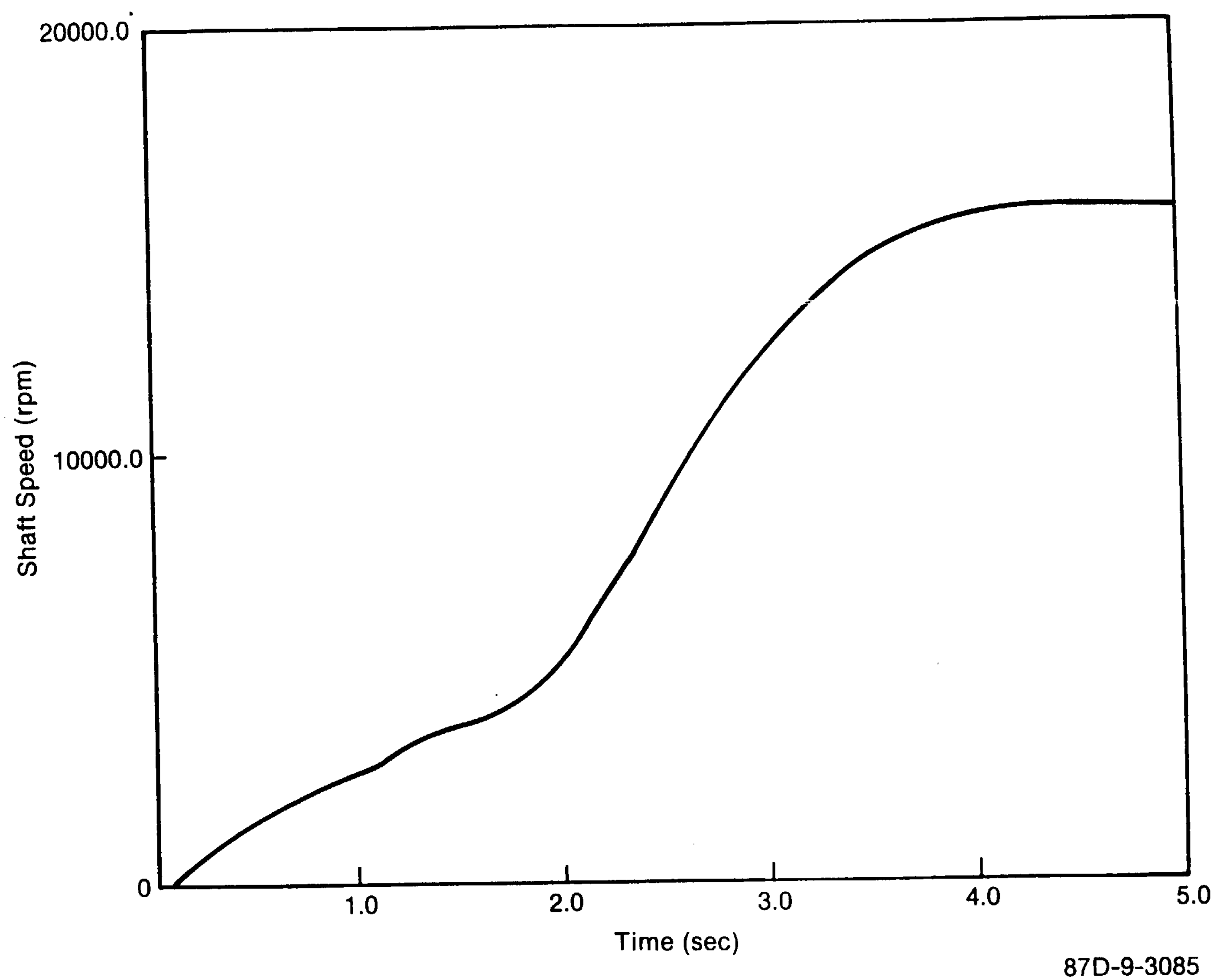

Figure 6-8. STME Helium Spin Start--LO_2 Pump Speed

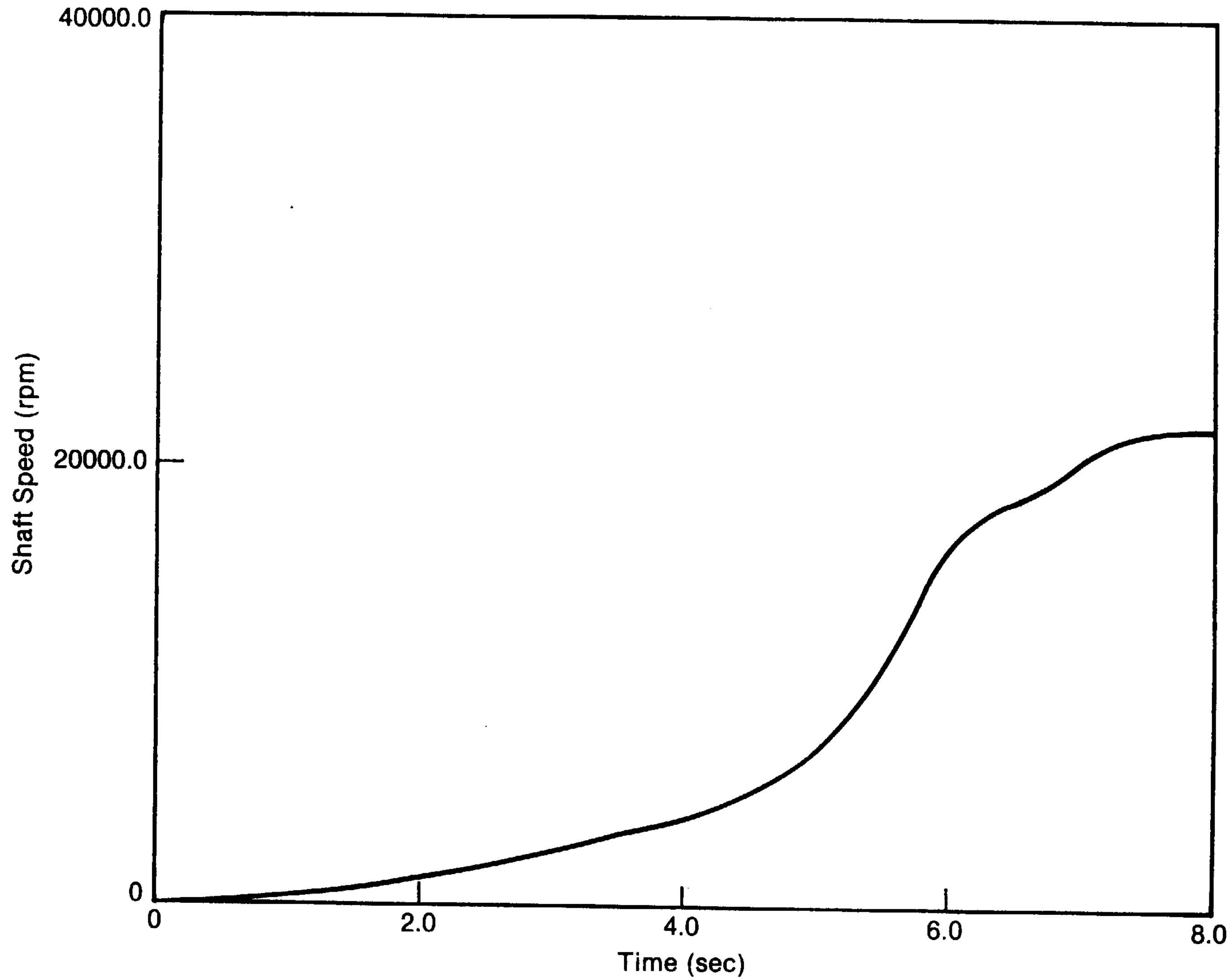

Figure 6-9. STME Tank Head Start--Fuel Pump Speed

87D-9-3076

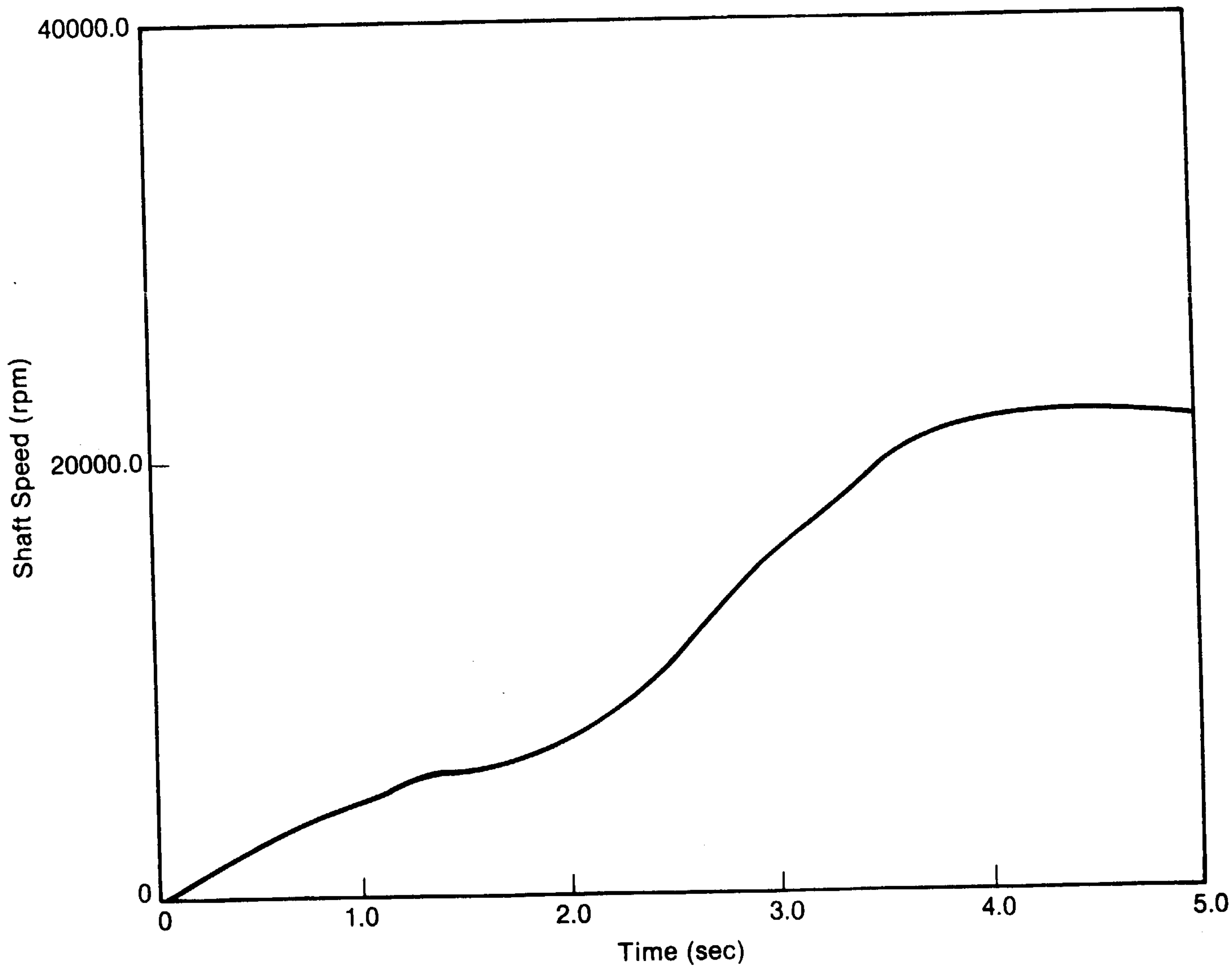

Figure 6-10. STME Helium Spin Start--Fuel Pump Speed

87D-9-3084

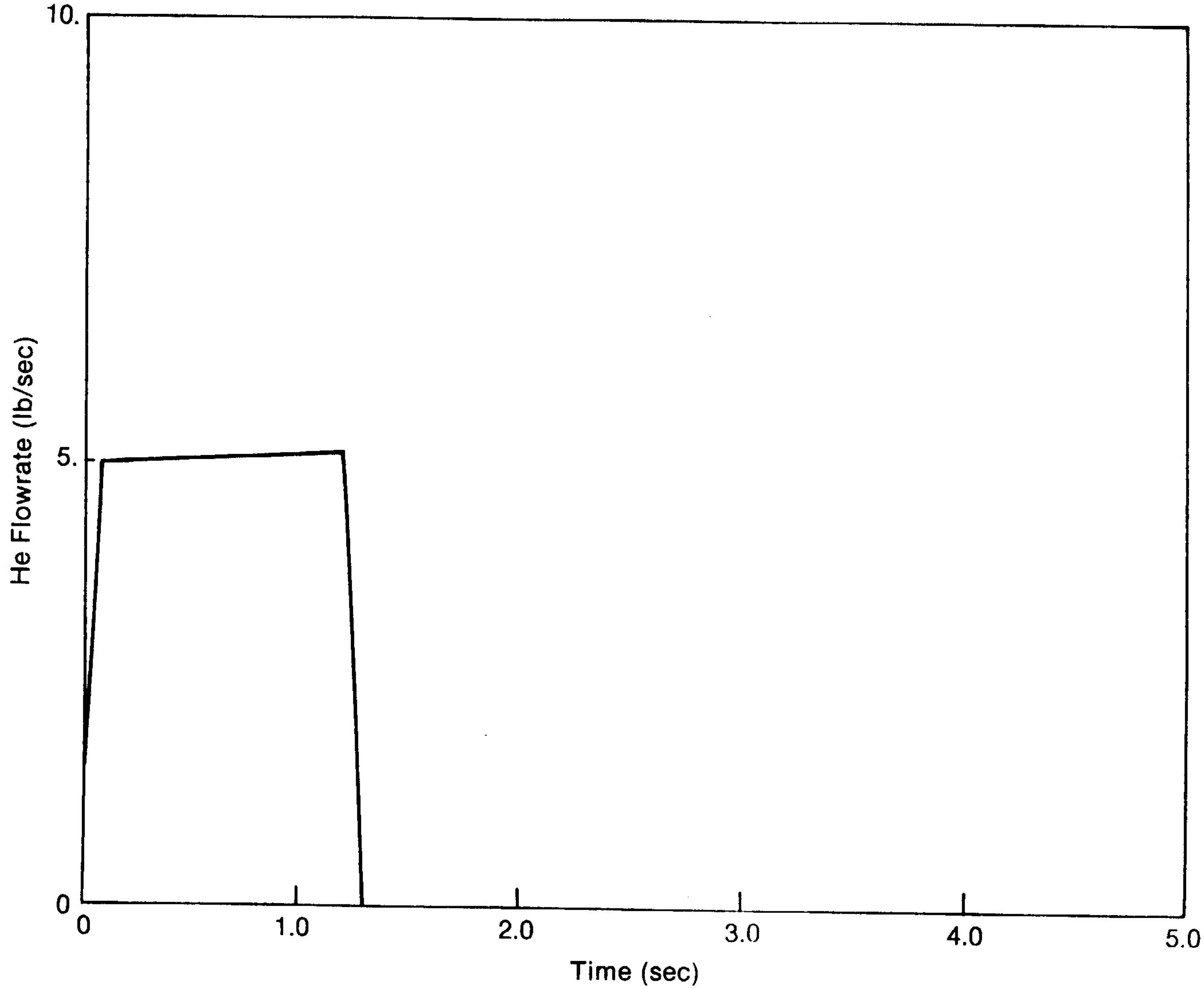

Figure 6-11. STME Spin Start--Helium Flow

87D-9-3080

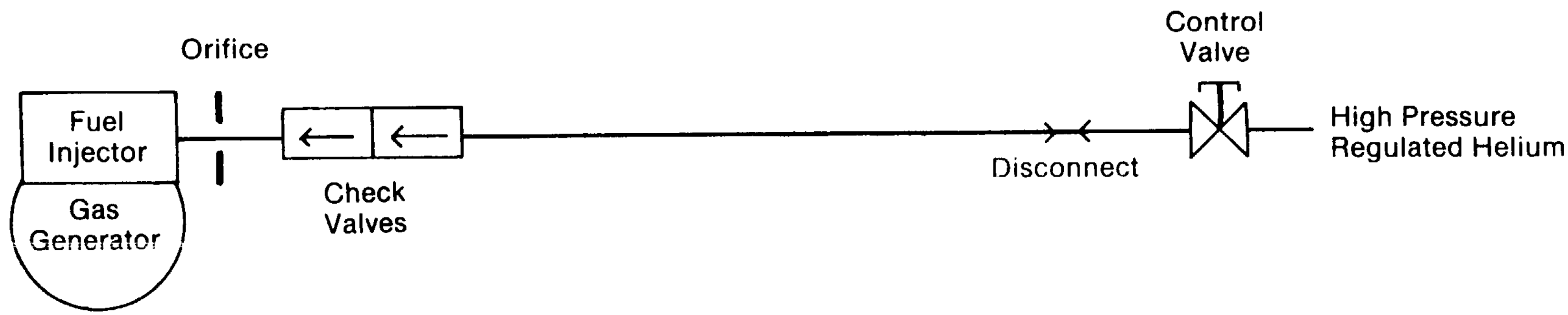

Vehicle Based

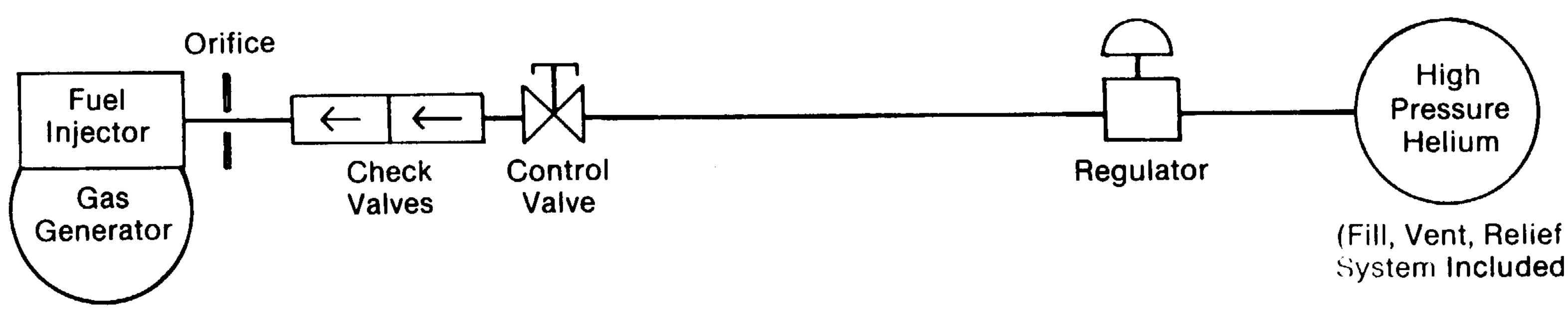

Figure 6-12. Helium Spin Systems--Ground Based

87D-9-3078

7.0 LAUNCH OPERATIONS

7.1 INTRODUCTION

A launch operations study was initiated to assess the problem of minimizing launch operations and between flight maintenance for the baseline engine. Design improvements were evaluated which would accomplish this task.

7.2 SUMMARY AND RESULTS

The major portion of this study concerned itself with the definition of requirements for launch operations and between flight maintenance. To do this, the SSME was utilized as a point of departure. Figure 7-1 provides a graphic representation of the number of labor shifts required for SSME turnaround and maintenance for 17 of the Space Transportation System (STS) flights. Additionally, current routine Orbiter Processing Facility (OPF) turnaround maintenance is represented in Figure 7-2. Tables 7-1, 7-2, and 7-3 contain current SSME inspection requirements, their purposes, and potential engine design features that would facilitate these inspections. The components assessed were combustion devices, turbomachinery, and the heat exchanger. Finally, in Table 7-4, electrical and leak checks for the SSME are identified and, again, engine design features are proposed to facilitate or automate these functional checkouts.

The second major part of the study considered the possibility of automating the maintenance decision process with a proposed condition monitoring system (CMS). This system will use data from conventional and advanced instrumentation as well as data accrued from the development program inspection history and SSME first generation system experience. Figure 7-3 depicts the potential turnaround time savings provided by a condition monitoring system. The system has the potential to reduce the complete turnaround maintenance procedure from several days to only a few hours. Based on this assessment, a preliminary list of operations and maintenance requirements for the STME was generated as shown in Table 7-5.

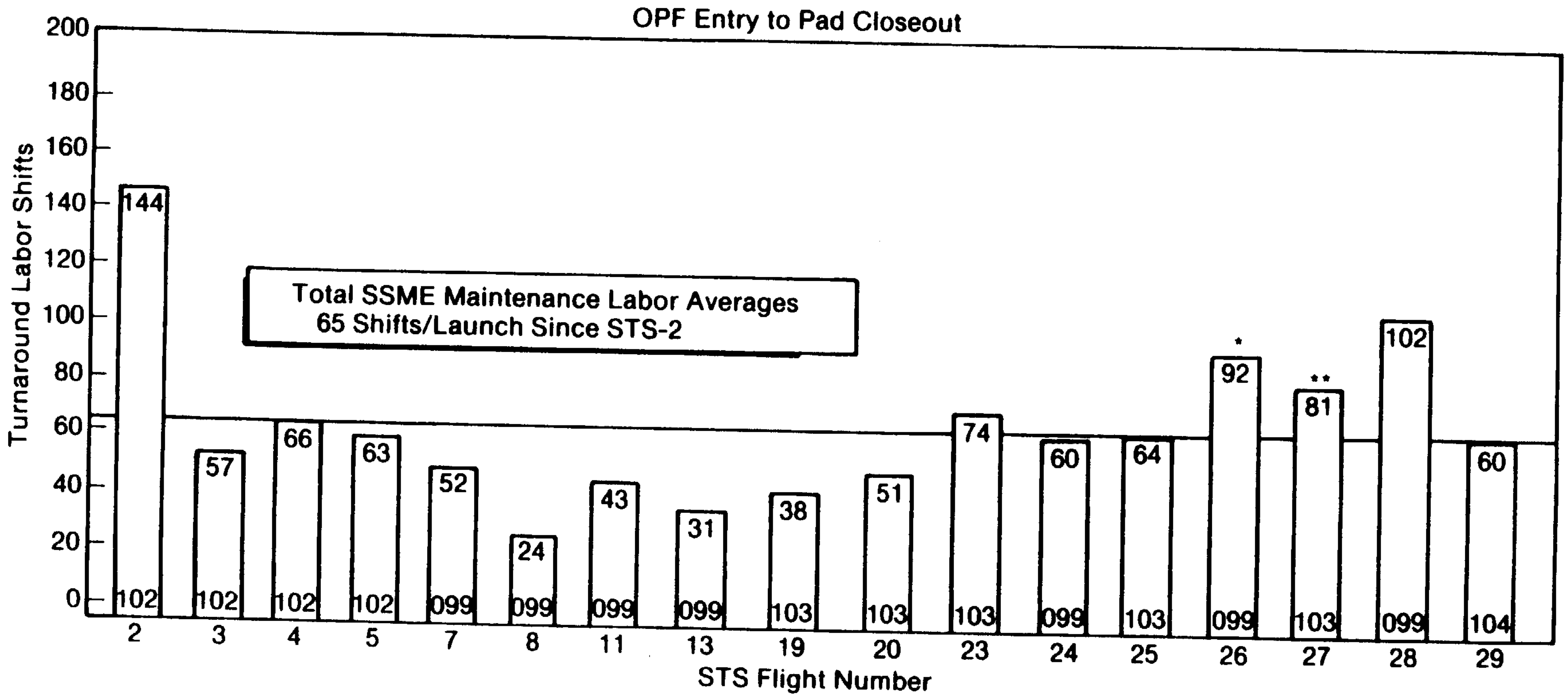

*Includes abort turnaround
**Includes launch scrubs (weather/GPC problem)

87D-9-3209

Figure 7-1. KSC SSME Turnaround Maintenance

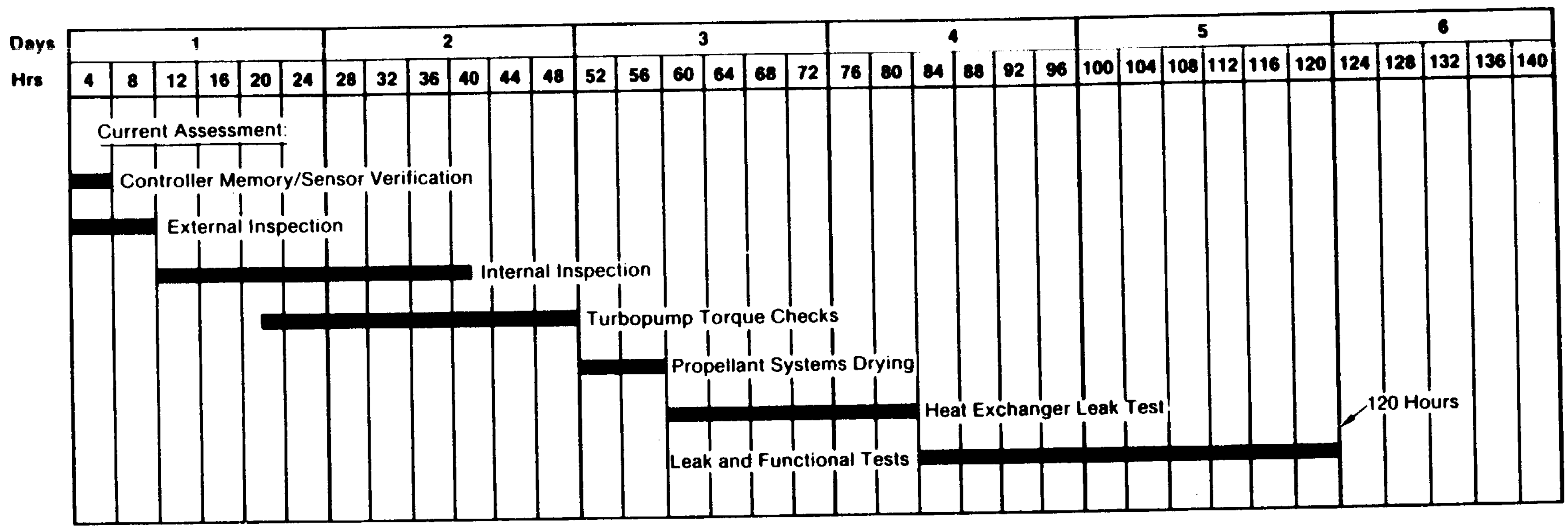

Figure 7-2. Current Routine OPF Turnaround Maintenance

87D-9-3207

Table 7-1. Internal Inspections--Combustion Devices

Current STS Requirement	Purpose	Engine Design Features
Main injector and preburner ● Face plate ● Fuel face nuts ● Lox post tips ● Baffles ● ASI chamber ● ASI spark igniters	Verify no ● Thermal distress ● Cracks ● Erosion ● Contamination	Built-in inspection ports
Main injector ● Interpropellant plate heat shield retainers ● Deflector shields ● Secondary faceplate retainers	Verify no damage	Heat shields eliminated Secondary faceplate eliminated Deflector shields eliminated

87D-9-3205
3-3-0

Table 7-2. Internal Inspections--Turbomachinery

Current STS Requirement	Purpose	Engine Design Features
Bearings ● Balls ● Cage ● Races	Verify No ● Wear ● Spalling ● Cracks	Double discharge volute Hydrostatic bearings Transient axial thrust bearing Enhanced balance piston Deflectometer, torquemeter, isotope wear detection
Impellers, inlets ● Seals	Verify no cavitation damage	Increased NPSP margin Inlet inducers Axial entry inlets Reduced tip speeds Material changes
Turbine ● Turbine housing ● Turbine sheet metal ● Nozzles ● Blades/shrouds/dampers ● Disks ● Seals	Verify no ● Cracks ● Erosion ● Chipping ● Plating loss	Eliminate temp spikes GG temp 1600°R max Material changes Segmented nozzles Shroud damping Eliminate plating Pyrometer

87D-9-3204
3-1-0

Table 7-3. Internal Inspections--Heat Exchanger

Current STS Requirement	Purpose	Engine Design Features
Borescope inspect coils	Verify no ● Discoloration ● Loose brackets ● Cracked welds	Eliminate requirement
Coil leak test (mass spec)	Verify coil integrity	Eliminate requirement
Eddy current test (every 10 starts)	Verify no coil wear	Increase structural margin Reduced environment
Proof test (contingency)	Verify no damage during HPOT installation	Not required

87D-9-3203
3-4-0

Table 7-4. Functional Checkouts

Current STS Requirement	Purpose	Engine Design Features
Electrical ● Sensor checkout ● Actuator checkout ● Pneumatic checkout ● FASCOS checkout ● Flight readiness test	Verify correct operation of engine systems	All software resident in engine Minimize required commands
Leak checks ● Valves ● Joints ● Aft fuselage	Verify no leakage	Automated leak detection ● Holographic ● Mass spec

87D-9-3202
3-2-0

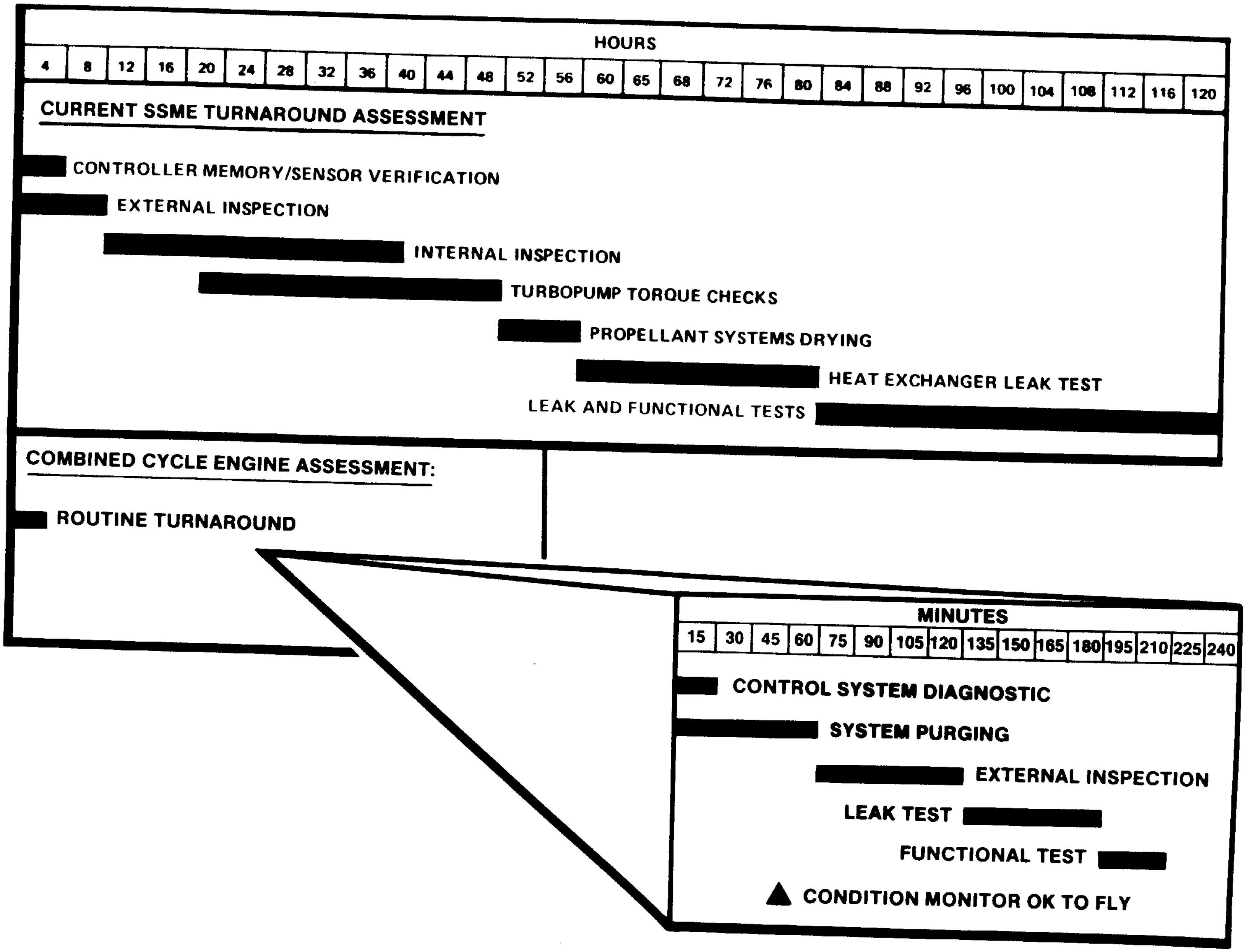

Figure 7-3. Condition Monitor System Improves Turnaround

Table 7-5. Operations and Maintenance Requirements

Installation	Launch Pad	Turnaround
• Install • Leak check interfaces • Functional (electrical) check • Closeout inspection	• Functional (electrical) check	• Diagnostic results • Safing (purging) • External inspection • Leak check • Functional (electrical) check • Closeout inspection

87D-9-3206
3-5-0

8.0 PRODUCIBILITY STUDIES

8.1 INTRODUCTION

In minimizing the recurring costs of the ALS program, the cost and flow time of manufactured engine components becomes a significant factor. Since cost and manufacturing complexity are strongly driven by initial design, a producibility study was undertaken to evaluate design options which would be less expensive, require less flow time, and maintain or enhance component reliability.

Selected SSME components were used to baseline the costs and schedules of what is called here "conventional" rocket engine hardware. In all cases, actual touch labor hours and procurement costs were obtained from existing records. While significant cost savings were determined by employing optional designs, they were only a fraction of the savings achievable since the analysis did not take into account the increased production rates, automated facilities, or lower overhead costs anticipated for ALS.

8.2 SUMMARY AND RESULTS

Baseline costs and schedules were obtained from the SSME program for the MCC, powerhead (including the main injector), 77:1 nozzle, and both of the high-pressure turbopumps. These five components comprise about 60% of the total cost of the SSME. A detailed study of the MCC, main injector, and the high-pressure LO_2 turbopump (HPOTP) housing were performed during this reporting period. Also, some initial work was performed relative to turbine blade costs. The results of this period's study are summarized below.

8.2.1 <u>Main Combustion Chamber</u>

Figure 8-1 shows a conventional MCC fabricated from a slotted copper alloy liner with an electrodeposited nickel close-out, wrought I-718 machined and welded manifolds, and a wrought I-718 machined and welded jacket and

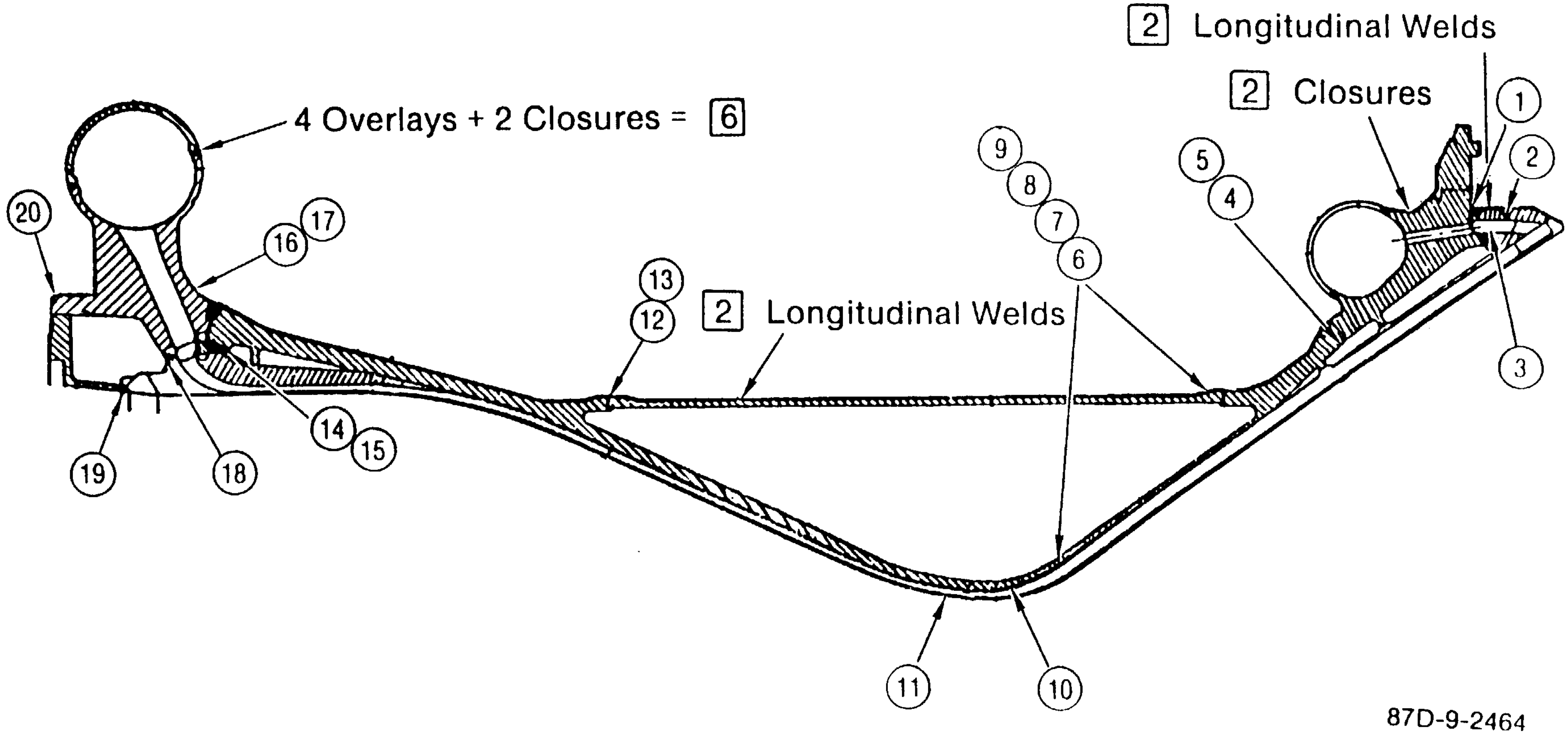

Figure 8-1. Conventional Main Combustion Chamber Liner Design (32 Welds)

thrust ring. The forward manifold requires HEE protection because of the sensitivity of I-718 to room-temperature hydrogen. This assembly requires 32 major weldments in the construction, including weld overlays of I-903, copper and gold plating for HEE protection, and extension fitting of jacket details to complete the assembly.

Figure 8-2 depicts a design option requiring only eight welds, no HEE protection, and no separate I-718 jacket details. The manifolds are made from material not sensitive to hydrogen. The use of diffusion bonding to attach the manifolds eliminates several welds, and the use of electrodeposited nickel-cobalt alloy precludes the necessity to attach a separate I-718 jacket, eliminating several more weldments.

A detailed cost and time study shows that this alternate approach to MCC fabrication can eliminate 19 of 42 major fabrication steps, 265 of 700 days flow time, 8,600 touch labor hours, and $8,000 in material costs. Further cost reductions can be achieved by providing investment cast manifolds and automation features in the process.

8.2.2 Main Injector

Figure 8-3 shows a conventional coaxial element injector design with 600 elements. The elements are partially machined, then inertia welded to a premachined and drilled interpropellant plate. The primary cost drivers in this construction are a variety of machining and inspection steps, which have to be performed 600 times each after the elements are in place on the injector body and the N/C machining and welding necessary to close out the LO_2 manifold and thrust structure.

Figure 8-4 is an ALS conceptual design incorporating several cost reduction features over the baseline. The injector elements are finish machined prior to installation and are attached all in one furnace brazing operation to simple drilled and reamed constant diameter holes in the interpropellant plate. The injector body and manifolds are made of investment casting which

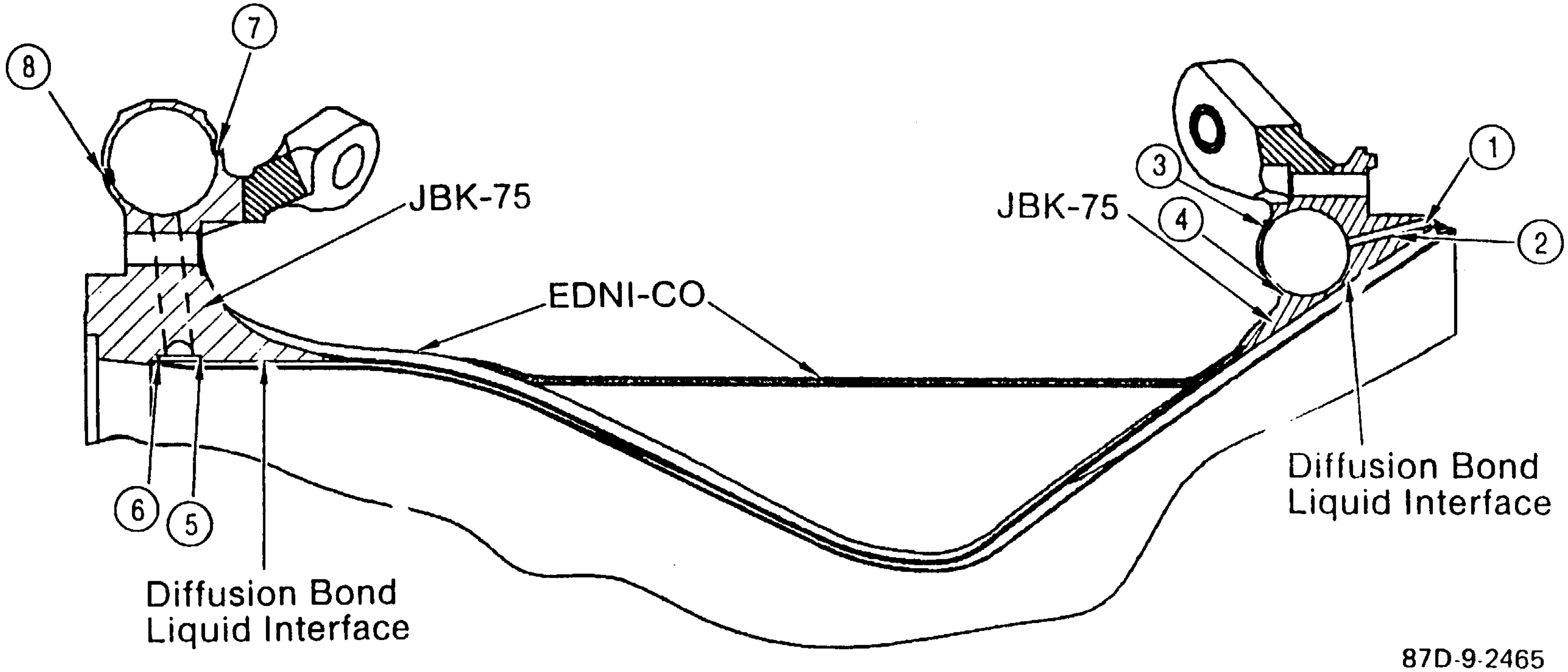

Figure 8-2. STBE/STME MCC Low Cost Design
(Alternate Concept 1) (8 Welds)

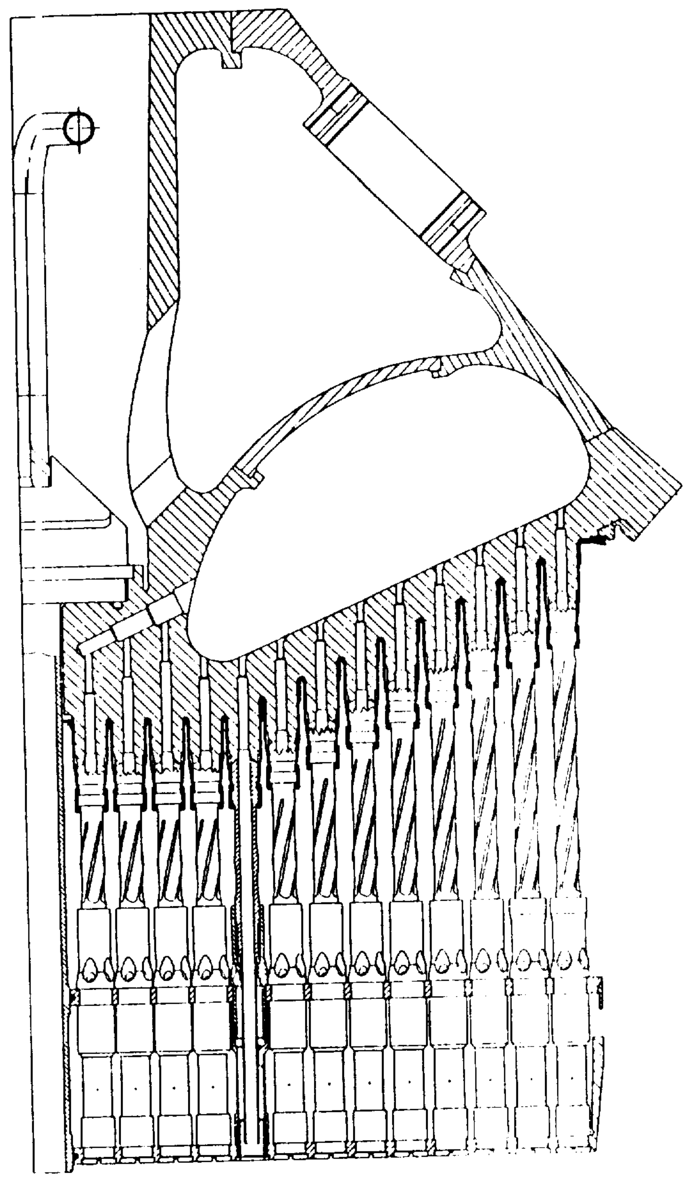

87D-9-2457

Figure 8-3. Conventional Main Injector

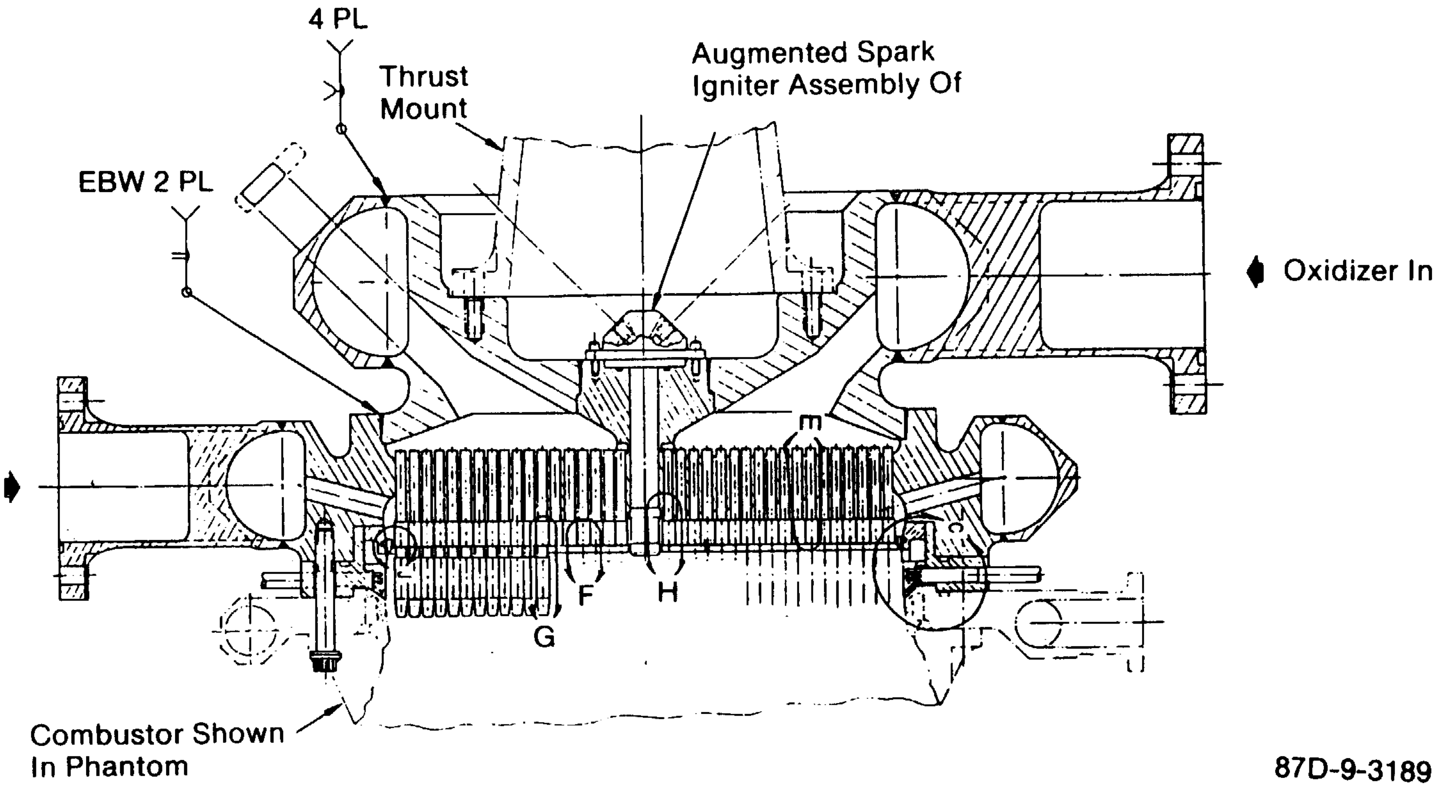

Figure 8-4. Main Injector Conceptual Design

require a minimum of machining and welding. The thrust structure is made as a separate detail and bolted to the LO_2 manifold structure.

The concept shown has not been priced in detail at this point. However, incorporating the single feature of brazed elements to the baseline design in Figure 8-3 eliminated 11 of 56 operations, 275 of 693 flow days, 7,475 touch labor hours, but increased the material cost by $90,000. Further work is in progress to assess the total benefit of the ALS injector concept.

8.2.3 HPOTP Housing

Figure 8-5 depicts the elements of an SSME HPOTP housing assembly. The center (discharge) manifold volute is now constructed of forged I-718 rings and shells, which are N/C and EDM machined and welded together. The two outer (inlet) manifolds are made of investment cast I-718 and are then electron beam welded to the center discharge assembly.

An alternate and feasible concept for reducing cost is to investment case the center volute in one piece, thus significantly reducing the machining and welding costs. We have received a bid from Precision Castparts Corp. to supply this assembly for $9,000, which is less than the current cost of the required I-718 starting forgings. Once the center volute is developed as a casting, it requires little more effort to attempt casting of the entire housing assembly (except the flange). This is accomplished by injecting waxes in the new casting tool and combining one center body wax with two outer (inlet) waxes (this tooling already exists) to create the entire housing in wax. After gates and risers are attached, this wax can be used to invest the mold used to pour the entire casting. This latter step is pushing the state of the art and is therefore high risk; however, the additional investment of this step is low compared to the potential $750,000 and 327 flow day savings per unit.

- **Results to date**
  - Performed detail studies for cast HPOTP volute housing (RS007232)
  - Designed one-piece cast HPOTP housing
    - Staged development planned
    - Cost estimates for development HPOTP casting received from foundries
- **Planned activity**
  - Fabricate tooling
  - Pour volute castings (4-6) HIP best one (RS007732)
  - After volute casting (RS007732) successfully demonstrated cast complete housing assembly
    - Weld waxes for inlet to volute wax
    - Pour 3RS007729 configuration castings (FY 1989)
- **Potential savings**
  - $750K per unit
  - 327 working days

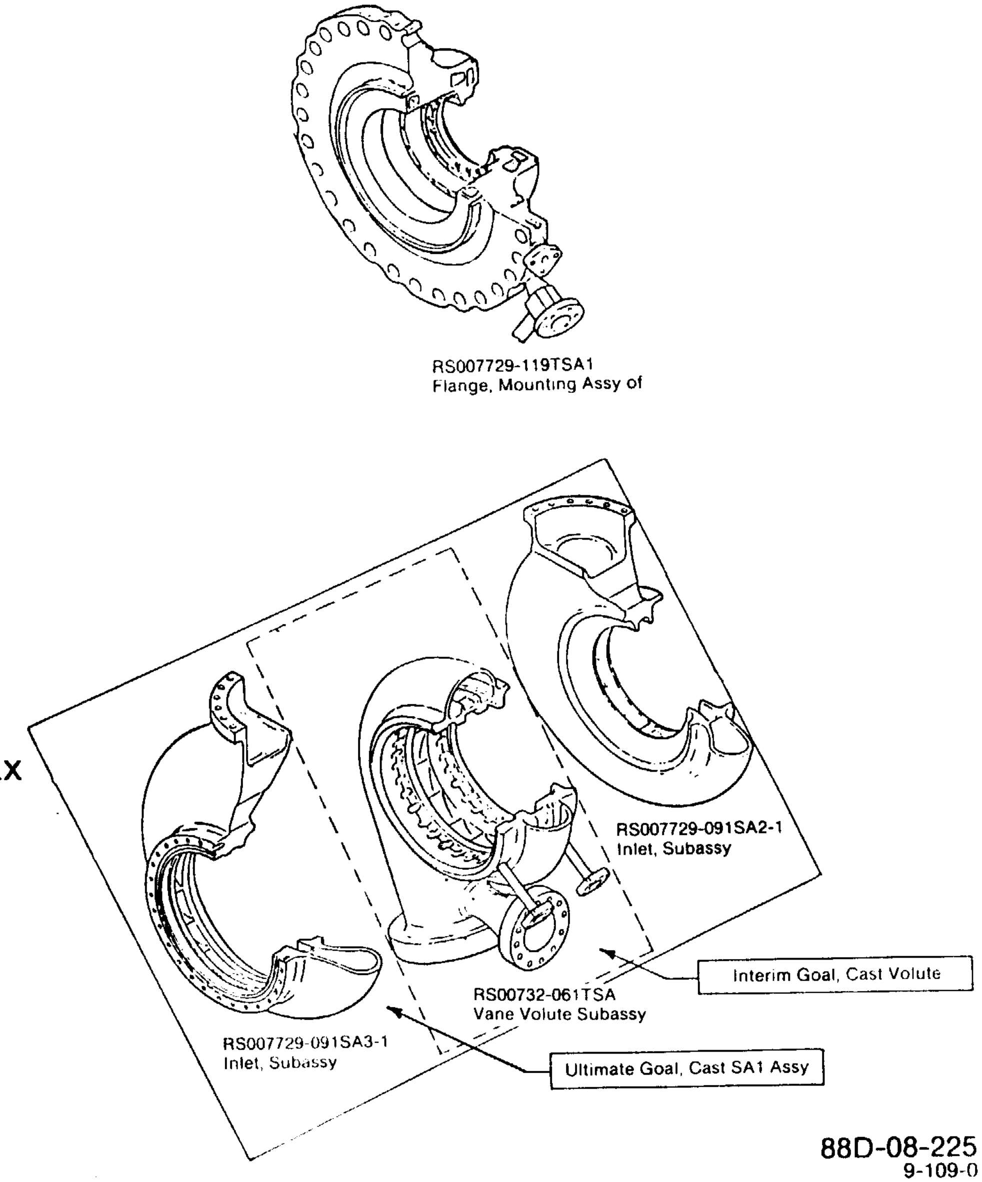

Figure 8-5. Structural Castings Evaluation

8.2.4 Turbine Blades

Current SSME turbine blades are reasonably priced as the supplier bases cost upon the low production quantities required. However, due to the extreme thermal shock characteristic of the SSME topping cycle, high steady-state temperature, and high life-cycle requirements, there is considerable in-house labor required after receipt to perform operations such as application of thermal coatings, hand blending of corners and damper pockets, special stress relieving, and shot peening.

In the ALS design concept for an expendable booster with a moderate temperature gas generator turbine drive, all of these special steps are deemed unnecessary. Table 8-1 shows a cost breakdown totalling $178,000 savings per engine if all of these special steps are eliminated.

5352e/rmr

Table 8-1. SSME Turbine Blade Cost Summary

Operation	HPFTP		HPOTP	
	1st Stage (63)	2nd Stage (59)	1st Stage (78)	2nd Stage (73)
	$	$	$	$
Casting per blade	41	43	51	50
Machining per blade	66	66	68	69
In-house touch labor per blade	1,490	1,176	124	72
Total cost per building	1,597	1,285	243	191
Cost if touch labor avoided	107	109	119	119
Savings per engine set	93,870	69,384	9,700	5,300
Savings per engine	$178,254			

87D-9-2463

9.0 COST UPDATE

9.1 INTRODUCTION

This section contains the results of the cost studies performed during Phase A'. This cost update is comprised of two areas of distinct study. The first area addresses general engine and program costs and the second area of study offers measures which seek to reduce engine production costs.

9.2 SUMMARY AND RESULTS

The STME Program, in total, comprises design, development, test and evaluation, production, and operations costs. As it is currently defined, the STME Program will involve a high level production rate with operations and support activity spanning 15 years from 1998 to 2012. Table 9-1 presents a summary of the total projected costs of the STME Program. Additionally, a nominal cost goal of $3.00/lb of thrust has been defined. This cost goal, relative to previous engine programs, in presented in Figure 9-1.

Figure 9-2 presents the average unit cost for a LO_2/LH_2 engine based on Rocketdyne's parametric cost model data. As shown, the engine's average unit cost is dependent upon the thrust level as well as the production rate. Based on the assumption of 10 missions/yr and four or more engines per vehicle, a reduction in average unit cost will occur due to large-scale prediction.

Engine production cost reduction was addressed in four study efforts during Phase A'. The first area constituted design concept changes which reduce costs without a compromise in performance. Figure 9-3 depicts a typical engine cost breakdown divided among components, systems, and acceptance testing. Table 9-2 shows that an overall 35% reduction in engine cost can be realized from component design changes that do not affect component performance. Still further, cost reductions can be achieved by design concept changes which do compromise engine performance.

Table 9-1. STME Program Cost Summary (FY 1987 $M)

		Total
• **DDT&E**		1,290
• Labor	**539**	
• Hardware	**701**	
• Tooling	**50**	
• **Production**		
• 28 engines		392
• **Operations and support**		658
Total		2,340

87D-9-1639A
49-31-1

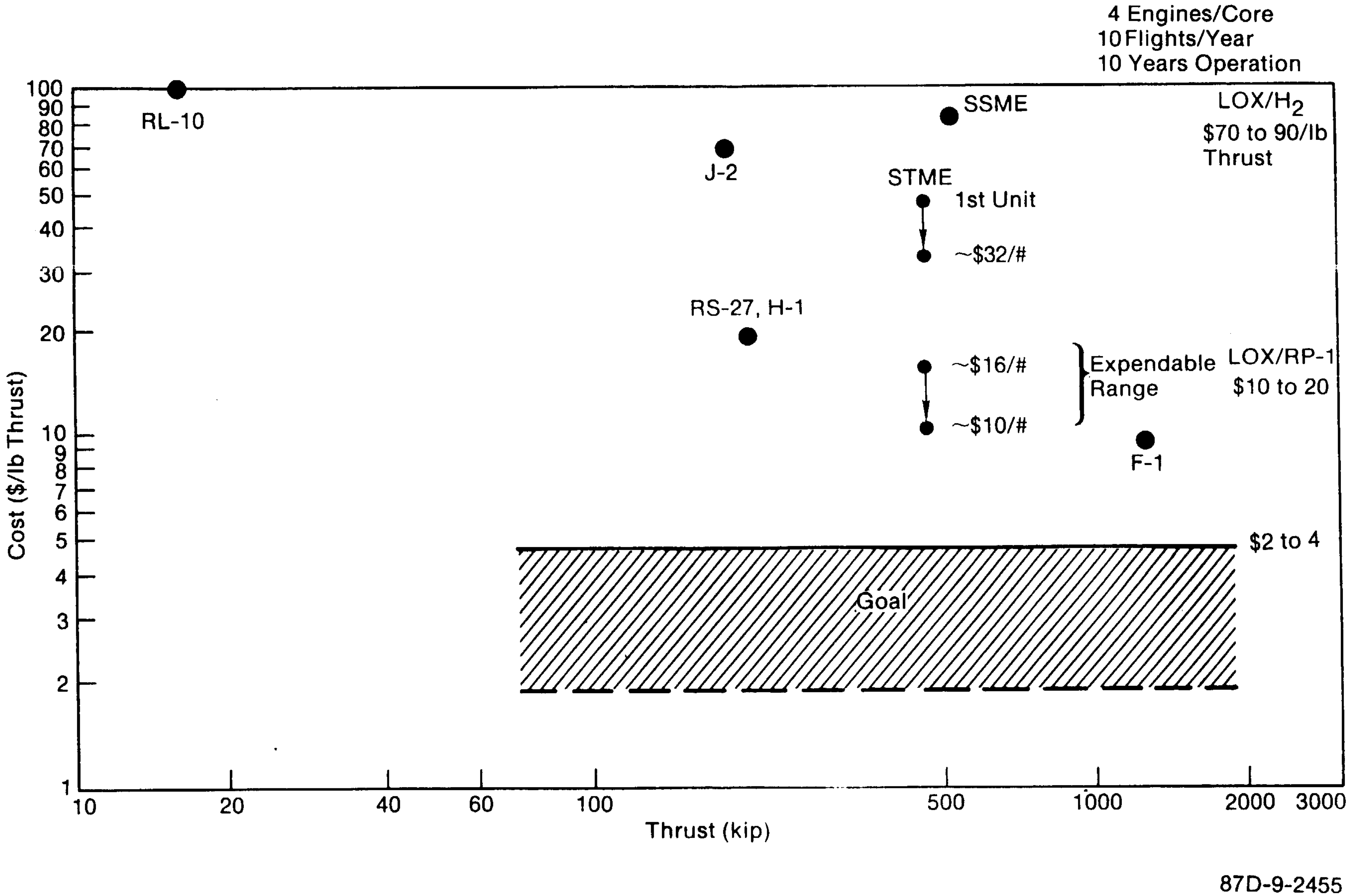

Figure 9-1. Engine Costs

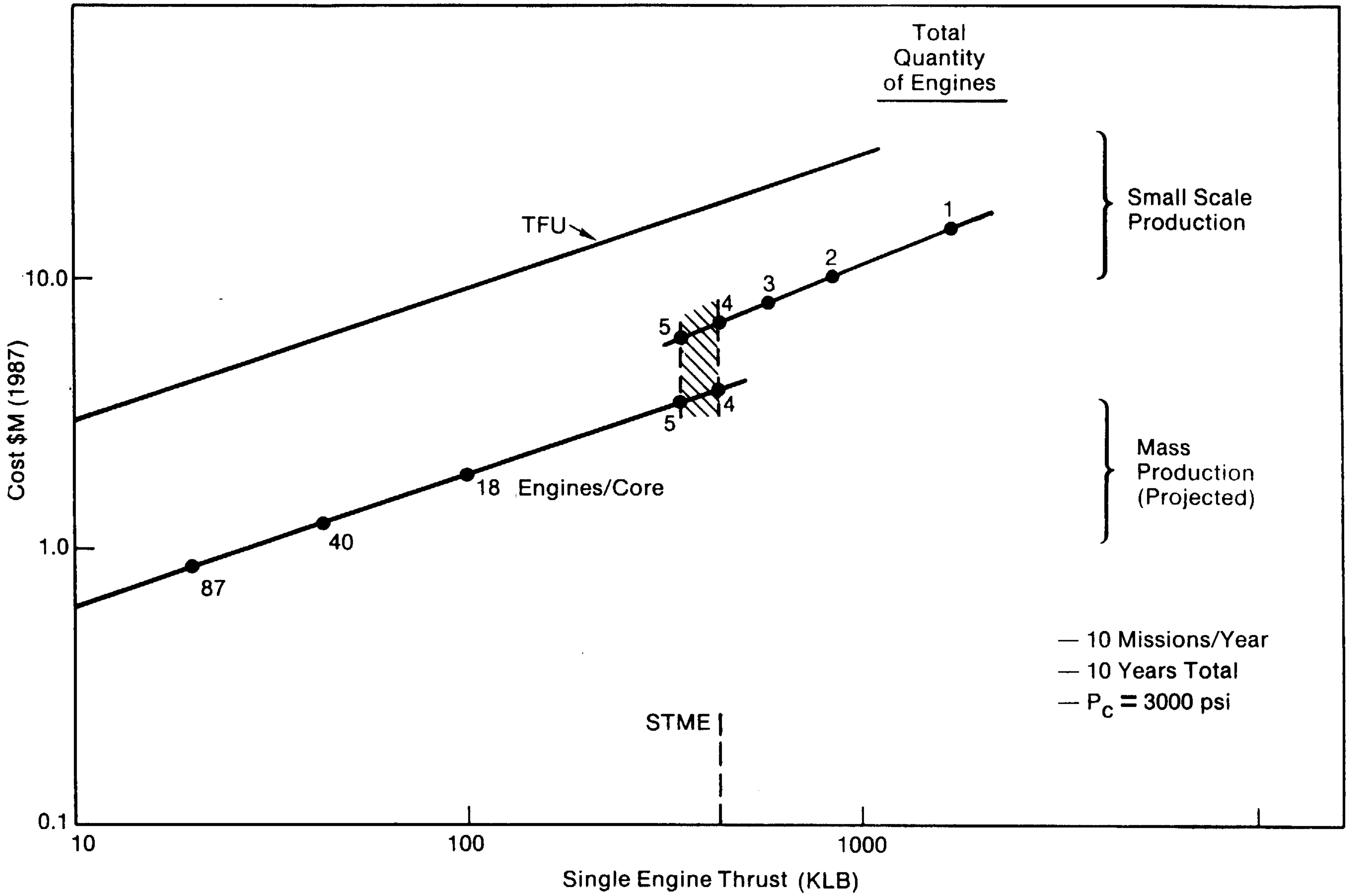

87D-9-2453

Figure 9-2. LOX/LH_2 Engine Average Unit Cost

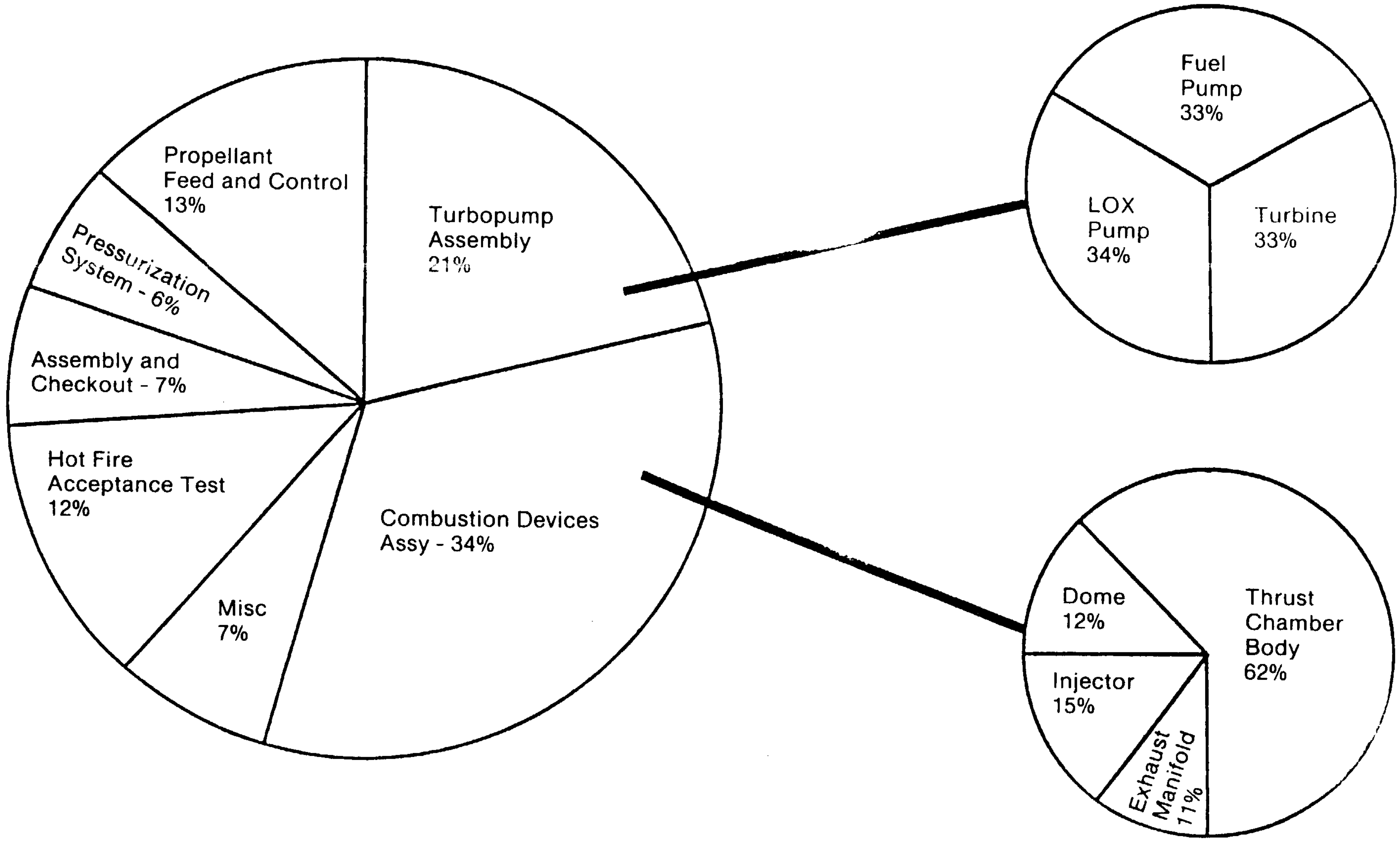

87D-9-2623A

Figure 9-3. Typical Engine Cost Breakdown

Table 9-2. Design Concept Changes--No Significant Change in Performance or Weight

Engine Subsystem	Engine Cost Breakdown %	Component Cost Reduction %	Engine Cost Reduction %
• Combustion devices	34	33	11.2
Combustion chamber			
Injector			
Nozzle			
• Turbopump assembly	21	30	6.3
Pump			
Turbine			
• Feed system and controls	13	45	6
• Pressurization system	6	30	2
• Engine assembly and checkout	7	50	3.5
• Acceptance testing	12	33	4
• Miscellaneous	7	30	2
Total	100		35

87D-9-2526

Another engine production cost reduction measure is the minimization of system requirements. Table 9-3 shows the cost savings gained from several engine system requirements changes.

Last, engine production costs are impacted by the product quantity and rate. Figure 9-4 shows the average unit cost reductions associated with increased production quantities and rates. It is observed that for small-scale reduction, costs are reduced by the learning curve. The more units produced per year, the greater the learning curve and the cheaper the cost. Further cost reduction is achieved by true mass production and automated production facilities. This case requires a large buy of greater than 500 engines at a high production rate of greater than 50 engines per year.

5352e/rmr

Table 9-3. System Impact--Requirement Reductions

	Cost Reduction, $*
• Eliminate boost pumps	1.0 M
• Eliminate fail-op in control system	1.5 M
• Eliminate throttling and closed loop control	1.0 M
• Lower chamber pressure (by 1000 psia)	1.0 M
• Eliminate power head/dual preburners	2.5 M
• Make expendable	1.0 M

*All costs are on Theoretical First Unit (TFU) basis ($20 M)

87D-9-2620C
2-149-0

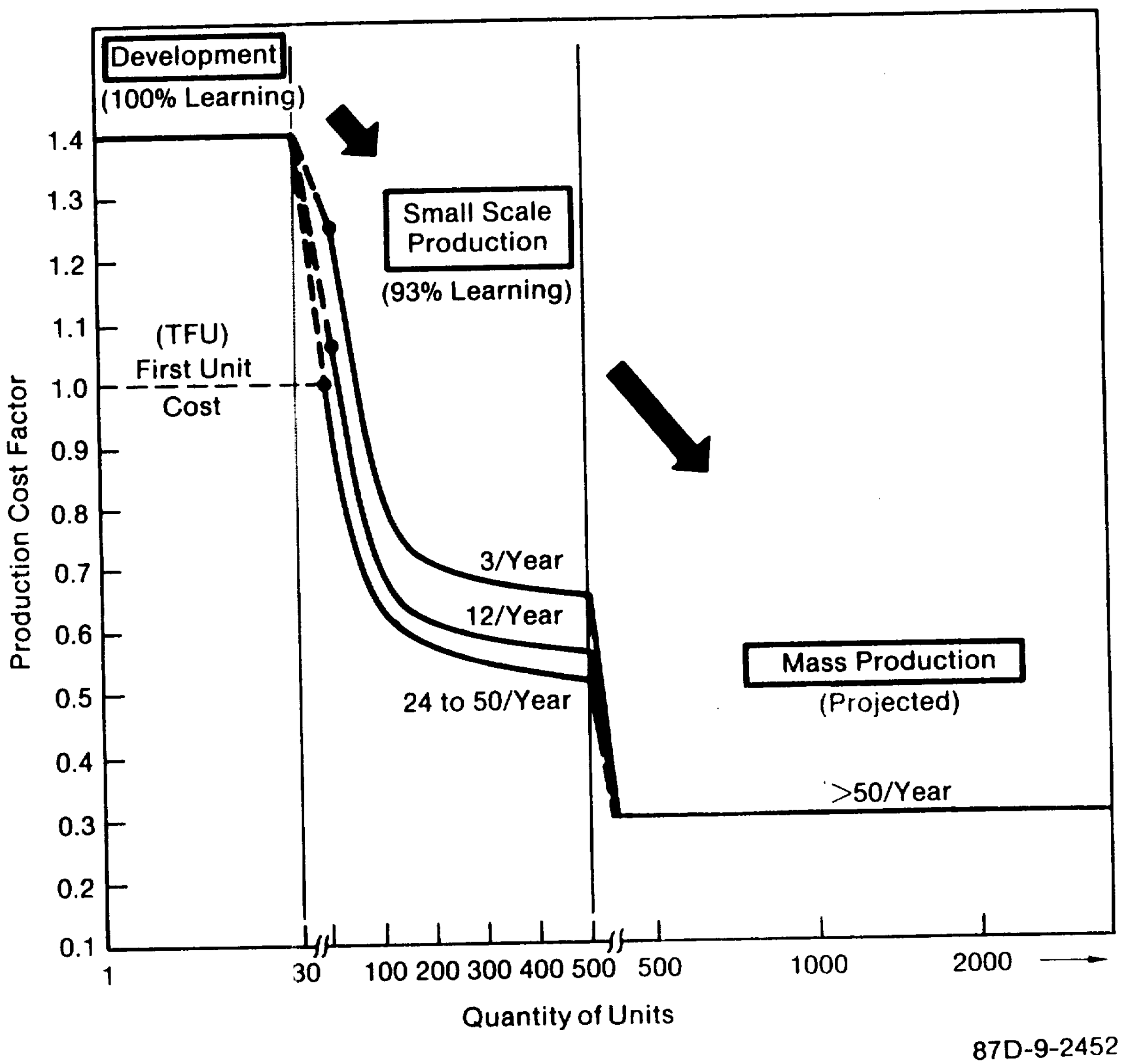

Figure 9-4. Production Cost Model

End DATE Nov 6, 1990